

**ELECTROCHEMICAL
REMOVAL OF CARBON MONOXIDE FROM HYDROGEN
USING NICKEL CATALYST**

By

AHMAD NAFEES

A Thesis presented to the
DEANSHIP OF GRADUATE STUDIES

In Partial Fulfillment of the Requirements of

MASTER OF SCIENCE
IN
CHEMICAL ENGINEERING

**KING FAHD UNIVERSITY
OF PETROLEUM & MINERALS**

Dhahran, Saudi Arabia

JUNE, 2005

**ELECTROCHEMICAL
REMOVAL OF CARBON MONOXIDE FROM
HYDROGEN USING NICKEL CATALYST**

BY

AHMAD NAFEES

A Thesis Presented to the
DEANSHIP OF GRADUATE STUDIES

KING FAHD UNIVERSITY OF PETROLEUM & MINERALS

DHAHRAN, SAUDI ARABIA

In Partial Fulfillment of the
Requirements for the Degree of

MASTER OF SCIENCE
In
CHEMICAL ENGINEERING

RABI-II, 1426 H

JUNE, 2005

KING FAHD UNIVERSITY OF PETROLEUM & MINERALS
DHAHRAN-31261, KSA

DEANSHIP OF GRADUATE STUDIES

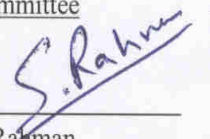
This thesis, written by

AHMAD NAFEES

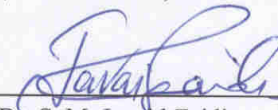
under the direction of his thesis advisor and approved by his thesis committee, has been presented to and accepted by the Deanship of Graduate Studies, in partial fulfillment of the requirements for the degree of

MASTER OF SCIENCE IN CHEMICAL ENGINEERING

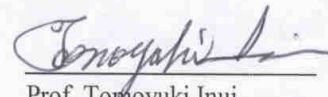
Thesis Committee



Dr. S. U. Rahman
(Thesis Advisor)



Dr. S. M. Javaid Zaidi
(Thesis Co-advisor)



Prof. Tomoyuki Inui
(Member)



Dr. N. A. Al-Baghli
(Member)



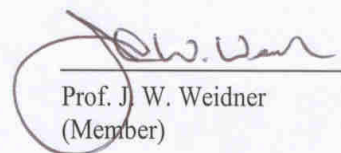
for Prof. Mohamed B. Amin
(Department Chairman)



Prof. Mohammad A. Al-Ohali
(Dean of Graduate Studies)

15/11/05

Date 15-11-2005



Prof. J. W. Weidner
(Member)



Dedication

My Late Chachu

Jb. Mohammad Khairul Anam (1960- 2001)

ACKNOWLEDGEMENT

In the name of Allah, Most Gracious, Most Merciful

“Read, In the name of thy Lord and Cherisher, Who Created. Created man from a [Leech-like] clot. Read, and thy Lord is most Bountiful, He who taught [the use of] pen. Taught man which he knew not. Nay, but man doth transgress all bounds. In that he looketh upon himself as self-sufficient. Verily, to thy Lord is the return [of all].”(The Holy Quran, Surah # 96, Verses 1-5).

I bow in reverence to almighty Allah for giving me confidence, strength and patience for undertaking and successful completion of this work.

The support provided by King Fahd University of Petroleum & Minerals to attain my MS degree, complete this research and overall to enrich my knowledge in the field of chemical engineering is gratefully acknowledge. The research facilities, computing facilities and other facilities were simply outstanding and excellent.

With deep sense of gratitude and appreciation, I would like to express my sincere thanks to my thesis advisor, Dr. S. U. Rahman for his invaluable support, guidance, encouragement throughout the period of my research. Working with him was indeed a wonderful learning experience, which I thoroughly enjoyed. I am also indebted to my thesis co-advisor, Dr. S. M. J. Zaidi, for his suggestions and analysis. I owe special thanks to my thesis committee members, Dr. Nadhir A. Baghli, Prof. Tomoyuki Inui and Prof. J. W. Weidner for their critical review and suggestions. Also I would like to thank Dr. Mohammed B. Amin, chairman, chemical engineering department for providing the required resources and facilities.

My Special thanks are due to Dr. Shakeel Ahmad, Research Engineer at Research Institute KFUPM, for helping me in the characterization of my samples. Also I am also thankful to Khursheed Ahmad, technician at CRP-RI for his support in various troubles shooting during my experimentations. I indeed received wonderful support from him throughout my research work.

I would like to thank the laboratory staff and technicians of CHE department especially Mr. Syed Kamal, Mr. Kamal Mahjoughb, Mr. Mahdi, Mr. Ebrahim, Mr. Bashir Ahmad Mr. Mofizul Islam for their help during the experimental work. I am especially thankful to Mr. Syed Kamal Ahmad, without who's help it might have been impossible for me to complete this work

My special thanks are due to Mohammed Fareeduddin, Mohd Irfan Ahmad, Mehboob Basha other friends and colleagues for their continuous encouragement and providing me a wonderful time during my stay at KFUPM.

Last but not least, I would like to appreciate my parents, brothers, sisters and other relatives for their prayers, encouragement and support that permitted me to indulge my passion for the long task for completing this work. It might be unjust on my part if I omit the name of my fiancé N. F. for her love, support and patience during this work and throughout my career.

(Ahmad Nafees Sajid)

Dhahran, Saudi Arabia

TABLE OF CONTENTS

LIST OF TABLES	X
LIST OF FIGURES	XI
ABSTRACT	XIV
ABSTRACT (ARABIC)	ERROR! BOOKMARK NOT DEFINED.
1. INTRODUCTION	1
1.1. CONCEPT OF FUEL CELL	1
1.2. ADVANTAGES AND DISADVANTAGES	2
1.3. CLASSIFICATION OF FUEL CELLS	2
1.4. PROTON EXCHANGE MEMBRANE FUEL CELL	4
1.5. FUEL PROCESSING SYSTEM	6
1.6. SCOPE AND OBJECTIVES	9
2. LITERATURE REVIEW	10
2.1. CO REMOVAL APPROACHES	11
2.1.1. LOW AND HIGH TEMPERATURE WATER GAS SHIFT PROCESS	13
2.1.2. PREFERENTIAL OXIDATION	14
2.1.3. PLASMA REFORMING	17
2.1.4. METHANATION	18
2.1.5. ADSORPTION	19
2.1.6. MEMBRANE PURIFICATION	21
2.1.7. INTEGRATED WGS MEMBRANE REACTOR	22
2.1.8. SORPTION PROCESS	24
2.1.9. ELECTROCHEMICAL FILTER	25
2.2. STUDY OF CO ADSORPTION AND OXIDATION ON Ni CATALYST	26
3. EXPERIMENTAL SETUP	29
3.1. MATERIALS USED	29

3.1.1.	PLANER Ni ELECTRODE	29
3.1.2.	RANEY-Ni CATALYST	29
3.1.3.	CARBON MONOXIDE GAS	31
3.1.4.	HYDROGEN GAS	31
3.1.5.	PLATINUM DISC	31
3.1.6.	ELECTROLYTE SOLUTION	31
3.1.7.	H-TYPE PYREX GLASS CELL	32
3.2.	EXPERIMENTAL DETAILS FOR PLANER Ni ELECTRODE	32
3.2.1.	EXPERIMENTAL SETUP	32
3.2.2.	EXPERIMENTAL PROCEDURE	38
3.3.	EXPERIMENTAL DETAILS FOR RANEY Ni STUDY	38
3.3.1.	EXPERIMENTAL SETUP	39
3.3.2.	EXPERIMENTAL PROCEDURE	41
4.	RESULTS & DISCUSSION	44
4.1.	CO ELECTROOXIDATION ON PLANER Ni ELECTRODE	44
4.1.1.	CYCLIC VOLTAMMETRY OF PLANER Ni ELECTRODE WITH N ₂	45
4.1.2.	CYCLIC VOLTAMMETRY OF CO EXPOSED PLANER Ni ELECTRODE	51
4.1.3.	CYCLIC VOLTAMMETRY OF H ₂ EXPOSED PLANER Ni ELECTRODE	56
4.1.4.	REMOVAL OF ADSORBED CO FROM PLANER Ni ELECTRODE	59
4.2.	PARAMETRIC STUDY OF CO REMOVAL ON PLANER Ni ELECTRODE	65
4.2.1.	EFFECT OF CO EXPOSURE TIME	65
4.2.2.	EFFECT OF CO CONCENTRATION	70
4.2.3.	EFFECT OF CO FLOW RATE	79
4.3.	CHARACTERIZATION OF RANEY-Ni CATALYST	85
4.3.1.	INDUCTIVE COUPLED PLASMA (ICP-AES)	86
4.3.2.	X-RAY DIFFRACTION (XRD)	86
4.3.3.	SCANNING ELECTRON MICROSCOPY (SEM)	91
4.3.4.	BET SURFACE AREA AND PORE SIZE DISTRIBUTION	92
4.4.	CO REMOVAL STUDY ON RANEY-Ni ELECTRODE	94
4.4.1.	CYCLIC VOLTAMMETRY OF RANEY-Ni ELECTRODE UNDER N ₂	94
4.4.2.	CYCLIC VOLTAMMETRY OF CO EXPOSED RANEY-Ni ELECTRODE	98
4.4.3.	REMOVAL OF ADSORBED CO FROM RANEY-Ni ELECTRODE	102

4.5. PARAMETRIC STUDY OF CO REMOVAL ON RANEY-NI ELECTRODE	104
4.5.1. EFFECT OF SCAN RATE	105
5. CONCLUSIONS & RECOMMENDATIONS	107
5.1. CONCLUSIONS	107
5.2. RECOMMENDATIONS	108
NOMENCLATURE	110
REFERENCES	111
APPENDIX	119
VITAE	130

LIST OF TABLES

Table 1-1: Classification of Fuel Cell based on Electrolyte	3
Table 3-1: Properties of Raney-Ni Catalyst	30
Table 3-2: Geometrical Details of Raney-Ni Electrode	40
Table 4-1: CV Parameters of N ₂ Exposed Planer Ni Electrode	47
Table 4-2: Cathodic Scan Parameters of N ₂ Exposed Planer Ni Electrode	50
Table 4-3: CV Parameters of CO Exposed Planer Ni Electrode	52
Table 4-4: Cathodic Scan Parameters of CO Exposed Planer Ni Electrode	55
Table 4-5: CV Parameters of H ₂ Exposed Planer Ni Electrode with H ₂	58
Table 4-6: CV Parameters of CO Electrooxidation Experimentation	61
Table 4-7: Details of Parametric Study on Planer Ni Electrode	66
Table 4-8: Details of Parametric Study on Planer Ni Electrode	71
Table 4-9: Details of Parametric Study on Planer Ni Electrode	80
Table 4-10: ICP-AES Analysis of H ₂ O ₂ Passivated Raney Ni Catalyst	87
Table 4-11: Elemental Analysis of H ₂ O ₂ Passivated Raney Ni Catalyst	90
Table 4-12: Pore Size Distribution of Passivated Raney-Ni Catalyst	93
Table 4-13: Characteristic Values of Passivated Raney-Ni Catalyst	93
Table 4-14: CV Parameters of N ₂ Exposed Raney-Ni Electrode	95
Table 4-15: Parameters of N ₂ Exposed Raney-Ni Electrode	97
Table 4-16: CV Parameters of CO Exposed Raney-Ni Electrode	99
Table 4-17: CV Parameters of CO Electrooxidation on Raney-Ni Electrode	103

LIST OF FIGURES

Figure 1-1: Schematic Diagram of PEM Fuel Cell	3
Figure 1-2: Cell Potential and Power Density of PEM Fuel Cell	5
Figure 1-3: Effect of CO Poisoning on Fuel Cell Performance	5
Figure 1-4: Schematic Diagram of Conventional Fuel Processing System	8
Figure 2-1: Schematic Diagram of New CO Removal Approaches	12
Figure 3-1: Geometric Dimensions of Planer Ni Electrode	30
Figure 3-2: Schematic Diagram of the Experimental Setup	33
Figure 3-3: Photograph of Experimental Measurement	34
Figure 3-4: Photograph of the Experimental Setup	34
Figure 3-5: Photograph of the Experimental Setup	35
Figure 3-6: Schematic Diagram of Raney-Ni Electrode	35
Figure 3-7: Photograph of Raney-Ni Electrode	40
Figure 3-8: Schematic Diagram of Experimental Setup for Raney-Ni Study	43
Figure 3-9: Photograph of Experimental Setup for Raney-Ni Study	43
Figure 4-1: Cyclic Voltammogram of N ₂ exposed Planer Ni Electrode	48
Figure 4-2: Cathodic Scan of N ₂ Exposed Planer Ni Electrode	50
Figure 4-3: Cyclic Voltammogram of CO and N ₂ Exposed Ni Electrode	53
Figure 4-4: Cathodic Scans of CO and N ₂ Exposed Planer Ni Electrode	55
Figure 4-5: CV of H ₂ , CO and N ₂ Exposed Planer Ni Electrode	57
Figure 4-6: Multiple CV of CO Electrooxidation on Planer Ni Electrode	61
Figure 4-7: Cathodic Scan of CO Electrooxidation on Planer Ni Electrode	62
Figure 4-8: Effect of Exposure Time at 1 % CO	67

Figure 4-9: Effect of Exposure Time on CO Electrooxidation at 10 ppm CO	68
Figure 4-10: Amount of CO Electrooxidized vs Exposure Time at 1 % CO	69
Figure 4-11: Amount of CO Electrooxidized vs Exposure Time at 10 ppm CO	69
Figure 4-12: Effect of CO Concentration at 25 ml/min	72
Figure 4-13: Amount of CO Electrooxidized vs Concentration at 25 ml/min	73
Figure 4-14: Amount of CO Electrooxidized vs CO Concentration at 125 ml/min	73
Figure 4-15: Effect of CO Concentration at 125 ml/min	74
Figure 4-16: Effect of CO Concentration at 200 ml/min	75
Figure 4-17: Effect of CO Concentration at 275 ml/min	76
Figure 4-18: Amount of CO Electrooxidized vs CO Concentration at 200 ml/min	77
Figure 4-19: Amount of CO Electrooxidized vs CO Concentration at 275 ml/min	77
Figure 4-20: Effect of Flow Rate at 1 % CO	81
Figure 4-21: Amount of CO Electrooxidized vs Flow Rate at 10 ppm CO	81
Figure 4-22: Effect of Flow Rate at 1 % CO	82
Figure 4-23: Amount of CO Electrooxidized vs Flow Rate at 10 ppm CO	82
Figure 4-24: Effect of Flow Rate at 100 ppm CO	83
Figure 4-25: Amount of CO Electrooxidized vs Flow Rate at 10 ppm CO	83
Figure 4-26: Effect of Flow Rate at 10 ppm CO	84
Figure 4-27: Amount of CO Electrooxidized vs Flow Rate at 10 ppm CO	84
Figure 4-28: XRD Patterns of H ₂ O ₂ Passivated Raney-Ni Catalyst	87
Figure 4-29: XRD Patterns of H ₂ O ₂ Passivated Raney-Ni Catalyst	88
Figure 4-30: SEM Micrograph of H ₂ O ₂ Passivated Raney-Ni Catalyst	89
Figure 4-31: SEM Micrograph of H ₂ O ₂ Passivated Raney-Ni Catalyst	89

Figure 4-32: EDS Spectra of H ₂ O ₂ Passivated Raney-Ni Catalyst	90
Figure 4-33: Complete CV of N ₂ Exposed Raney-Ni Electrode	95
Figure 4-34: CV of N ₂ Exposed Raney-Ni Electrode	97
Figure 4-35: CV of CO Exposed Raney-Ni Electrode	99
Figure 4-36: CV of CO and N ₂ Exposed Raney-Ni Electrode	101
Figure 4-37: Cyclic Voltammogram of CO Electrooxidation on Raney Ni Electrode	103
Figure 4-38: Effect of Scan Rate on CO Electrooxidation on Raney-Ni Electrode	106
Figure 4-39: Amount of CO Electrooxidized vs Scan Rate	106

ABSTRACT

NAME OF STUDENT: AHMAD NAFEES
TITLE OF STUDY: Electrochemical Removal of Carbon Monoxide
from Hydrogen Using Nickel Catalyst
MAJOR FIELD: CHEMICAL ENGINEERING
DATE OF DEGREE: JUNE 2005

A large and complex CO gas clean up system is usually required to bring down carbon monoxide content in reformat gas to acceptable levels for fuel cell application (<10 ppm). Recently an electrochemical filter has been proposed promising to simplify the gas clean up. In this device, a pulsating potential is applied to a conventional PEMFC, the configuration results in preferential oxidation of CO. The present work was undertaken to investigate the possibility of replacing the expensive Pt catalyst with non-noble metal catalyst. It has been shown experimentally that CO adsorbs and electrooxidizes on Ni/Raney-Ni catalyst akin to Pt catalyst.

It has been found that CO present in the H₂ gas gets adsorbed over the catalyst surface causing delay in hydrogen evolution reaction and prevents the Ni dissolution. The adsorbed CO was successfully removed by application of suitable anodic potential. It was observed that almost 100 % CO removal takes place from the electrode surface. The amount of CO electrooxidized depends upon a number of parameters such as CO exposure time, CO flow rate, CO concentration, scan rate and catalyst loading. The effect these parameters were investigated.

MASTER OF SCIENCE DEGREE

King Fahd University of Petroleum & Minerals
Dhahran, Saudi Arabia

رسالة الماجستير

اسم الطالب: أحمد نفيس

بعملية (H₂) من الهيدروجين (CO) موضوع الرسالة: إزاحة أول أكسيد الكربون
كهروكيميائية باستخدام محفز النيكل .

حقل التخصص: الهندسة الكيميائية

تاريخ الحصول على الدرجة: يونيو 2005 م

يستخدم نظام كبير ومعقد عادةً لإزالة غاز أول أكسيد الكربون أو تخفيض مستوى الغاز إلى حد مقبول في تطبيقات خلايا الطاقة (أقل من عشرة جزء من المليون). في هذه الدراسة تم تطوير منظم كهروكيميائي أعطى نتائج مشجعة لهذه العملية . في هذا الجهاز، قدرة كهربائيه متغيره تعرض على خليه عاديه من نوع (PEMFC) هذه الطريقه تعطي الأفضليه لتأكسد أول أكسيد الكربون. كما تم في الدراسة الماليه بحث إحتماالية تغيير المحفز العالي الكلفه Pt إلى محفز معدني غير نفيس.

وتم تجربة المحفز البديل في المعمل، وأظهر نفس مستوى إمتصاص غاز أول اكسيد الكربون وتم فحص المحفز البديل ووجد أن أول أكسيد الكربون الموجود في غاز الهيدروجين يمتص على المحفز مسبباً تأخيراً في تفاعل الهيدروجين ويمنع إخمال النيكل المحفز النشط. وقد تم إزالة CO الممتص بنجاح بتطبيق أو تعريض قدرة أنوديه مناسبه . ولو حظ بأنه تقريباً تم إزالة كل الـ CO تقريباً من سطح القطب. وقد وجد أن كمية الـ CO المؤكسدة تعتمد على عدد من العوامل مثل مدة تعرض الـ CO، وكذلك مستوى الإنسياب ، والتركيز ، وكمية القدرة ، وكمية المحفز . وتم دراسة هذه العوامل .

1. INTRODUCTION

1.1. Concept of Fuel Cell

Fuel cell is an electrochemical device that directly converts the chemical energy of reactants (a fuel and an oxidant) into electrical energy. Since fuel and oxidant both are stored outside the cell, fuel cell is an energy converter only. There are several different types of fuel cell but they are all based around a central design, which consists of two electrodes, an anode and a cathode. These are separated by a solid or liquid electrolyte that carries ions between the two electrodes. Fuel is supplied to the fuel electrode (anode) and oxidant is fed to the oxidant electrode (cathode) as shown in the Figure 1-1 for a H_2/O_2 fuel cell. Simultaneous and separate occurrence of oxidation of fuel at anode and reduction of oxidant at cathode causes a potential difference that promotes electron flow in external circuit. In a PEM fuel cell Pt-Ru and Pt-C are used as anode and cathode electrocatalyst respectively.

1.2. Advantages and Disadvantages

Most significant advantage of fuel cell is that chemical energy is directly converted into electrical energy thus avoiding the limitation of Carnot cycle, which results into higher efficiencies. Other advantages of fuel cells are absence of moving parts, low noise level, high reliability, high power and energy densities with respect to volume, low operating temperature ranges and low pollution. Fuel cell can be made in variety of sizes and they are modular. This advantage is particularly important in congested urban centers where the needed transmission and distribution facilities are expensive to install. Although fuel cell offers attractive advantages as cited above, there are some disadvantages associated with it. This includes high initial cost of the system, large weight and volume of gaseous fuel storage, liquefaction expenses of H₂ fuel, cleaning requirements of fuel and oxidant gases, specific power limitation, and deactivation of precious metal catalyst by S and CO.

1.3. Classification of Fuel Cells

Fuel cells can be classified either according to the type of electrolyte, electrode, electrocatalyst, temperature and end use or applications. Among these, classification based on the nature of the electrolyte is most popular. Some of the common types of fuel cells and their salient features are listed in Table 1-1. General categories of fuel cells are as follows;

1. AFC: alkaline fuel cell
2. PAFC: phosphoric acid fuel cell
3. MCFC: molten carbonate fuel cell

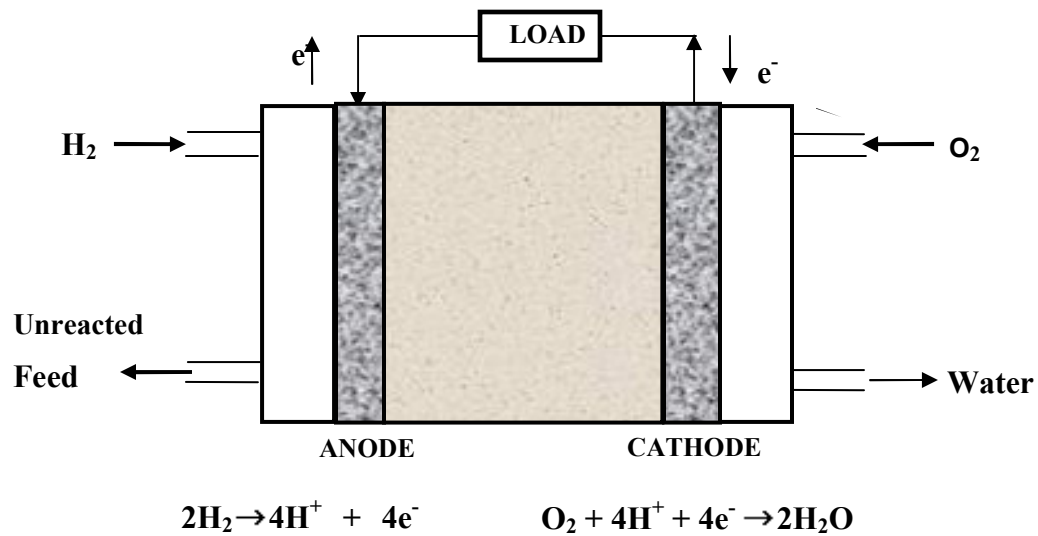


Figure 1-1: Schematic Diagram of PEM Fuel Cell

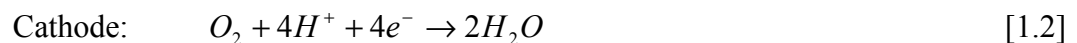
	<i>AFC</i>	<i>PEMFC</i>	<i>DMFC</i>	<i>PAFC</i>	<i>MCFC</i>	<i>SOFC</i>
Temp (° C)	80	40-80	60-130	200	650	1000
Fuel	H ₂	H ₂	Methanol	H ₂ (/CO ₂)	H ₂ , CO	H ₂ , CO
Electrolyte	KOH	Polymeric Membrane	Polymer	Phosphoric Acid	Molten Carbonate	Solid Oxide
Mobile ion	OH ⁻	H ⁺	H ⁺	H ⁺	CO ₃ ²⁻	O ₂ ²⁻

Table 1-1: Classification of Fuel Cell based on Electrolyte

4. SOFC : Solid Oxide Fuel Cell
5. PEMFC: Proton Exchange Membrane Fuel Cell
6. DMFC: Direct Methanol Fuel Cell

1.4. Proton Exchange Membrane Fuel Cell

Proton exchange membrane fuel cell (PEMFC) consists of a proton conducting membrane as electrolyte contained between two platinum impregnated porous electrodes. The back of the electrodes are coated with a hydrophobic compound forming a wet proof coating which provides a gas diffusion path to the catalyst layer. This technology was invented by General Electric in the 1950s and was used by NASA to provide power for the Gemini space project [1]. Typical components and reactions occurring in PEMFC fuel cell are given in Figure 1-1. Hydrogen flows into the fuel cell on to the anode and gets split into protons and electrons. Hydrogen ions permeate across the electrolyte to the cathode, while the electron flows through an external circuit and provides power. Oxygen in the form of air is supplied at the cathode that combines with the electrons and the hydrogen ions to produce water. The electrochemical reactions occurring at the electrodes are as follows:



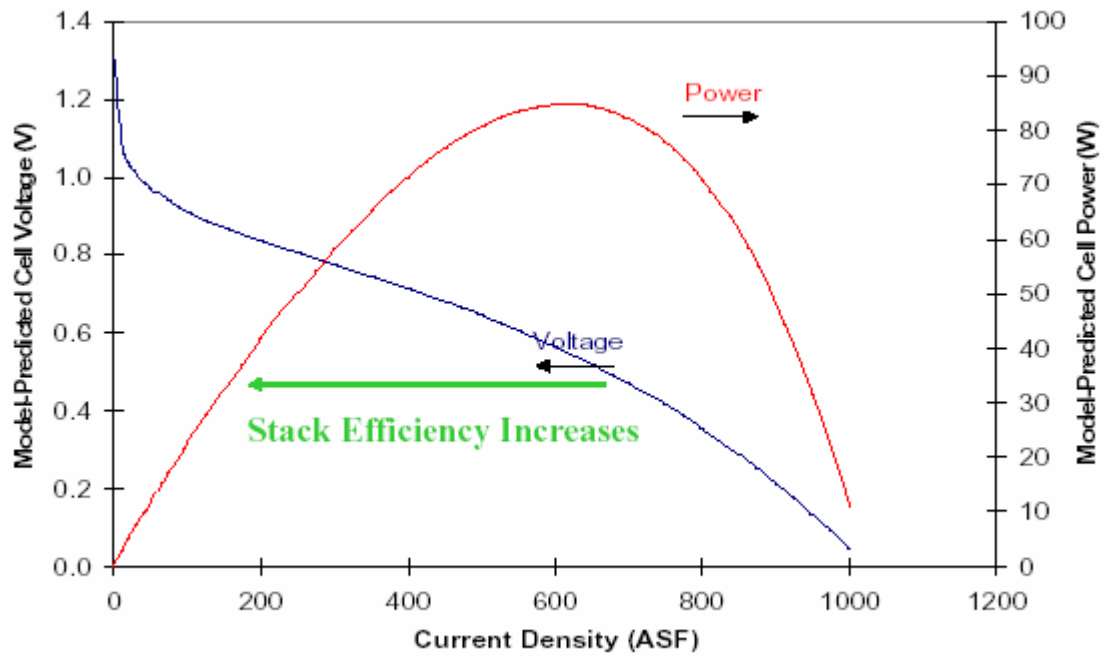


Figure 1-2: Cell Potential and Power Density of PEM Fuel Cell [2]

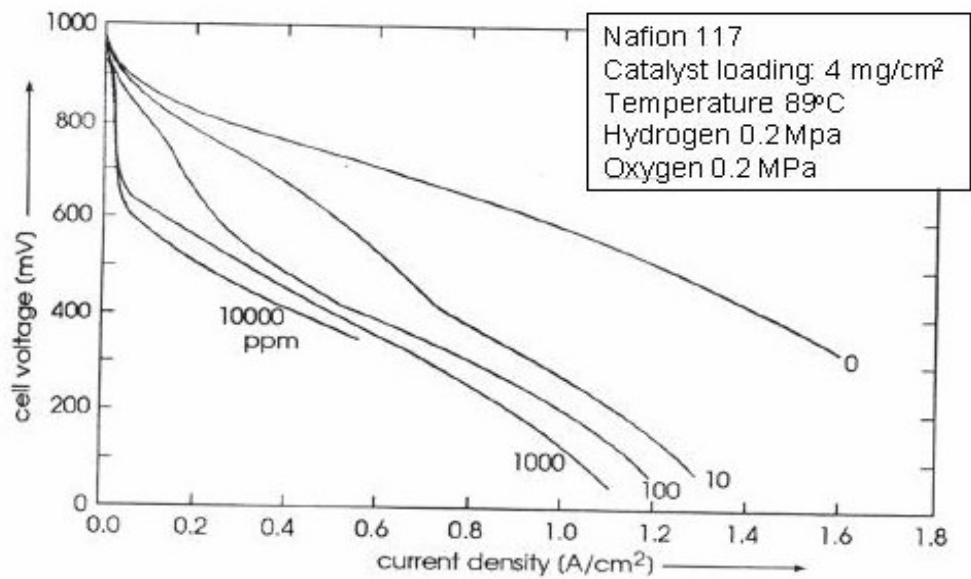
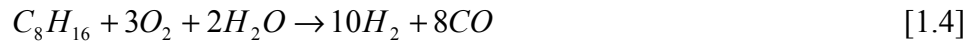


Figure 1-3: Effect of CO Poisoning on Fuel Cell Performance [2]

A PEMFC typically operates at a temperature of around 80 ° C. Each cell produces approximately 0.7 volt. A higher voltage can be generated by combining a number of individual cells in series called fuel cell stack. The potential of the PEMFC drops as a function of current drawn from the cell [2]. Figure 1-2 shows the effect of current density on cell potential and power density. After an initial steep drop in potential, there is an almost linear relation between current density and potential. The main limitation of the PEM fuel cell is that it needs pure hydrogen, as it is highly susceptible to poisoning by carbon monoxide and other impurities. Figure 1-3 represents the effect of carbon monoxide poisoning of on the performance of a PEM fuel cell.

1.5. Fuel Processing System

The objective of fuel processing is to produce pure H₂ from the reforming of the easily available hydrocarbons and fossil fuel, i. e. natural gas, gasoline, diesel, propane, methanol and ethanol. A conventional fuel processing system primarily consists of two stages namely reforming and carbon monoxide clean up [3-6]. In reformer, fuels are converted into a hydrogen rich stream, called reformat. Reformat, is a mixture of N₂ (40–50 %), H₂ (35–45 %), CO₂ (10–20 %), carbon monoxide, water vapor and traces of other gases. In order to lower the carbon monoxide content, multiple stages of carbon monoxide clean up are required. A conventional fuel processing system is shown in Figure 1-4. It consists of an autothermal reforming reactor, high temperature and low temperature converter water gas shift reactors (HTS & LTS) and a preferential oxidation reactor. In the autothermal reformer, fuel is converted to a hydrogen rich stream by autothermal reforming in presence of air and water vapors, at temperature 600-900 ° C.



The reformat is now fed to high temperature and low temperature converter water gas shift reactors (HTS & LTS) to convert the carbon monoxide content present in the reformat to CO₂. The temperature for water gas shift is 180 °C, and 450 °C in low and high temperature water gas shift reactors respectively.



The hydrogen rich stream exiting from LTS is then fed to the preferential oxidation reactor, where the concentration of carbon monoxide is brought down to ppm levels. Typically operating temperature range of this reactor is 100 -180 °C.



The conventional fuel processing has several limitations such as, total volume requirements of the CO clean up stages are more than one order of magnitude larger than that of reformer and fuel cell stack combined and poor selectivity of the PrOx reactor for oxidizing CO over H₂. The typical selectivity of a PrOx reactor towards CO oxidation is less than 1: 10 (i. e. for every mole of CO oxidized 10 moles of H₂ is also oxidized). In addition, it is reportedly problematic during transient operation because CO oxidation reaction is highly exothermic and has limited operating temperature. Hence there is

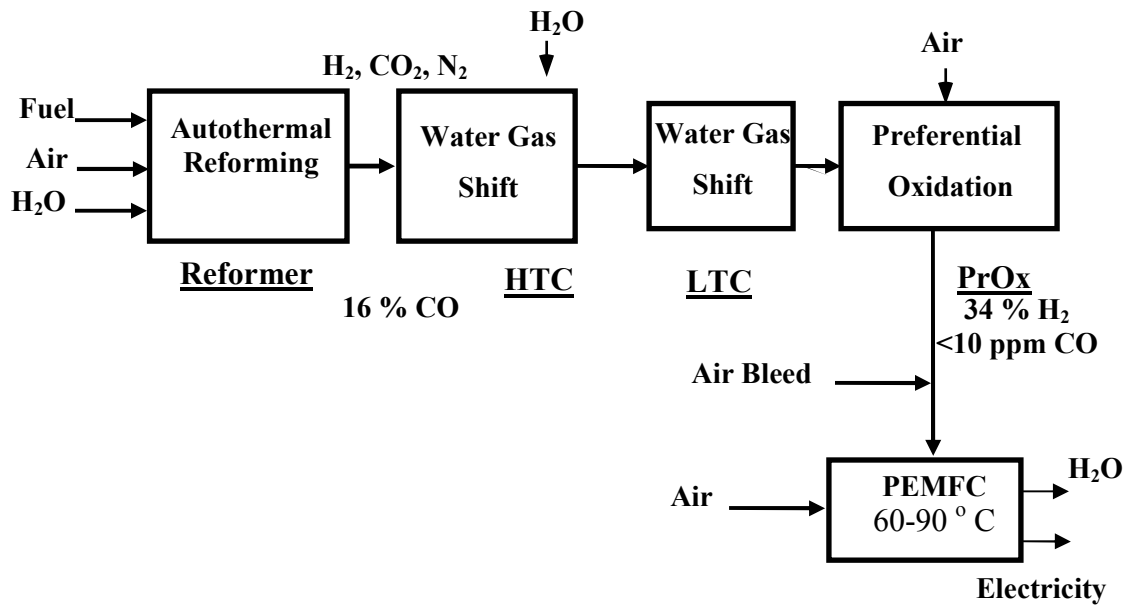


Figure 1-4: Schematic Diagram of Conventional Fuel Processing System [3]

urgent and growing need to develop new methods and technologies for the removal of carbon monoxide, effectively and efficiently from the reformat gas.

1.6. Scope and Objectives

The present work was undertaken with the aim of exploring the possibility of using Ni/Raney-Ni catalyst for electrochemical removal of carbon monoxide from hydrogen. The point that was focused while working with the new methodology was to come up with cheaper and more efficient carbon monoxide removal method. Currently available methods involve application of precious metal catalysts (such as Pt), which are costly, and affects the economy of the carbon monoxide removal. The objectives of this study can be classified broadly in two categories. First part mainly deals with the study of carbon monoxide adsorption and electrooxidation at a planer nickel electrode while second part focuses on the study of carbon monoxide removal by using Raney-nickel catalyst. Effect of parameters such as carbon monoxide concentration, carbon monoxide exposure time and carbon monoxide flow rate have been investigated in order to assess the suitability of the nickel based electrochemical filter that can be used in conventional fuel processing system.

The objectives of the current work can be briefly stated as follows;

1. To investigate the suitability of using Ni/Raney-Ni catalyst in electrochemical filter for CO removal from reformat gas (H₂).
2. To study the effect of CO exposure time, CO concentration, CO flow rate and scan rate on CO electrooxidation performance of the Ni/Raney-Ni.

2. LITERATURE REVIEW

The available literature was comprehensively reviewed with zeroed in on CO removal approaches and kinetics of carbon monoxide adsorption and oxidation on Ni/Raney-Ni catalyst. Literature review has been categorized in two sections, with the first section emphasizes on the new and conventional carbon monoxide removal approaches, while the second section deals with fundamental studies on the kinetics and mechanism of carbon monoxide adsorption and oxidation or removal over Ni/Raney-Ni catalyst.

There is a general agreement among fuel cell researchers that the best possible solution is the development of a new carbon monoxide removal method that should be free from the shortcoming of the current carbon monoxide removal methods [7-9]. Other researchers have advocated development of new electrocatalyst and high temperature operation as possible solution of carbon monoxide poisoning of fuel cells [10-17]. This section

focuses on recent advancement and breakthrough in the conventional carbon monoxide removal approaches i. e preferential and selective carbon monoxide oxidation as well as new carbon monoxide removal approaches such as methanation, membrane purification, integrated water gas shift membrane reactor (WGS), adsorption, sorption process and electrochemical filter.

2.1. CO Removal Approaches

During last decades extensive efforts have been made to develop an effective and viable method for carbon monoxide removal that can reduce even traces of CO present in the reformat gas with good efficiency and economy. In order to develop efficient monoxide removal processes, there is need to understand the kinetics of carbon monoxide adsorption and electrooxidation at Pt-Ru anode electrocatalyst. Leading researchers have tried to gain insight of mechanism and kinetics details of carbon monoxide adsorption and oxidation at the anode electrocatalyst and a number of other metal catalysts [18-21].

The conventional approaches of carbon monoxide removal are low temperature and high temperature water gas shift process (LTS & HTS) and preferential or selective carbon monoxide oxidation with air bleeding. However, new carbon monoxide removal approaches such as methanation, membrane purification (Palladium and Knudsen diffusion membrane), integrated WGS membrane reactor, sorption process, plasma induced preferential oxidation, adsorption, and electrochemical filter and some other processes are at various stages of development. Figure 2-1 shows the ways these new CO removal approaches can be incorporated in conventional fuel processing system.

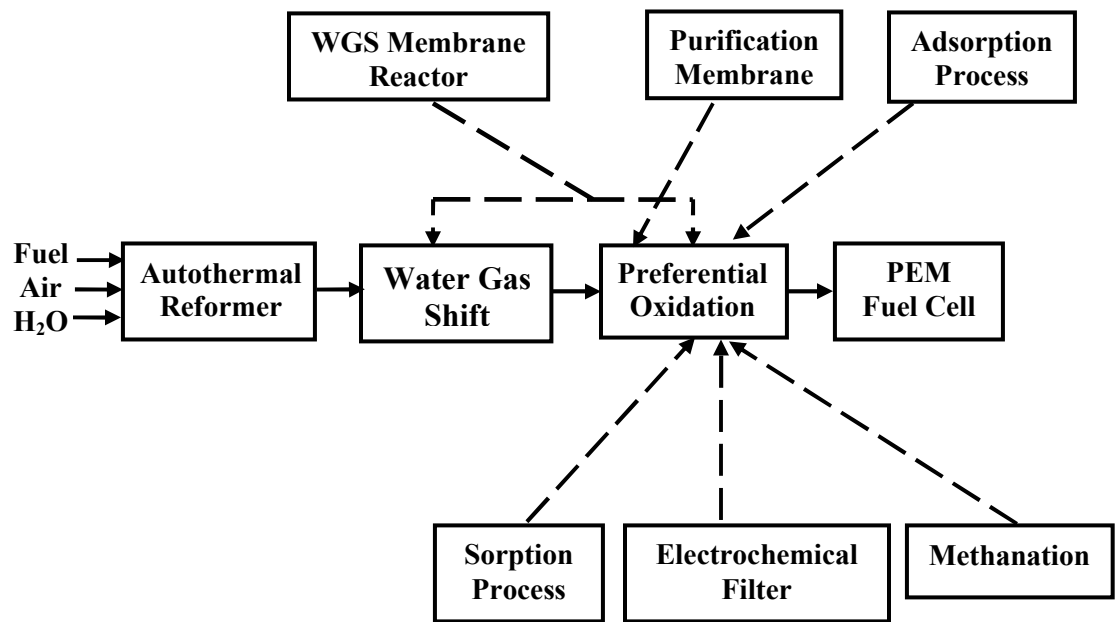


Figure 2-1: Schematic Diagram of New Carbon Monoxide Removal Approaches [3]

Some of the important carbon monoxide removal approaches are discussed in the following sections;

2.1.1. Low and High Temperature Water Gas Shift Process

Conventionally, low temperature water gas shift and high water gas shift process is used for CO removal from the reformat gas containing primarily H₂, CO₂, water vapors and CO. Majority of the CO content is converted to CO₂ in these reactors. The reformat gas exiting from the low temperature WGS reactor can have a CO concentration in the range of 1 % or even less than that. The water gas shift process is given by equation [2.1];



Usually, Cu/Zn/Al₂O₃ based catalyst is employed to speed up the water gas shift process. The main limitations of the conventional water gas shift process with Cu/Zn/Al₂O₃ catalyst or other commercial catalyst are relatively larger reactor volume and equilibrium controlled carbon monoxide conversion. In addition, both low temperature and high temperature water gas shift process catalysts are pyrophoric, they spontaneously generates heat to dangerously high temperature, when exposed to air after activation.

Therefore advanced water gas shift catalysts for both low temperature and high temperature water gas shift processes are need of the hour for effective removal of carbon monoxide from reformat. Considerable attention has been paved to the development of advanced catalyst with superior performance than currently used catalyst. However

developments of an effective commercial water gas shift catalyst either for low temperature and high temperature water gas shift operation remains elusive.

The search for non-pyrophoric alternative to commercial catalyst led to the synthesis of base metal catalyst called, ‘Selectra Shift’ by Ruettinger et al. [22]. Most significant advantage associated with the ‘Selectra Shift’ catalyst is that, it is non-pyrophoric and has activity comparable to that of the commercial catalyst. High stability up to 350 ° C, wider range of operating temperature, safety during accidental exposure and in-situ and ex-situ regenerability makes, ‘Selectra Shift’ as a potential choice for water gas shift catalyst.

It was found by Jacobs et al. [23] that ceria based catalyst loaded with promoter metals, such as Pt, Rh, Pd and Au has much improved performance than commercial catalyst. Pt/ceria, Cu_x/ceria and Au/ceria catalysts were developed by Bunluesin et al. [24] and Li et al. [25] respectively. These catalysts are very attractive and promising alternative to the commercial used water gas shift catalyst (Cu/Zn/Al₂O₃) primarily due to high activity and good stability.

2.1.2. Preferential Oxidation

carbon monoxide content of the reformat gas exiting from the water gas shift reactor is reduced to fuel cell acceptable levels (<5 ppm) by preferential oxidation. The preferential oxidation is given by equation [2.2];



The main disadvantage of preferential oxidation is its poor selectivity for oxidizing carbon monoxide over hydrogen, which is typically less than 1:10. In addition, it is reportedly problematic during transient operation because the oxidation reaction is highly exothermic and has very limited operating temperature. A number of new catalyst systems have been investigated but only few catalysts have shown promising features. Hence, so far search for an efficient PrOx catalyst is marginally achieved.

Sedmak et al. [26] reported that Au, Pt, Ru, Rh and Cu based catalysts have improved performance and could be used for preferential oxidation reactions.

Luengnaruemitchai et al. [27] investigated the potential and suitability of gold-based catalyst for preferential oxidation of carbon monoxide in a typical PrOx reactor and found that gold based catalyst has superior performance in temperature range of 323 - 463 ° K.

Avgouropoulos et al. [28] proposed CuO-CeO₂ catalyst, as a candidate catalytic system for carbon monoxide removal from reformed gas. The catalyst showed much better performance than typical PrOx catalyst.

Menacherry et al. [29] developed a new method for the selective oxidation of carbon monoxide in a gas stream comprising carbon monoxide, hydrogen and oxygen in an adiabatically operated fixed-bed catalytic reactor. It involves control of inlet temperature based upon the space velocity of the gas stream through the reactor.

Meltser et al. [30] developed a method to determining the minimum amount of air to be supplied to preferential reactor. It involves the controlling air supply to by monitoring the concentration of H_2 entering and exiting to the reactor, the difference is correlated to the amount of air needed, and based on that the air supply to reactor is adjusted.

Vanderborgh et al. [31] developed a new approach for selectively oxidizing CO in H_2 rich feed stream. It comprises mixing a feed stream consisting essentially of H_2 , CO_2 , water and carbon monoxide with a first predetermined quantity of oxygen (air). The mixed feed/oxygen stream is then sent to reaction chambers having an oxidation catalyst contained therein. The carbon monoxide content of the feed stream preferentially absorbs on the catalyst and reacts with the oxygen in the chambers with minimal simultaneous reaction of the hydrogen to form an intermediate hydrogen rich process stream having lower carbon monoxide content than the feed stream. Three or more continuous stages are required to bring down the concentration of carbon monoxide up to 5 ppm.

Soma et al. [32] developed a new method for removing carbon monoxide from reformed gas. The method consist of two steps, first treating the reformed gas by a H_2 purifier and then converting carbon monoxide of the reformate stream into another gas (CO_2) thus simultaneously high-purity H_2 is obtained which leads to higher fuel efficiency.

Buswell et al. [33] developed a two-stage reactor for selective oxidation of CO from H_2 gas. Their apparatus consists of two reaction chambers, a primary and a secondary chamber, which deliver pure H_2 gas having a CO concentration of less than about 5 ppm.

Dudfield et al. [34] developed a precious metal based catalytic CO oxidation reactor. Based upon the measured catalyst activity and CO oxidation, they developed a simplified simulation model. They found that it can reduce CO from 1 % to less than 15 ppm. They found good agreement between the experimental data and simulation results.

Nagamiya et al. [35] developed a new carbon monoxide removal method from reformat gas. The method involves supplying oxygen to reformat gas to oxidize carbon monoxide. A controller is used for precise controlling of the amount of oxygen to be supplied to oxidize carbon monoxide. The amount of oxygen for oxidizing carbon monoxide is adjusted appropriately so that a pure reformat gas can be obtained.

Park et al. [36] studied selective oxidation of carbon monoxide in hydrogen rich steam over Cu-Ce/ γ -Al₂O₃ catalyst promoted with transition metals. They found that a maximum carbon monoxide conversion of ~ 80 % is attainable at 150 ° C and up to 99 % conversion at 150 - 220 ° C. By carbon monoxide-TDP test, they found that at temperature lower than 200 ° C, carbon monoxide adsorption strength of on the catalyst surface is high enough to increase the concentration of carbon monoxide, resulting in the selective carbon monoxide oxidation.

2.1.3. Plasma Reforming

Many researchers have advocated the application of plasma reforming as an alternative to autothermal reforming of hydrocarbons in conventional fuel processing system, as it significantly reduces the amount of carbon monoxide formation [37-43]. In plasma

reforming a high voltage electrical discharge is applied to produce gas phase free radicals, which produces synthesis gas without use of any catalyst. Catalyst elimination is one of the important features of the plasma reforming.

There are two types of the plasma, hot and cold plasma, and either of two can be used for the production of synthesis gas. The temperature of hot plasma can be in the range of 3000-10000 ° K while that of the cold may be 1000-2000 ° K. Plasma reactors can be operated on air and/or steam as reactant. Other advantage of this approach is that it reaches to equilibrium at 500-800 ° C, which is considerably lower than the reforming reactor. Higher consumption of the electrical energy is a limiting factor for this approach.

2.1.4. Methanation

Significant studies have been carried out to access the potential of methanation for carbon monoxide removal, by Dudfield et al. [44], Led Jeff et el. [45] and Murthy et al. [46]. Methanation is a process of formation of methane from carbon monoxide and H₂. The reaction is catalyzed by a supported N catalyst. The advantage of using methanation is that reactants are fully mixed and complete removal of carbon monoxide from reformat gas is possible. The methanation process is given by the following reaction [2.3];



Other feature of this approach is its good transient response and elimination of air feed control. One of the limitations of this approach is its exothermicity, hence accurate

temperature control must be employed to prevent unintentional methanation of carbon monoxide. Other limitations of this approach are that it causes thermal integration mismatch and a loss of 300 % more loss of H₂ than the conventional PrOx approach.

Takenaka et al. [47] have developed two advanced Ni and Ru based metal catalysts (Ni/ZrO₂ and Ru/TiO₂) for the methanation process that significantly improves the performance of this process. They found that these catalysts can decrease a concentration of carbon monoxide from 0.5 % to less than 20 ppm. In addition, they found that catalytic activities of these supported metal catalyst strongly depends upon the type of the support. Among the various investigated support they concluded that ZrO₂, TiO₂ are optimum supports for Ni and Ru. Another significant advantage of these catalysts is that these catalysts are highly effective in the presence of 25 volume % of carbon dioxide.

2.1.5. Adsorption

The concept of application of carbon monoxide adsorption on a suitable metal salt is one of the relatively newer carbon monoxide removal approaches. The advantage of the adsorption method is that in addition to carbon monoxide removal, final traces of impurities such as ammonia and carbon dioxide can also be removed. Copper and Ni-platinum salts have received great attention due to their strong ability to remove traces of carbon monoxide from the synthesis gas [48-49]. The advantage of using these adsorbent are that it achieves total carbon monoxide removal and has very good transient response. Major limitations of adsorption approach include non-availability of commercial adsorbent, difficulty in regeneration and limited capacity per cycle time.

Tamon et al. [50] investigated the adsorption characteristics of the carbon monoxide on the active carbon impregnated with several metal halides. Among the several metal halide studied, they found that only carbon impregnated with CuCl, CuBr, CuI and PdCl₂ yield high adsorption capacity. Especially they found that the amount of carbon monoxide adsorbed on PdCl₂/CuCl₂ impregnated carbon has around eight to twenty times capacity to that of the unimpregnated carbon.

Iyuke and Daud [51] studies carbon monoxide removal or reformat purification with Sn based catalyst in pressure swing adsorption (PSA). They investigated the effect of the support on the selectivity of the Sn catalyst towards carbon monoxide adsorption. They investigated pure carbon and impregnated carbon as possible support for Sn catalyst and found that adsorption of carbon monoxide was relatively higher with impregnated carbon. From the experimental findings they proposed that Sn catalyst based on impregnated carbon is more effective to than pure carbon based adsorption application (PSA system).

Rehg et al. [52] developed a new method of CO removal from fuel cell reformat gas. The new method, electro-catalytic oxidations uses adsorption for the removal of CO. The reformer comprises of a cell containing electrode catalytic material that preferentially adsorbs and react with CO. The principle of the operation is that CO gets adsorbed on the electrode surface an oxidizing agent reacts with the adsorbed CO converting it to CO₂.

Yasumoto et al. [53] developed a series of new catalyst materials that are capable of effectively removing carbon monoxide from H₂ gas. The salient feature of the process is

that same catalyst can also be used in proton exchange membrane (PEM) fuel cell anode. The newly developed catalyst comprises of zeolite carrying at least one metal from the group consisting of Pt, Pd, Ru, Au, Rh & Ir, or an alloy of two or more metals.

2.1.6. Membrane Purification

One of the novel method of carbon monoxide removal from reformat is membrane purification by the application of either hydrogen selective or carbon monoxide selective membranes. Hydrogen purification membrane will only allow hydrogen gas to permeate through it, while blocking passage of carbon monoxide and other impurities, resulting in pure hydrogen gas (>99.999 %). Similarly a carbon monoxide selective membrane only permits carbon monoxide gas to flow through it while preventing flow of hydrogen, resulting in pure hydrogen. The purity of the H₂ obtained from the membrane purification method can be much higher than any of the alternative method.

Membrane purification method was proposed by Yasuda et al. [54] and Saracco et al. [55]. Palladium alloy membranes and Knudson diffusion membranes have particularly received great attention because of there ability to remove other hydrocarbon reformat gas contaminants H₂S, CO₂ and NH₃ in addition to the effective carbon monoxide removal. The important advantage of using the H₂ purification membrane over that of the conventional carbon monoxide removal approaches is that it eliminates the further need of CO clean up, as complete carbon monoxide removal is possible. The disadvantage of using the purification membranes are that H₂ loss is quite high (10-20 %). In addition, it also requires additional air compressor, which affects the economy of the process. In spite

of the above limitations the membrane purification process is still a viable alternative for carbon monoxide removal over the conventional carbon monoxide removal methods.

2.1.7. Integrated WGS Membrane Reactor

Integrated WGS membrane reactor is conventional WGS reactor with the incorporation of selective membranes. Instead of using two different reactors, a water gas shift reactor and a preferential oxidation reactor, integrated membrane water gas shift reactor (WGS membrane reactor) can be used for the same duty as proposed by Uema et al. [56], Paglieri et al. [57] and Winston et al. [58]. Hydrogen enrichment membranes and/or CO₂ selective membrane can be incorporated with the conventional water gas shift reactor to make either hydrogen selective integrated WGS reactor or CO₂ selective integrated WGS reactor. Since membranes remove either product of water gas shift reaction (H₂ or CO₂), it is anticipated that integrated WGS membrane reactors can possibly overcome the restraint of equilibrium. Palladium alloy and Knudson diffusion membranes are typical H₂ enrichment and CO₂ selective membranes, which can be used in any conventional water gas shift reactor to give integrated WGS membrane reactor. The reaction in an integrated WGS membrane reactor will be the typical reaction occurring in water gas shift reactor, as given below;



The selective membrane will remove either products of the water gas shift process resulting in much better carbon monoxide removal or H₂ purification. Advantages of this

approach are that it can overcome the restraint of equilibrium, smaller reactor volume, optimum utilization of hydrogen up to 96 %, Nernstian voltage of 30 mV and almost pure hydrogen. The product stream exiting from the reactor contains almost pure hydrogen due to almost complete removal of all contaminants such as CO, NH₃, CO₂ and H₂O.

Utaka et al. [59] investigated supported copper catalyst for carbon monoxide removal in an oxygen supported water gas shift reactor. By the addition of O₂ in the gas mixture, they observed enhanced effectiveness of water gas shift reaction as well of CO oxidation reaction. They found that mixed oxide catalyst of Cu/Al₂O₃-ZnO exhibited excellent activity for removal of a small of CO reformat with O₂ assisted water gas shift reaction.

Wilkinson et al. [60] developed a new method for removal of carbon monoxide from the reformat gas. The method is based on the oxidation of the CO present in reformat stream by the reverse water-shift reaction to CO₂. They found that the exit stream from such process has carbon monoxide concentration <5 ppm which is ideal for a PEMFC.

Hashimoto et al. [61] developed a new Pt-Re supported catalyst for water gas shift (WGS) reactor as an alternate to the currently used Cu-Zn catalyst. They found that Pt-Re based catalyst has good oxidation resistance and superior catalytic reactivity.

Keulen et al. [62] developed a process for the purification of H₂ gas. The process consisting of one or more catalyzed reactions for the selective removal of CO from the gas stream wherein a controlled amount of H₂O is introduced into the gas stream prior to

some of the catalyzed reactions so as to lower the temperature of the gas stream to a predetermined value at which preferential removal of CO takes place in the associated catalyzed reaction. The catalyzed reactions may be selective oxidation, selective methanation or combination of both. This process may be operated in combination with a water gas shift reaction for the reduction of CO in the H₂-containing gas stream.

Edlund et al. [63] & Aranda et al. [64] developed novel hydrogen purification membranes that can be used in integrated water gas shift reactor for hydrogen purification. The new purification membranes are a composite of metal based palladium membrane with trace amounts of carbon, silicon, and/or oxygen. Using a reformat gas stream containing predominantly hydrogen, they found excellent selectivity for carbon monoxide removal from these composite membrane based integrated water gas shift reactor.

2.1.8. Sorption Process

Sorption is a process of reversible complex formation by carbon monoxide with metal catalysts. Lee et al. [65] developed the sorption process, which was based on the reversible complex forming and dissociation reactions of CO with Cu (I). The advantage of sorption process is that CO can be easily captured and released from CuCl-dispersed sorbents. The sorption process can successfully remove CO from a reformat gas stream containing 1 % CO to a level of 50 ppm or even lower than that. The advantages of the sorption process includes the sorbents flexibility to operate at a wide range of temperature from room temperature to 250 ° C, fast CO sorption, easy regenerability, and ability to operate over wide concentration ranges. Above mentioned advantages makes it

capable of instantaneous cold start and dynamic carbon monoxide removal prompted the sorption process as one of the best carbon monoxide removal process for PEM fuel cell.

Cordaro et al. [66] showed that sorption process could reduce carbon monoxide from 1% to than 100 ppm. They established that amount of the carbon monoxide sorption increases with temperature and inlet concentrations. Also they found that copper based sorbents possesses the instantaneous cold start capability at room temperature and can reduce carbon monoxide from 1 % to much lower carbon monoxide concentrations.

2.1.9. Electrochemical Filter

The concept of the electrochemical filter was proposed by Laxmanan et al. [67-69]. It is an electrochemical device that preferentially oxidizes carbon monoxide over hydrogen present in reformat by using current proton exchange membrane fuel cell technology. It operates under pulse potential mode to achieve high selectivity for carbon monoxide adsorption and oxidation over hydrogen oxidation. The overall reaction of the electrochemical filter is given by equation [2.5];



The preliminary result about the electrochemical filter shows that by varying the pulse-potential profile (*e.g.*, on time, off time, and pulse potential) the carbon monoxide and H₂ oxidation currents can be varied independently. They found that adsorption carbon monoxide was promoted during the off portion of the pulse (*i.e.*, open circuit), while

during on-portion of the pulse potential, oxidation of the adsorbed carbon monoxide was preferred as the catalyst surface is covered with carbon monoxide. The filter is still at its incipient stage of development and very little information is available about its performance. One of the prominent limitations of the filter is that it uses Pt-Ru as electrocatalyst for carbon monoxide adsorption and subsequent oxidation.

From the available literature, it could be concluded that Pt-Ru bifunctional catalyst were prepared in view that Ru imparts carbon monoxide tolerance to pure Pt catalyst. Hence Pt-Ru may not be the best choice for electrochemical filter as it will prevent CO adsorption on the anode electrocatalyst, which in turn reduces the carbon monoxide removal potential of the filter. Obviously pure Pt is a better choice for the electrochemical filter, but it is a highly expensive. In addition, world have only limited supply of platinum. Approximately 86 % of world's platinum reserves are in South Africa [70-71]. Hence a less costly catalyst needs to find that could be used in the electrochemical filter.

2.2. Study of CO Adsorption and Oxidation on Ni Catalyst

The study of adsorption and oxidation of carbon monoxide on nickel catalyst is one of the prerequisites for the development of efficient nickel based carbon monoxide removal method. So far only little attention has been given to Ni as a catalyst for carbon monoxide removal by researcher. Therefore the studies concerning on Ni/Raney-Ni catalyst are relatively small and rare. Previous studies on Ni were mainly focused on electrochemical reduction of carbon monoxide to hydrocarbon as a method to remove carbon monoxide, which forms as an intermediate product during the electroreduction of CO₂. However

studies specifically related to the electrochemical oxidation of CO on Ni catalyst is non-existent. In the following section some of the important studies that deal with the electrochemical reduction or CO adsorption on Raney-Ni catalyst have been presented.

Hori et al. [72-73] were one of the first researchers to study the electrochemical reduction of carbon monoxide to hydrocarbons at various metal electrodes such as Ag, Au, Pb, Zn, Cd, In, Cu, Fe and Ni. Based on the cyclic voltammetric and coulometric measurements in aqueous media, they found that only considerable extent of hydrocarbons was formed on Ni. This predominant behavior of Ni catalyst towards carbon monoxide reduction was attributed to the predominant H₂ evolution at room temperature.

Azuma et al. [74] have studied the carbon monoxide reduction at low temperature on various metal electrodes namely, Ti, V, Mn, Co, Zr, Nb and Ni. They found that at lower temperature (2 ° C), CO reduction efficiency at Ni electrode increases to many fold from that of the room temperature efficiency. In addition, they also observed that the amount of carbon monoxide reduction increases linearly with charge passed .

Hori and Murata [75] investigated the electrochemical reduction of CO on various metal electrodes by using voltametric and coulometric measurement approaches in aqueous electrolytes. They found that, adsorption of CO on Ni electrode is of such nature that CO is not desorbed even when dissolved CO is purged by continuous sparging of Ar gas in the saturated electrolyte solution. In addition, they also observed that, the phenomena of dissolution or passivation of the Ni electrode is markedly suppressed by the adsorbed CO.

Wang, et al. [76] studied the electrochemical characteristics of CO adsorbed on a Ni (111) surface. They found that the adsorbed CO layer remains intact up to the moment of contact with the electrolyte and can be subsequently electro-oxidized to yield CO₂.

Koga and Hori [78] studied the affect of adsorbed CO on Ni electrode in connection with the electrochemical reduction of CO₂. They observed that during the electroreduction, CO is formed and strongly adsorbed on the surface. The adsorbed CO prevents the H₂ evolution on electrode as most of the surface sites were covered by CO. They were able to reduce it at a negative potential of -0.1 V vs. SCE (saturated calomel electrode). They proposed a new correlation to estimate the coverage of the adsorbed CO and the reduction of the CO from the extent of prevention of H₂ evolution and the time course of the cathodic current in constant potential measurement. They found good agreement between the values of the CO reduction rate predicted from this model with that of the coulometric measurements reported in literature.

Cuesta et al. [79] used cyclic voltammetry and potential modulated reflectance (PMR) spectroscopy to study the electroadsorption of the carbon monoxide at the Ni electrode, and reported the chemisorption of carbon monoxide on the electrode surface.

From the above literature review, it is clear that reduction of carbon monoxide has attracted considerable attraction from researcher but no attention has been yet directed towards oxidation of CO. The aim of the current work was to study the oxidation of CO on Ni/Raney-Ni catalyst to demonstrate that Pt could be replaced by a cheaper catalyst.

3. EXPERIMENTAL SETUP

3.1. Materials Used

3.1.1. Planer Ni Electrode

A planer cylindrical electrode of Ni (more than 99.99 % pure) was procured from Bayouni Trading Co. Al-Khobar, Saudi Arabia (Subsidiary of Sigma-Aldrich, USA). The geometrical dimension and other details of the working electrode are given in Figure 3-1. The active area of the electrode was 0.3 cm^2 .

3.1.2. Raney-Ni Catalyst

Raney-Ni-Al catalyst material was procured from Merck-Schuchardt, 8011 Hihenbrunn Bi Munich, Germany (Art. No: 820875). The catalyst was supplied in active state with 50 % water. Some of the properties of this catalyst have been listed in Table 3-1.

Parameters	Ranges
Ni content	88 %
Al content	12 %
Mol. Weight	58.71
Storage Medium	50 % Water

Table 3-1: Properties of Raney-Ni Catalyst

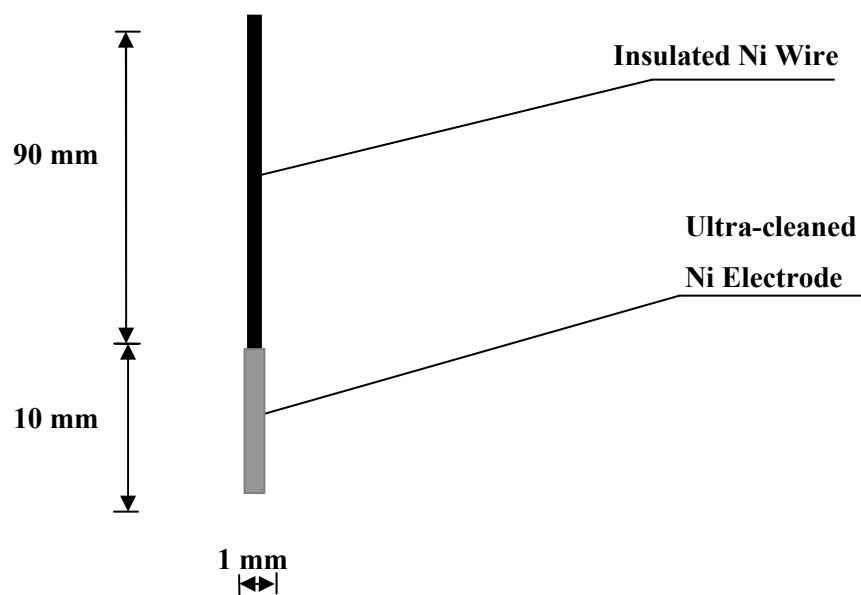


Figure 3-1: Geometric Dimensions of Planer Ni Electrode

3.1.3. Carbon Monoxide Gas

High purity carbon monoxide gases were procured from Abdullah Hashim Gas Company, Saudi Arabia. The supplied gases were 99.9999 % pure. For this study, hydrogen gas containing 10 ppm, 100 ppm, 1000 ppm, 10000 ppm and 100000 ppm carbon monoxide in hydrogen and pure carbon monoxide gases were purchased.

3.1.4. Hydrogen Gas

High purity research grade H₂ gas was obtained from Abdullah Hashim Gas Company, Saudi Arabia. The supplied gas was 99.999999 % pure.

3.1.5. Platinum Disc

A platinum disc was used as current collector. In the working electrode, it was placed between the Raney-Ni working catalyst bed and fritted glass bottom of the tube. A platinum wire of 0.05 mm diameter was glued at the center of the disc. These materials were procured from Bayouni Trading Co. Ltd. Al-Khobar, Saudi Arabia (Subsidiary of Sigma-Aldrich, USA).

3.1.6. Electrolyte Solution

A phosphate buffer solution was used as electrolytic solution. It was prepared by using the buffer salt (Fisher Gram-Pac) procured from Fisher Scientific Company, USA. The salt contains Potassium Phosphate Monobasic/Sodium Phosphate Dibasic. The pH of the buffer solution was 6.86 at room temperature. In order to make one liter of the buffer

solution, 7.0 g of buffer powder was dissolved in distilled water, as per the preparation instructions of the supplier.

3.1.7. H-type Pyrex Glass Cell

A Pyrex H-type cell was fabricated for this study. It has three different chambers for housing working electrode, reference electrode and counter electrode respectively and two gas inlet points. A finely fritted glass separated the reference and working electrode compartments. The cell has also has a lugging capillary between the working electrode and the reference electrode chambers.

3.2. Experimental Details for Planer Ni Electrode

This section deals with the details of the experimental setup used for the carbon monoxide adsorption and electrooxidation on planer nickel electrode in this study.

3.2.1. Experimental Setup

A planer cylindrical electrode (Ni wire of 1mm diameter) functions as working electrode in the electrochemical study. The active area of the electrode was 0.3 cm^2 . An insulating paint was applied on Ni wire so that a desired active surface is exposed. A series of the steps were used to clean the electrode. The electrode surface was carefully cleaned with the emery paper of 1500 grit until mirror finished surface is obtained. Subsequently it was washed with deionized water to remove any impurity present at the surface. The electrode was further washed in acetone to remove any oil or grease present on the

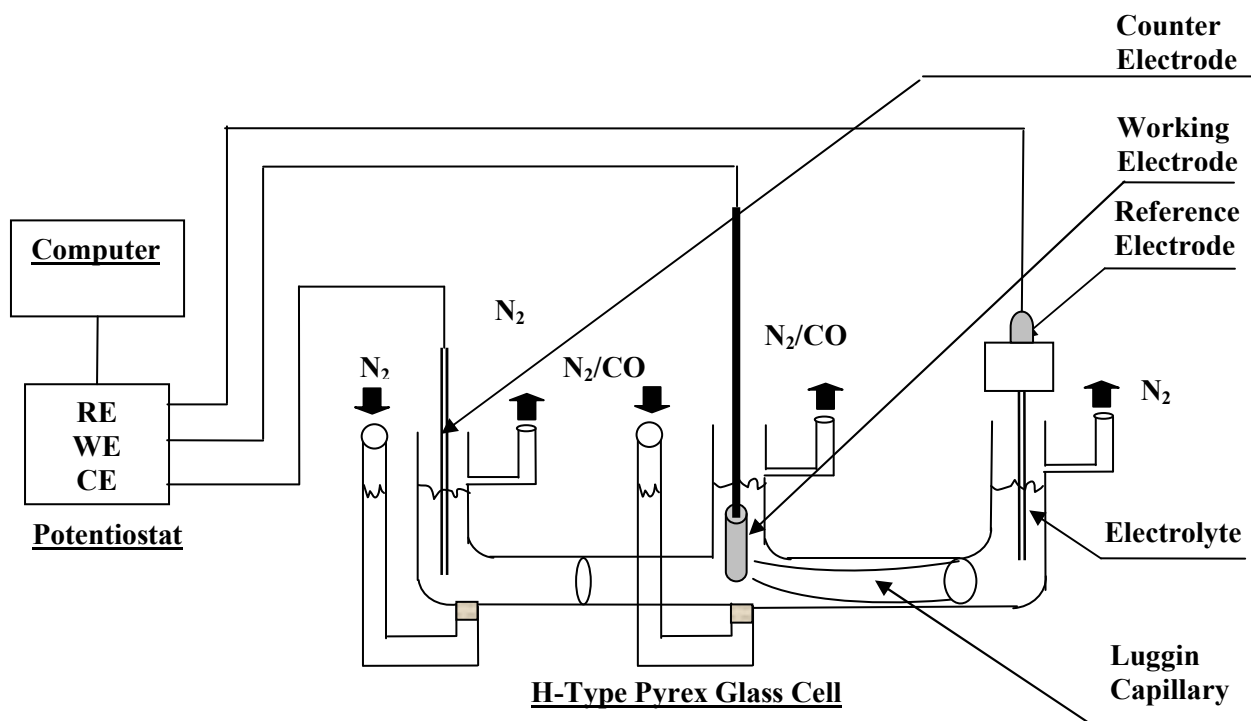


Figure 3-2: Schematic Diagram of the Experimental Setup



Figure 3-3: Photograph of Experimental Measurement

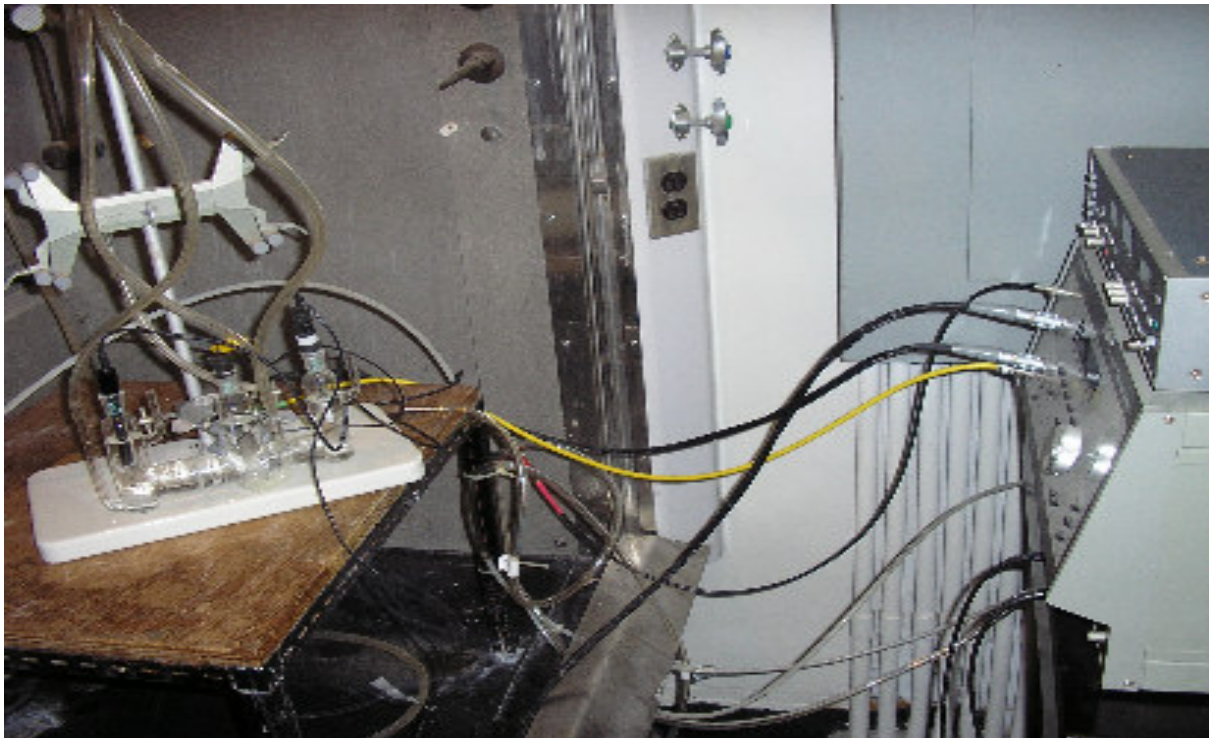


Figure 3-4: Photograph of the Experimental Setup



Figure 3-5: Photograph of the Experimental Setup

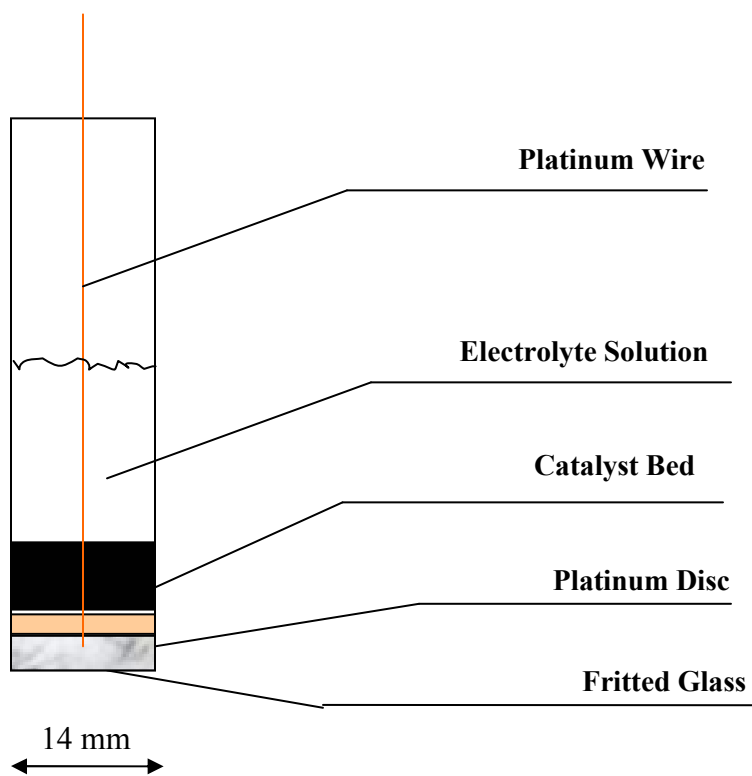


Figure 3-6: Schematic Diagram of Raney-Ni Electrode

surface. At ambient conditions, nickel surface has a stable passive film. It was necessary to remove this film so that nickel surface is available for adsorption and reactions. The process of etching or removal of passive layer from the working electrode surface is called anodization. Anodization was carried out by passing anodic current while the nickel electrode was dipped into 85 % phosphoric acid against large area platinum electrode. Initially a small current was passed through the electrochemical cell for a given period of the time. The value of the current was gradually increased to $30 \mu\text{A cm}^{-2}$ so that hydrogen evolution is avoided. Following is the possible reaction occurring during the anodization of the nickel electrode:



The anodized electrode was again washed carefully by deionized water. The cleaned electrode was then used in the electrochemical study. A phosphate buffer solution of 6.86 ± 0.02 pH was used as electrolytic solution in all the experimentation. Figure 3-2 shows the schematic diagram of the cell while Figure 3-3 to Figure 3-5 shows the photograph of the experimental setup and electrochemical cell. The cell has three chambers for housing working electrode, reference electrode and counter electrode, respectively and two gas inlet points in the working and reference electrode chambers. In addition, the cell is equipped with three gas exit points each at the top of each chamber separately. The gas exit point was provided for purging out dissolved gases from each electrode compartments. The reference and working electrode compartments were separated by a fritted glass. The central chamber was used to house the working electrode, while

reference electrode was placed in the right chamber of the working electrode and the counter electrode was placed in the left chamber of the cell. A lugging capillary was placed between the working electrode and the reference electrodes chambers for minimizing the uncompensated resistance. Electrolyte solution was filled to a reasonable height in all the three electrode chambers. The electrolyte solution in the working electrode chamber and reference electrode chamber can communicate through the fritted glass that separates the two chambers. The inlet for the gases in working and reference electrode chambers was provided at the bottom of the respective chambers. The cell was also equipped with two gas spargers at the working and counter electrode compartments for the uniform distribution of the gases.

Cyclic voltammetry and cathodic scan of the working electrode were carried out in this study. Single and multiple CV were performed. In a cyclic voltammetry experiment, the potentiostat linearly changes the potential of the working electrode with a given scan rate and then reverses the scan, returning to the initial potential. During the potential sweep, the potentiostat measures the current resulting from the applied potential. The values are then used to plot the CV graph of current versus the applied potential, commonly referred as voltammogram.

The electrochemical cell, consisting of working, counter and reference electrodes was connected to a potentiostat which controls the experiments via a microcomputer. The potentiostat used in this study was model 283 from EG & G, Princeton Applied Research, USA. The potentiostat was driven by a manufacturer software package Powersuit. The

electrode potential was measured with respect to a saturated calomel electrode (SCE). All the experiments were carried out at room temperature.

3.2.2. Experimental Procedure

In this section details about the procedure followed during the electrochemical experiments is presented. The electrolyte solution which was phosphate buffer solution of 6.86 pH was firstly decanted in all the three electrode chambers of the H-Type Pyrex cell. Nitrogen gas with a significantly higher flow rate was purged in all the three electrode chambers for at least 30 minutes in order to completely remove the dissolved oxygen or any other oxygen containing species from the electrolyte solution. The cyclic voltammetric experiments were performed while N₂ gas was being passed slowly.

Whenever the voltammogram of the carbon monoxide exposed Ni electrode surface was desired, carbon monoxide gas mixture was passed in the electrolytic solution of the working electrode chamber for a predetermined period and flow rate. Subsequently N₂ gas was purged in this chamber for about 30 minutes to ensure the removal of dissolved carbon monoxide from the electrolytic solution. The cyclic voltammetric experiment was performed under N₂ flow to avoid the dissolution of the ambient O₂ into the electrolyte.

3.3. Experimental Details for Raney Ni Study

In this section the experimental setup and procedure used for the electrochemical study of carbon monoxide adsorption and electrooxidation on Raney-Ni catalyst have been given.

3.3.1. Experimental Setup

Figure 3-6 shows the schematic details, while Figure 3-7 shows the photograph of the Raney-Ni electrode. The electrode consists of a hollow cylindrical Pyrex glass body having fritted glass at the bottom with open top. At the bottom of the tube, a platinum disc is placed for current collection purpose. A platinum wire was attached at the center of the platinum disc for connection to the potentiostat. A known quantity of Raney-Ni catalyst slurry was placed at the platinum disc forming a catalyst bed. The height of the catalyst bed was approximately 2 mm. The lower end of the working electrode was fritted to facilitate the electrochemical communication between working and counter electrodes during the electrochemical measurements. Other geometrical dimensions of the working electrode are presented in Table 3-2. Due to the equipment limitations only little quantity of Raney Ni catalyst was used in the present work. In future studies, both height of the catalyst bed and diameter of glass tube can be increased to many folds to adsorb more carbon monoxide and in turn removal of more carbon monoxide from hydrogen.

The schematic diagram of the experimental set up used for electrochemical study has been illustrated in the Figure 3-8. The photograph of the experimental set up is shown in Figure 3-9. The electrochemical cell consisting of Raney-Ni working electrode, large area platinum counter electrode and saturated calomel electrode was connected to a potentiostat which controls the experiments via a microcomputer. The potentiostat used in this study was procured from EG & G Princeton Applied Research, USA. The potentiostat was driven by a manufacturer software package Powersuit. The electrode potential was measured with respect to a saturated calomel electrode (SCE). The

Parameters	Values
Catalyst	Raney-Ni
Weight of the catalyst (gm)	0.9
Diameter of the platinum wire (mm) (Current collector)	0.5
Diameter of the glass tube (mm)	14
Height of the working electrode (mm)	80
Height of the catalyst bed (mm)	2

Table 3-2: Geometrical Details of Raney-Ni Electrode



Figure 3-7: Photograph of Raney-Ni Electrode

electrode potential was corrected for the uncompensated resistance. The electrolyte solution used was a phosphate buffer solution of 6.86 pH. The experimentation has been carried out at room temperature. The procedures for conducting the electrochemical experiments are given in the next sections.

3.3.2. Experimental Procedure

The electrolyte solution, which is phosphate buffer solution of 6.86 pH, was decanted into the glass cell to the required height. Nitrogen gas was purged in the electrolyte solution for at least 30 minutes in order to completely remove the dissolved oxygen or any other oxygen containing species from the electrolyte solution. The working electrode, reference electrodes and counter electrodes were placed in their respective slots in the electrochemical cell as shown in the Figure 3-8. Nitrogen was passed in the electrolytic solution of the working electrode to remove dissolved oxygen from the electrolyte solutions of the working electrode. The flow of gas was maintained in such a way to keep the catalyst bed in fluidized state. This assures the complete removal of any active species present at the electrode surface. Following this cyclic voltammetry was performed by using Powersuit software.

Subsequently the flow of nitrogen gas at the working electrode was switched to a 1 % carbon monoxide gas mixture. The gas was allowed to flow for 25 minutes to get significant amount of carbon monoxide adsorbed at the working electrode surface. The flow rate of the carbon monoxide gas was maintained higher enough to keep the catalyst bed in pulverized state. This assures the optimum adsorption of carbon monoxide at the

catalyst surface. After ensuring significant adsorption of carbon monoxide at the catalyst surface, flow of carbon monoxide gas was again switched to nitrogen gas. The purpose of the nitrogen gas was to remove carbon monoxide that may have been dissolved in the electrolyte solution. After ensuring complete removal of carbon monoxide from the electrolyte solution flow of the nitrogen gas was stopped and the catalyst bed was allowed to settle down. It has been observed that in 10 minutes the catalyst settles down completely. The CV experiments were performed nitrogen flow to keep the working electrode under nitrogen blanket to avoid any dissolution of ambient oxygen into the electrolyte solution.

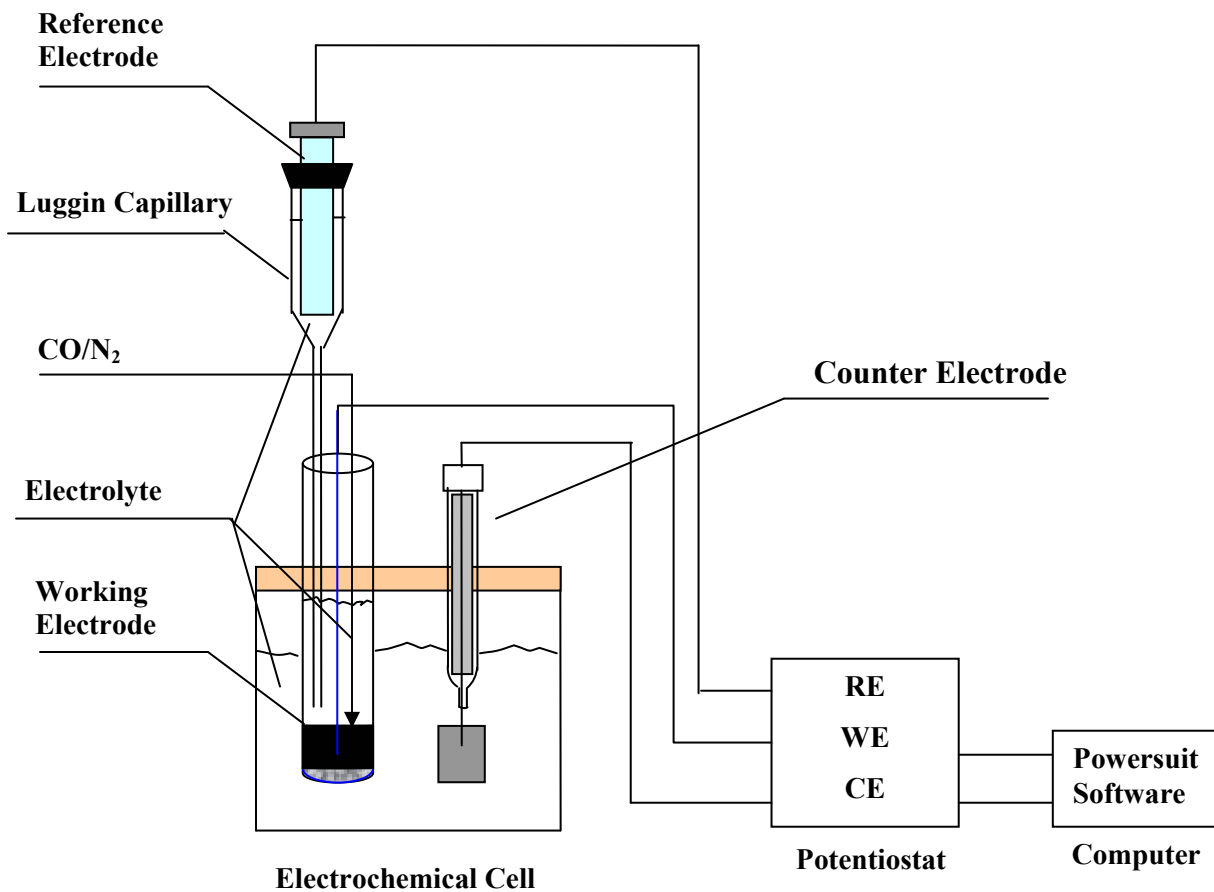


Figure 3-8: Schematic Diagram of Experimental Setup for Raney-Ni Study

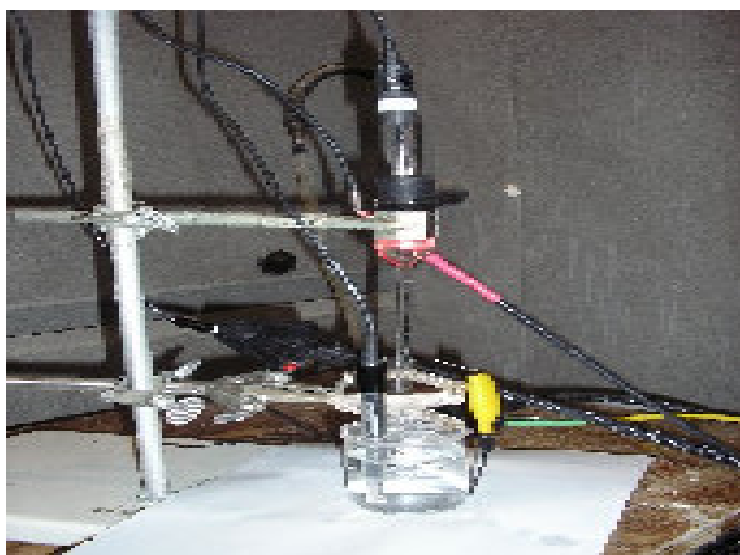


Figure 3-9: Photograph of Experimental Setup for Raney-Ni Study

4. RESULTS & DISCUSSION

The result and discussion have been broadly categorized in two sections. The first section deals with carbon monoxide adsorption and electrooxidation on planer Ni electrode and effect of various parameters such as CO concentration, CO exposure time and CO flow rate on the electrochemical removal on planer Ni electrode. Second part of this chapter focuses on the study of CO adsorption and electrooxidation on Raney-Ni catalyst. Characterization of the Raney-Ni catalyst has also been presented in the second part.

4.1. CO Electrooxidation on Planer Ni Electrode

In the first part of this study, concept of the electrochemical adsorption and electrooxidation of CO on planer Ni electrode surface has been presented. One percent CO gas in H₂ was used for this purpose. This particular concentration of the carbon monoxide gas was selected as it corresponds to the typical CO concentration being used

in the low temperature water gas shift reactor or preferential oxidation reactor. Cyclic voltametric experiments were carried out to establish the adsorption and electrooxidation of CO on the catalyst surface. The electrochemical setup consist of planer cylindrical Ni electrode of 1mm diameter and 10 mm length as working electrode, a saturated calomel electrode as reference electrode and a large area platinum electrode as counter electrode.

Firstly a voltammogram of the clean working electrode with an inert gas (N_2) was obtained in the potential range of -1.4 V (NHE) to 0.4 (NHE). Above range of potential was selected based on the available published information. Then similar voltammogram of carbon monoxide exposed working electrode was obtained. In addition voltammogram of pure hydrogen exposed working electrode was also observed. The discussion of the features and characteristics of these voltammogram has been presented in next sections.

It order to support the cyclic voltammetric results and findings of the carbon monoxide adsorption and electrooxidation on Ni electrode surface, cathodic scan of the planer nickel electrode was also recorded under nitrogen, carbon monoxide and pure hydrogen environment. The analysis of these cathodic scan experiments have been presented along with the discussion of cyclic voltammetric data.

4.1.1. Cyclic Voltammetry of Planer Ni Electrode with N_2

Cyclic voltammogram of the N_2 exposed working electrode (planer Ni electrode) under N_2 environment were obtained by following the procedures given in the experimental sections. The electrochemical set up used for CV has also been already discussed in the

previous sections. The surface area of the planer Ni electrode (working electrode) was 0.3 cm². The parameters that were maintained during the experimentation have been listed in the Table 4-1. The voltammogram was obtained from an initial potential -0.4 V (NHE) to first vertex potential -1.4 V (NHE) and then up to a second vortex potential 0.4 V (NHE) and back to the initial potential (-0.4 V). Figure 4-1 represents the voltammogram of the planer Ni electrode obtained under these conditions.

From the voltammogram, it is clear that at the beginning of the cathodic scan (-0.4 V), current response of the nickel electrode is zero representing absence of any electrochemical activity at the catalyst surface. As the electrode is negatively scanned the current starts rising at -0.7 V potential and keeps on rising with the potential. This cathodic current is essentially due to the occurrence of the hydroegn evolution reaction at the Ni electrode surface. Hori et al. [78] have also recorded the hydroegn evolution process at the Ni electrode under inert environment of Ar. They reported the onset potential for hydrogen evolution process at -0.5 V (NHE) which is significantly different than observed during this experiment. Apparently this variation of the onset potentials can be attributed to the significantly higher surface area used by the Hori et al. The area of the electrode used in this study is 1/12th of the area of electrode used by Hori et al [78].

During the anodic scan, the current response of the electrode is essentially zero due to the absence of any electrochemical activity at the electrode surface. As the electrode is further anodically scanned the current starts increasing slowly and sharp peak is observed

Parameters	Range/Values
Equilibration time (sec)	120
Initial potential (V vs NHE)	-0.4
Vertex potential (V vs NHE)	-1.3
Vertex potential (V vs NHE)	+0.4
Final potential (V vs NHE)	-0.4
Scan rate (mV/sec)	50
Open circuit potential (V vs NHE) (measured)	-0.578
Sample area (cm ²)	0.3
Reference electrode	SCE

Table 4-1: CV Parameters of N₂ Exposed Planer Ni Electrode

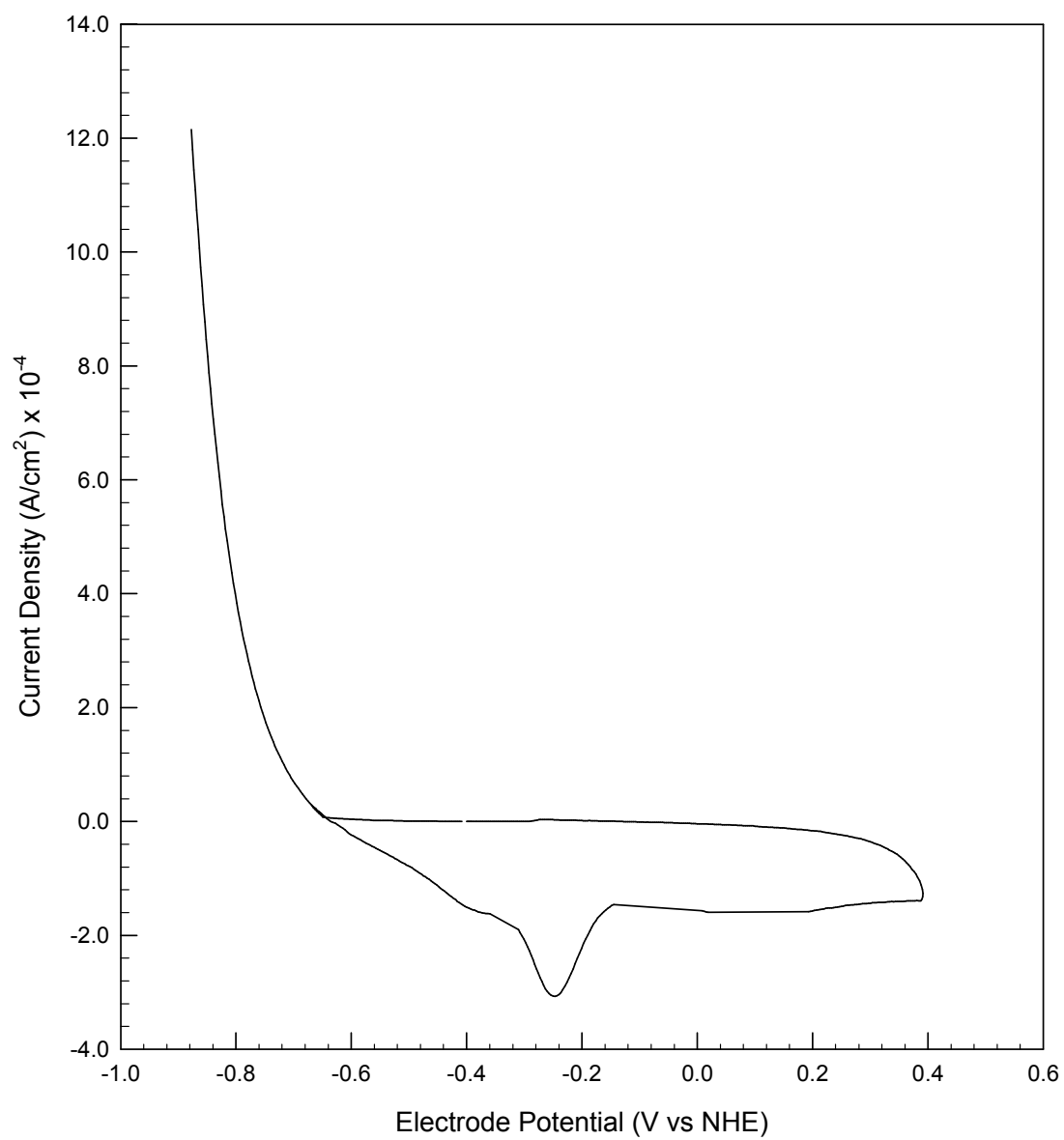


Figure 4-1: Cyclic Voltammogram of N₂ exposed Planer Ni Electrode

at approximately -0.25 V. This anodic peak can be attributed to the anodic oxidation of the Ni as the standard potential for the Ni/Ni⁺⁺ is -0.23 V. Dissolution of the Ni readily leads to the formation of Ni⁺⁺ at the electrode surface, that subsequently form a Ni (OH)₂ film. Hori et al. [78] have also reported occurrence of similar peak at -0.25 V during the cathodic scan of the Ni electrode in their study. They have attributed this peak to the Ni dissolution reaction. Hence the occurrence of the peak at -0.25 V electrode potential essentially corresponds to the dissolution and passivation of the Ni electrode.

From the preceding discussion two important conclusions can be made. First conclusion is the occurrence of the anodic peak at -0.25 V electrode potential during the anodic scanning and second conclusion is the occurrence of the H₂ evolution process at -0.7 V. Nickel oxidation or dissolution is in close agreement with the Ni oxidation results reported by Hori et al. [78].

In order to support the above voltammometric finding about the planer Ni electrode, independent cathodic scan of the electrode was performed. The experimental parameters that were maintained during the cathodic scan experiment have been listed in Table 4-2. The cathodic scan plot of the N₂ exposed planer Ni electrode under N₂ environment is shown in Figure 4-2. The electrode was cathodically scanned from an initial potential of -0.4 V to a final potential value of -1.4 V.

As in the case of N₂ exposed cyclic voltammogram, at the start of the cathodic scan, the current response of the electrode is zero, suggesting no activity at the electrode surface.

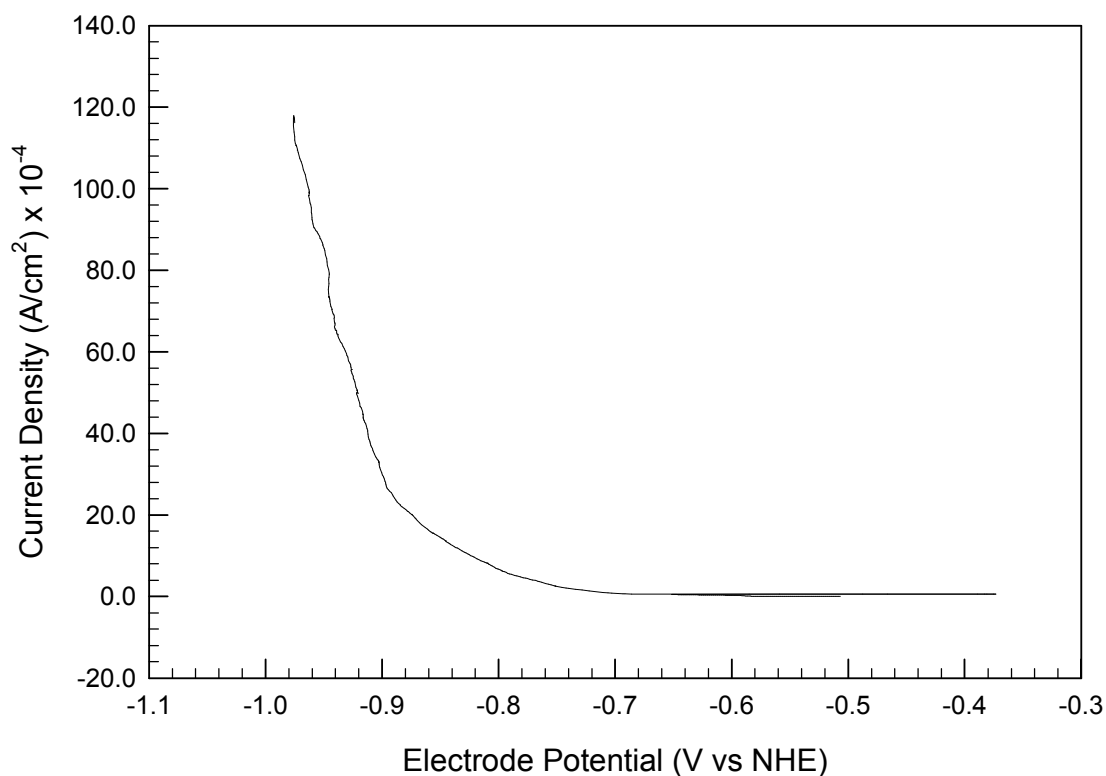


Figure 4-2: Cathodic Scan of N₂ Exposed Planer Ni Electrode

Parameters	Range/Values
Equilibration time (Sec)	120
Initial potential (V vs NHE)	-0.4
Final potential	-1.4
Scan rate (mV/sec)	10
Open Circuit Potential (V vs NHE) (Measured)	-0.533

Table 4-2: Cathodic Scan Parameters of N₂ Exposed Planer Ni Electrode

As the potential is scanned to further negatively at -0.7 V potential the current starts rising representing the onset of the electrochemical process at the electrode surface. The current response of the electrode rises sharply after this onset potential as potential is further negatively scanned up to -1.4 V. This observation supports the above cyclic voltammetric findings that H₂ evolution reaction takes place at -0.7 V.

4.1.2. Cyclic Voltammetry of CO Exposed Planer Ni Electrode

Cyclic voltammetry of carbon monoxide exposed planer nickel electrode in phosphate buffer (pH=6.86) was obtained by following the procedure discussed in the experimental section. The electrode was exposed to carbon monoxide gas by continuously bubbling 1 % carbon monoxide gas in the electrolyte solution of the working electrode at a flow rate of 100 ml/min for 20 minutes. Carbon monoxide gets adsorbed on the active sites of the nickel electrode surface. Some carbon monoxide might have been dissolved in the electrolytic solution also, which were presumably removed by continuous purging of N₂ through the electrolyte solution after flow of carbon monoxide was stopped. It was anticipated that a continuous nitrogen purging of 30 minutes removes all dissolved carbon monoxide from the electrolyte solution.

The cyclic voltammogram was obtained at 50 mV/sec scan rate. Other parametric details of the experimentation have been listed in Table 4-3. The voltammogram of the planer Ni electrode with 20 minutes carbon monoxide exposure to 1 % carbon monoxide is shown in Figure 4-3. The comparison of the cyclic voltammogram of Ni electrode under nitrogen and when it was exposed to carbon monoxide are shown in Figure 4-3.

Parameters	Range/Values
Equilibration time (Sec)	120
Initial potential (V vs NHE)	-0.4
Vertex potential (V vs NHE)	-1.3
Vertex potential (V vs NHE)	+0.4
Final potential	-0.4
Scan rate (mV/sec)	50
Open Circuit Potential (V vs NHE) (measured)	-0.578
Reference electrode	SCE

Table 4-3: CV Parameters of CO Exposed Planer Ni Electrode

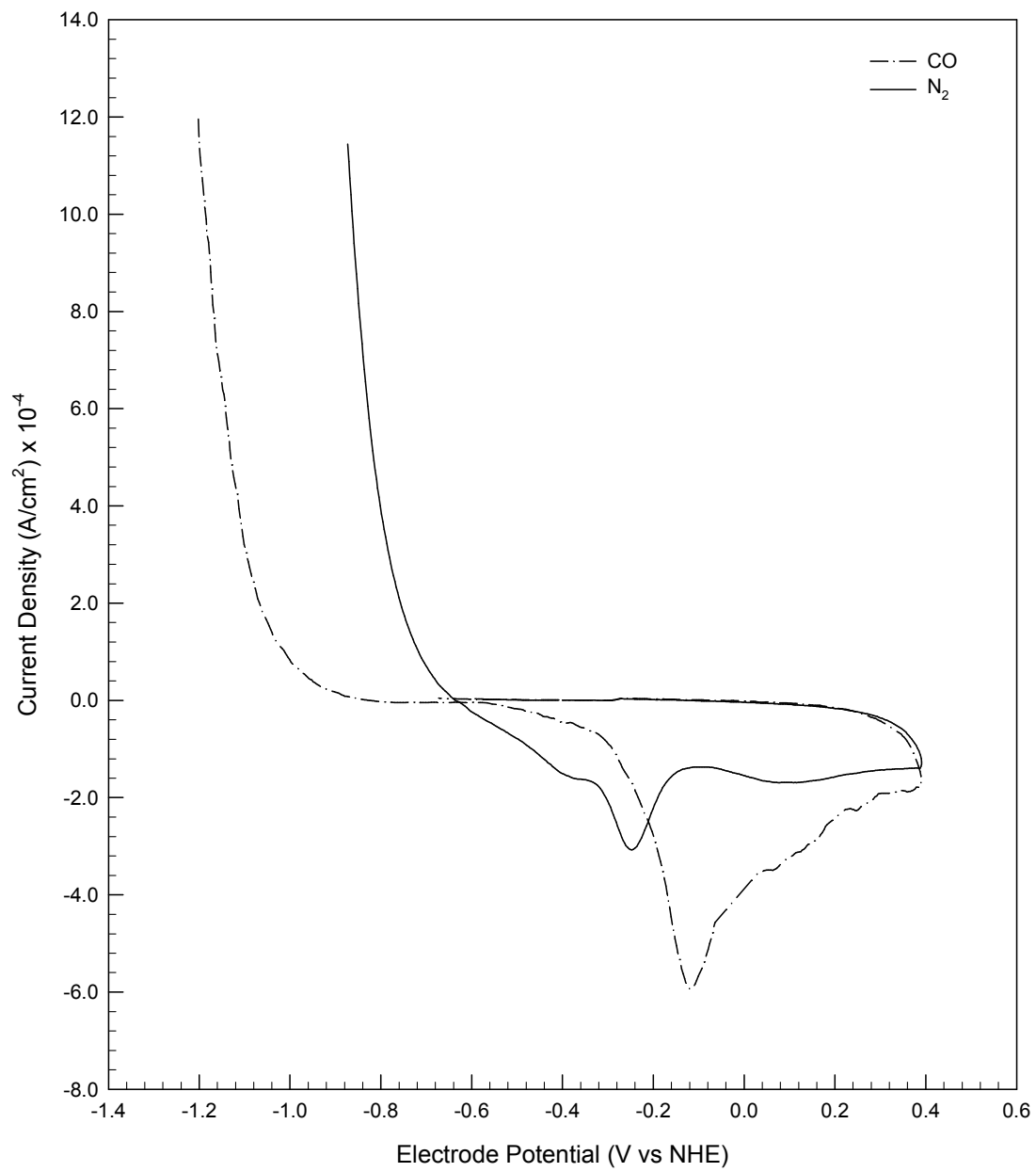


Figure 4-3: Cyclic Voltammogram of CO and N₂ Exposed Ni Electrode

During the anodic scanning of the electrode, a peak is observed at -0.13 V, in contrary to the Ni electrode under N₂ environment, where it occurs at -0.25 V. This means that the presence of carbon monoxide on Ni electrode has a major shift of 130 mV in the anodic oxidation peak position. Hori et al. [77] has observed similar shift but of 400 mV. They have attributed this peak to the Ni oxidation that shift towards positive values due to the presence of CO. However, the observation of the peak at -0.13 V may not be due to Ni oxidation as discussed by Hori et al. It was observed repeatedly that the peak at -0.13 V occurs whenever Ni electrode was exposed to CO. But it does not appear during second scan or higher scans of the electrode. Hence it can be inferred that the peak occurring at -0.13 V is not due to the Ni oxidation but due to the oxidation of the adsorbed CO. It is hypothesized that in the presence of CO, dissolution of Ni is prevented and or suppressed.

During cathodic scanning of the carbon monoxide exposed Ni electrode, the H₂ evolution process starts at a potential of -0.96 V. This onset potential is significantly different than that obtained in the case of the Ni electrode under N₂ environment, which is at -0.7 V. The delay of the H₂ evolution is approximately 260 mV, which is significantly higher. Apparently this was due to the poisoning of the active sites of Ni electrode. Since adsorbed carbon monoxide form strong bond with the active sites, only a fraction of the active sites are available. Hence from the cyclic voltammogram of the carbon monoxide exposed Ni electrode, it can be concluded that CO is getting adsorbed on Ni electrode. It can also be inferred that the adsorbed CO form strong bond with the active sites of the electrode, resulting in the poisoning of the electrode surface. Hori et al. [77] have also observed a significant difference in the onset potential of H₂ evolution process.

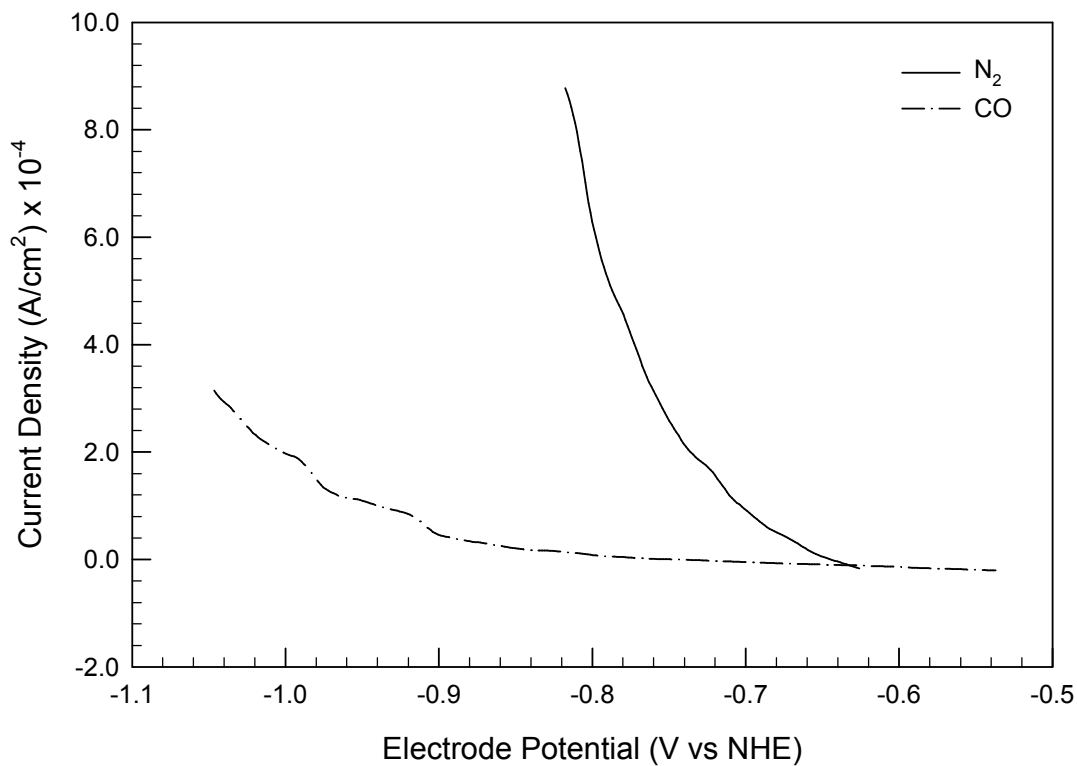


Figure 4-4: Cathodic Scans of CO and N₂ Exposed Planer Ni Electrode

Parameters	Range/Values
Equilibration time (Sec)	120
Initial potential (V vs NHE)	-0.4
Final potential	-1.4
Scan rate (mV/sec)	10
Open Circuit Potential (V vs NHE)	-0.533
Electrode Area (cm ²)	0.3

Table 4-4: Cathodic Scan Parameters of CO Exposed Planer Ni Electrode

Since H₂ evolution reaction potential differs remarkably between CO and N₂ exposed electrodes, this characteristic behavior can be used as an indication of the presence of CO on the Ni electrode. For example cathodic scans between -0.4 V to -1.4 V were done.

As in the case of cyclic voltammogram, cathodic scan were also obtained 50 mV/sec scan rate. Figure 4-4 shows the cathodic scans Ni electrode exposed CO and under N₂ environment. Parametric details of the experimentation have been listed in Table 4-4. As expected features of the cathodic scans of the CO exposed electrode have similar characteristics to that of the cyclic voltammogram. It is clear that H₂ evolution reactions start at the potential of -0.96 V (vs NHE), which supports the voltammetric findings.

4.1.3. Cyclic Voltammetry of H₂ Exposed Planer Ni Electrode

Cyclic voltammetry experiments of Ni electrode exposed to pure H₂ gas were carried out to study the effects of the H₂ on the Ni electrode surface. A high purity H₂ gas (>99.9999% purity) was passed continuously for 30 minutes through the phosphate buffer electrolytic solution of the working electrode chamber. During which it was anticipated that significant H₂ will get adsorbed on the electrode surface. Then, cyclic voltammogram of the H₂ exposed Ni electrode surface was obtained at 50 mV/sec scan rate. Exact parameters of the experimentation have been listed in Table 4-5.

Figure 4-5 show the comparison of the cyclic voltammogram of the H₂ exposed Ni electrode with CO and N₂. The performance of the H₂ exposed Ni electrode differs significantly. It is evident that in the case of the H₂ exposed Ni electrode the anodic

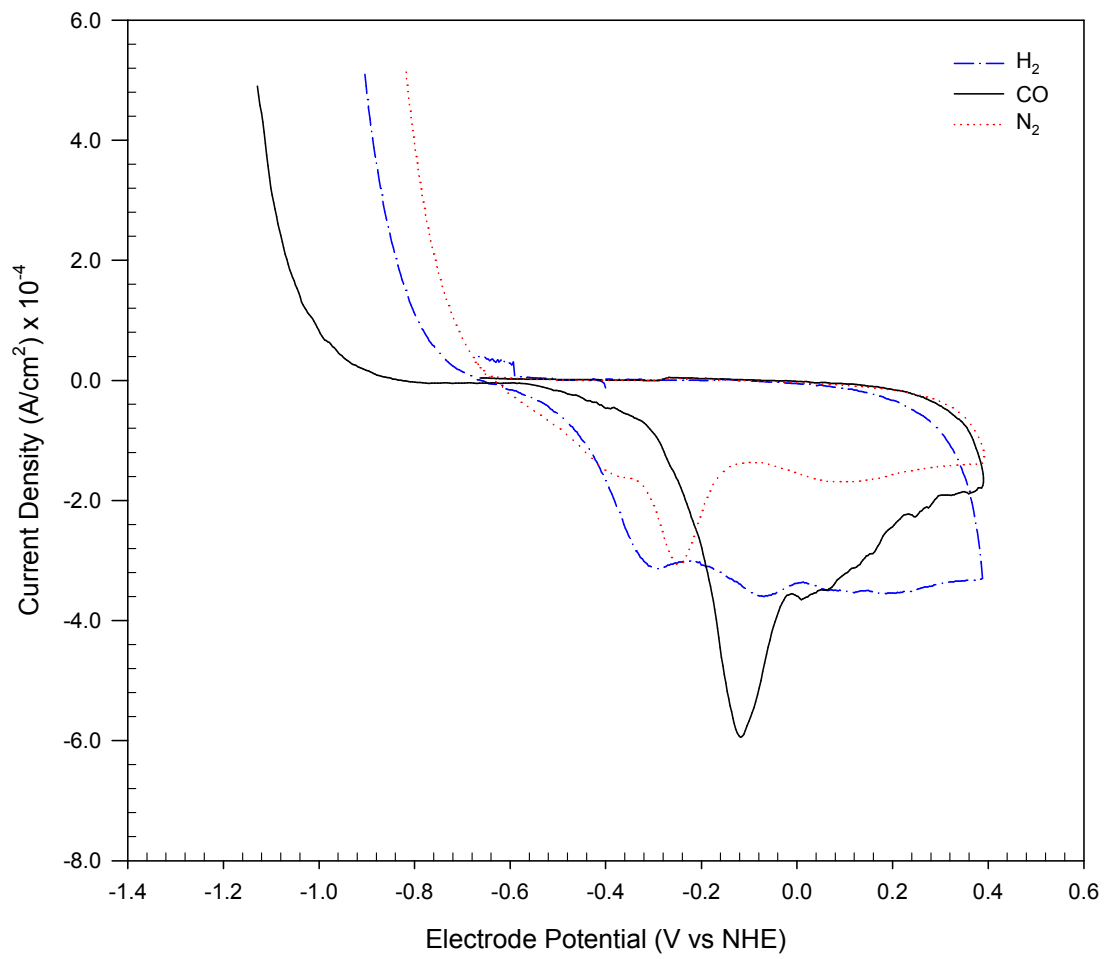


Figure 4-5: CV of H_2 , CO and N_2 Exposed Planer Ni Electrode

Parameters	Range/Values
Equilibration time (Sec)	120
Initial potential (V vs NHE)	-0.4
Vortex potential (V vs NHE)	-1.3
Vortex potential (V vs NHE)	+0.4
Final potential (V vs NHE)	-0.4
Scan rate (mV/sec)	50
Open circuit potential (V vs NHE)	-0.525
Sample Area (cm ²)	0.3
Reference electrode	SCE

Table 4-5: CV Parameters of H₂ Exposed Planer Ni Electrode

oxidation peak is completely absent. It seems that H₂ oxidation is occurring across the complete anodic potential range (from -0.4 V to 0.4 V range). As in the case of carbon monoxide exposed electrode, the adsorbed H₂ prevents the Ni dissolution. In addition it is also clear that the anodic currents in the case of the H₂ exposed Ni electrode are much higher than carbon monoxide exposed planer Ni electrode and those of under nitrogen.

During the cathodic scanning, as in the case of the N₂ exposed electrode, H₂ evolution reaction starts at a potential of -0.7 V. This value is essentially similar that observed under N₂. This suggests that the H₂ exposed Ni electrode is behaving very similar to the electrode under N₂, indicating absence of any reducible species.

From these observations of pure H₂ exposed Ni electrode, it can attributes that whatever characteristic features of 1 % CO gas in H₂ is entirely due to carbon monoxide. These findings verify that CO gets preferentially adsorbs at the Ni electrode surface.

4.1.4. Removal of Adsorbed CO from Planer Ni Electrode

Hori et al. [78] tried to remove adsorbed carbon monoxide by electroreduction to hydrocarbons. This was done by repeated cathodic scanning. It is a time consuming method not practical for an electrochemical filter. As observed by Saleh et al. [80], the adsorbed CO can be removed from PTFE bonded Raney-Ni gas diffusion electrode surface by continuous purging of inert gas for 100 or more hours. Therefore this approach is also not pragmatic for electrochemical filter. Above mentioned limitations of these CO removal approaches necessitates the development of a new CO removal method.

This work describes a new approach of carbon monoxide removal by electrochemical oxidation of adsorbed carbon monoxide. By using cyclic voltammetry, adsorbed carbon monoxide was removed from the Ni electrode surface. Figure 4-6 shows the cyclic voltammogram of the CO exposed Ni electrode obtained during the CO removal from the electrode. The parametric details of this experiment have been listed in Table 4-6.

During the start of the anodic scan at -0.4 V, the current response is zero representing the absence of any electrochemical activity. As the electrode is further scanned anodically, current starts increasing at -0.3 V, representing the onset of some electrochemical activity. The anodic current keeps on rising with potential and a clear peak is observed at -0.13 V. As discussed in the earlier sections, this peak is essentially due to the electrooxidation of adsorbed carbon monoxide.

Figure 4-6 shows the multiple cyclic voltammogram of the CO electrooxidation, which were observed in order to investigate whether or not CO is completely removed from the electrode surface. From the voltammogram, clear that CO electrooxidation peak is absent in second and subsequent scans. From this observation, it can be inferred that complete removal of the carbon monoxide takes place during the first scan of the electrode.

In order to verify these findings, cathodic scans of nickel electrode was carried out after the completion of the carbon monoxide oxidation. Figure 4-7 shows the cathodic scans of the Ni electrode exposed to N₂, carbon monoxide and after carbon monoxide oxidation. It is clear from this figure that the curves of

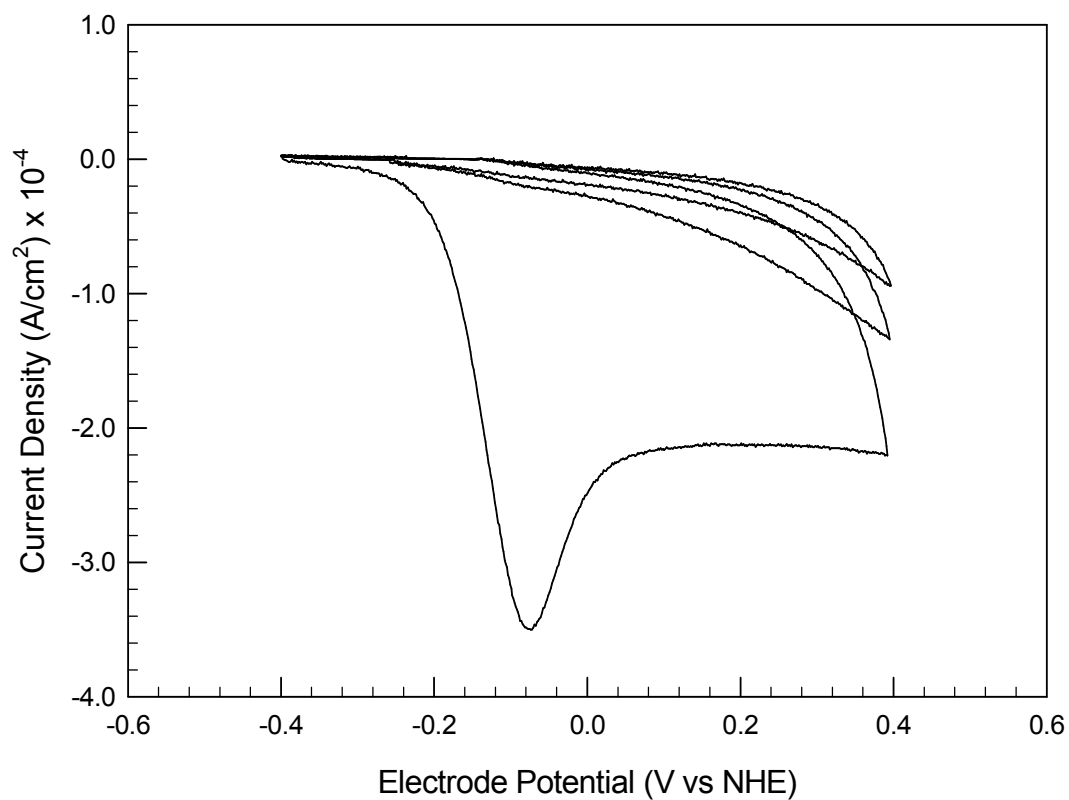


Figure 4-6: Multiple CV of CO Electrooxidation on Planer Ni Electrode

Parameters	Range/Values
Equilibration time (Sec)	120
Initial potential (V vs NHE)	-0.4
Final potential (V vs NHE)	+0.4
Scan rate (mV/sec)	20
Open Circuit Potential (V vs NHE)	-0.555

Table 4-6: CV Parameters of CO Electrooxidation Experimentation

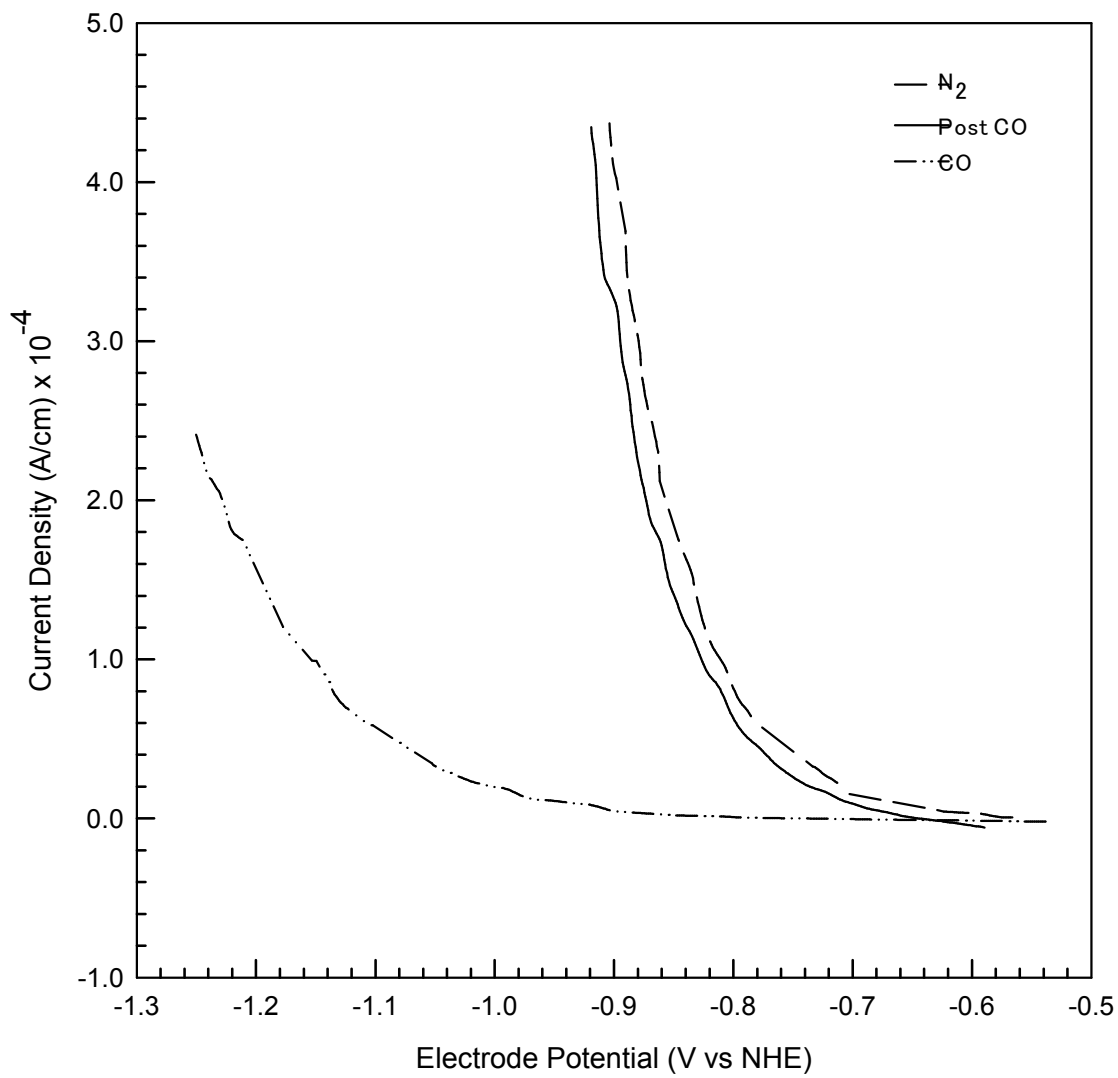
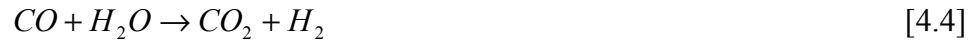


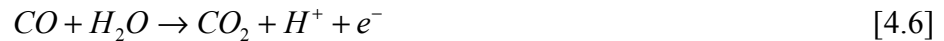
Figure 4-7: Cathodic Scan of CO Electrooxidation on Planer Ni Electrode

Ni electrode after carbon monoxide oxidation almost coincides with the initial Ni electrode under N₂. These curves are markedly different from the CO exposed electrode. Hence from it can be inferred that complete removal of carbon monoxide from the Ni electrode surface has been achieved by the anodic electrooxidation.

Laxmanan et al. [67-69] have given the detailed mechanism of CO electrooxidation on Pt-Ru anode electrocatalyst. It is anticipated that similar electrooxidation mechanism will also take place on Ni catalyst surface. The overall reactions occurring during the electrochemical removal of carbon monoxide can be given by reaction [4.4]:

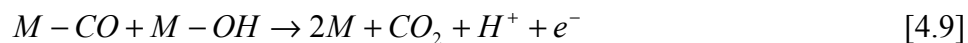


During the anodic scanning of the electrode, carbon monoxide oxidation will be preferred over H₂ oxidation as the catalyst surface is saturated with the carbon monoxide. Reaction 4.5 represents that whatever H₂ gets oxidized during the carbon monoxide electrooxidation formed back during the cathodic scanning of the Ni electrode. Electro-oxidation of carbon monoxide takes place through the following reaction [4.6]:



The mechanistic steps of the above reaction are given as follows:





Where, M refers to active Ni catalyst sites.

Reaction [4.7] corresponds to the adsorption of carbon monoxide onto the active sites of Ni catalyst (i.e., CO poisoning). Reaction [4.8] corresponds to the formation of hydroxyl ions via the oxidation of water, and reaction [4.9] corresponds to the oxidation of adsorbed carbon monoxide by reaction with the hydroxyl species.

The area under the carbon monoxide electrooxidation peak relative to the background current can be used to calculate the amount of carbon monoxide removed by the anodic scanning. According to the Faraday's law, the number of moles of CO oxidized is;

$$N = \frac{Q}{nF} \quad [4.1]$$

Where,

N = Number of moles of carbon monoxide electrooxidized

Q = Peak area

n = Number of the electron involves in the reaction

F= Faraday's constant = 96500

The peak area or charge transfer during the CO electrooxidation in the above voltammogram (Figure 4-6) is -180 μ C. This corresponds to $1.88 \cdot 10^{-4}$ μ moles of CO.

4.2. Parametric Study of CO Removal on Planer Ni Electrode

In order to fortify the observation of the previous sections, the effect parameters such as CO exposure time, CO concentration and CO flow rate have been investigated. Any significant variation in the amount of carbon monoxide electrooxidized with these parameters will establish that in case of carbon monoxide exposed electrode, oxidation of the carbon monoxide takes place rather than dissolution of Ni. In this section details about the effect of these parameters has been presented. In order to study the effect of concentration, different concentration of carbon monoxide gases namely 10 ppm, 100 ppm, 1000 ppm and 1 % CO in H₂ and pure CO were used. Similarly in order to establish the effect of exposure time, the gas was passed for 2, 5, 10, 15, 20, 25 and 30 minutes. Four different flow rates namely 25, 125, 200 and at 275 ml/min have been investigated.

4.2.1. Effect of CO Exposure Time

The amount of the carbon monoxide adsorbed on the Ni electrode surface significantly increases with the exposure time. In turn oxidation of carbon monoxide also increases as more CO is available at the electrode surface. These study were carried out by using 10 ppm and 1 % CO gas in H₂. Other details of the parameters are given in Table 4-7. CO electrooxidation voltammogram was obtained after CO exposure of 2, 5, 10, 15, 20 and 25 minutes. Figure 4-8 and Figure 4-9 shows the variation of the CO electrooxidation curves with exposure time at 1 % and 10 ppm CO, respectively. These results can be represented in a more meaningful way in terms of the number of moles of CO electrooxidized with exposure time plot, which is shown in Figure 4-10 and Figure 4-12.

Concentration of CO (in H₂)	Flow Rates (ml/min)	Exposure Time (min)
10 ppm & 1 % CO	25 ml/min	2
		5
		10
		15
		20
		25
		30
	35	
	125 ml/min	2
		5
		10
		15
		20
		25
30		
35		

Table 4-7: Details of Parametric Study on Planer Ni Electrode

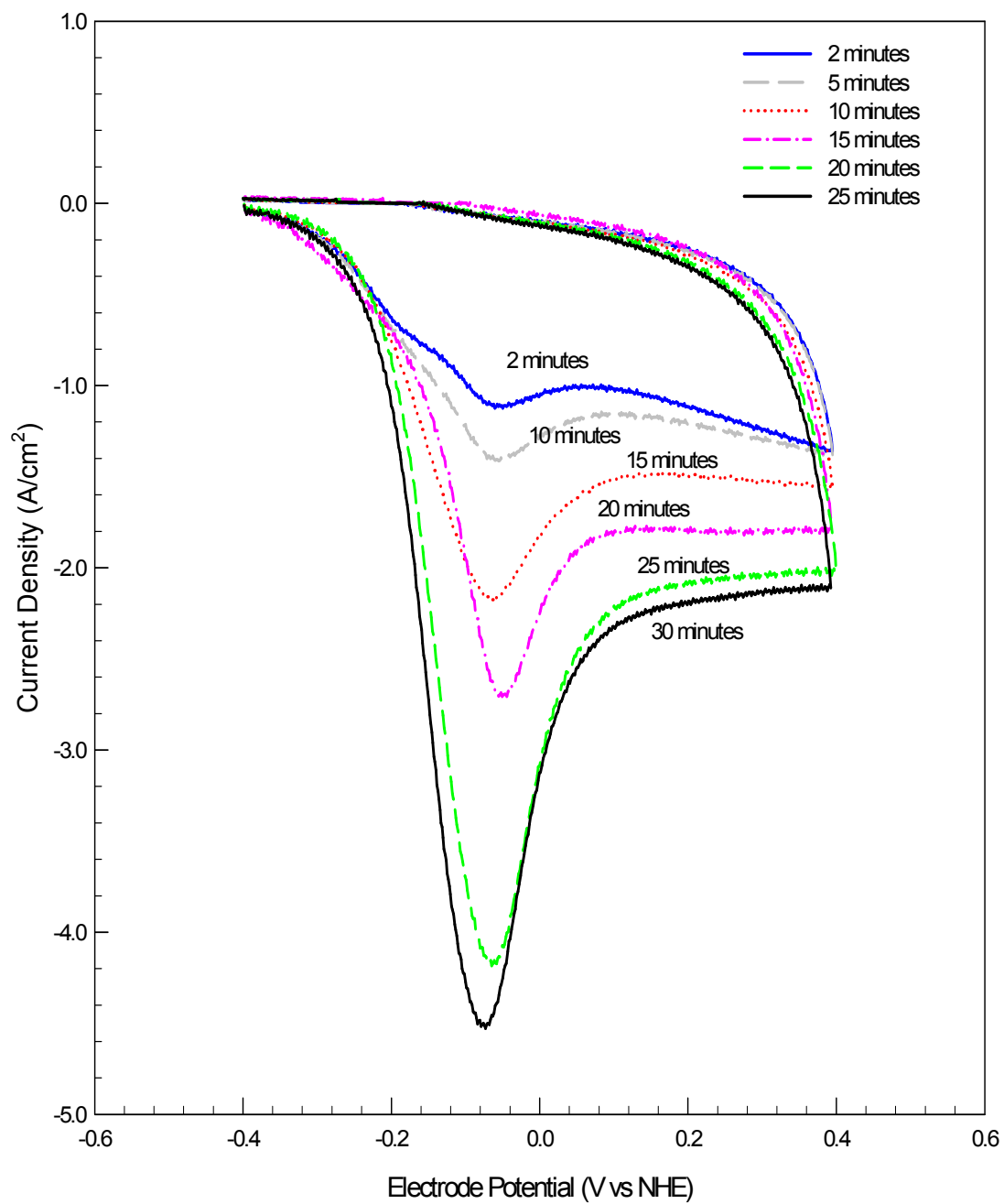


Figure 4-8: Effect of Exposure Time at 1 % CO

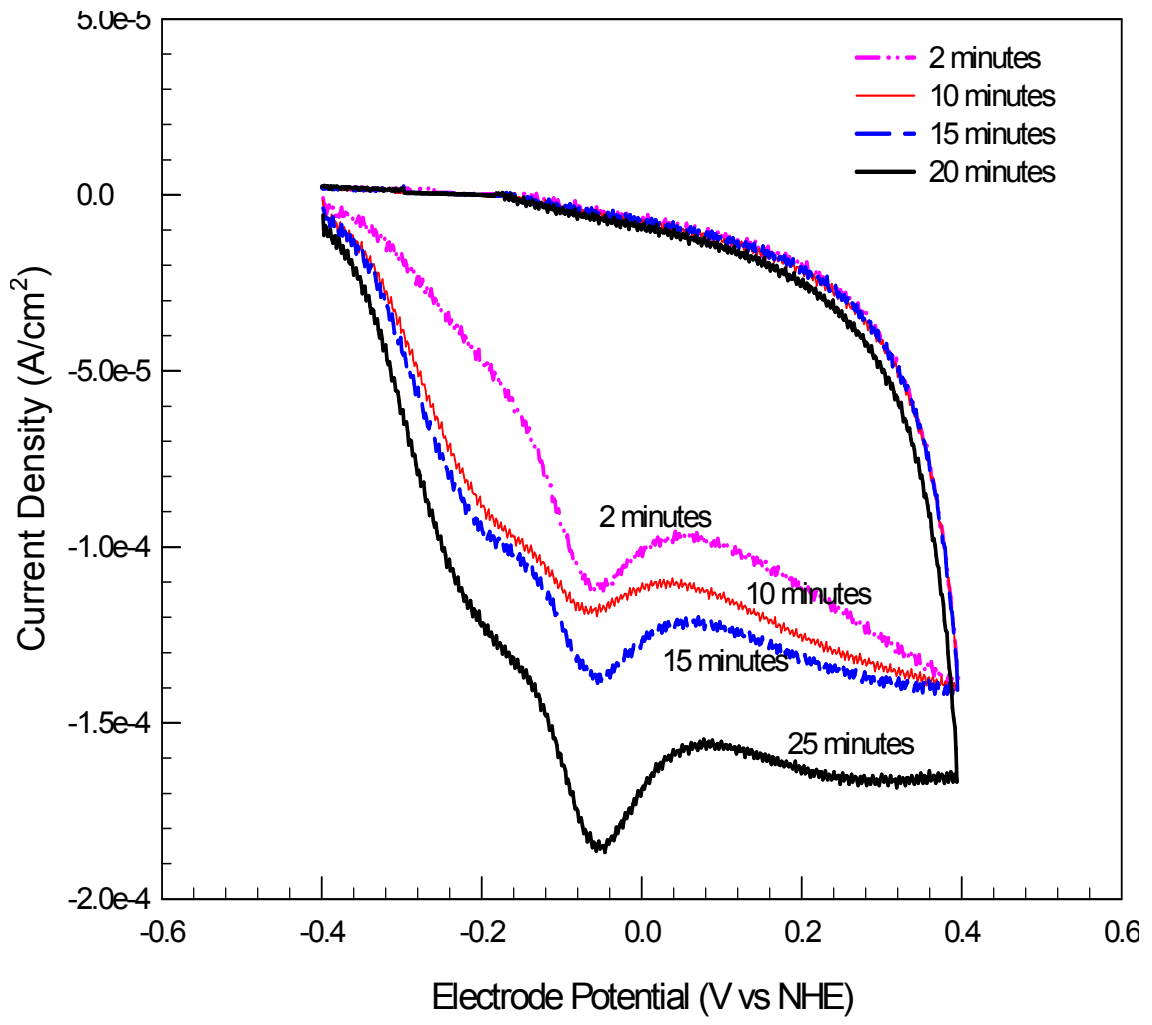


Figure 4-9: Effect of Exposure Time on CO Electrooxidation at 10 ppm CO

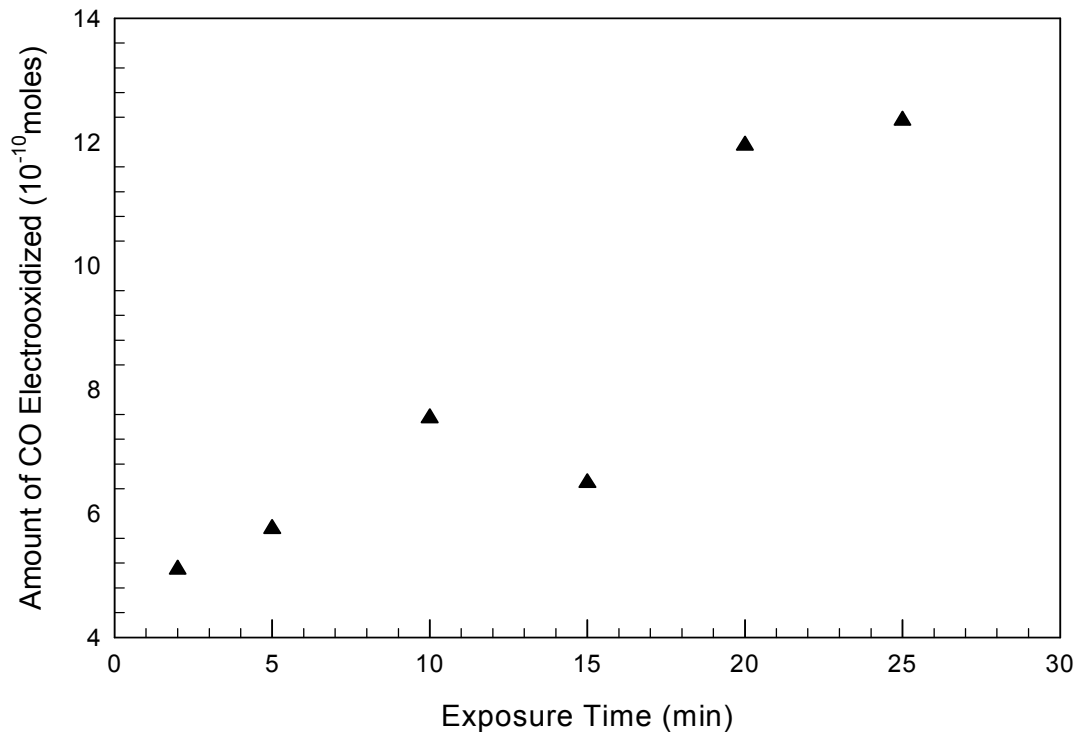


Figure 4-10: Amount of CO Electrooxidized vs Exposure Time at 1 % CO

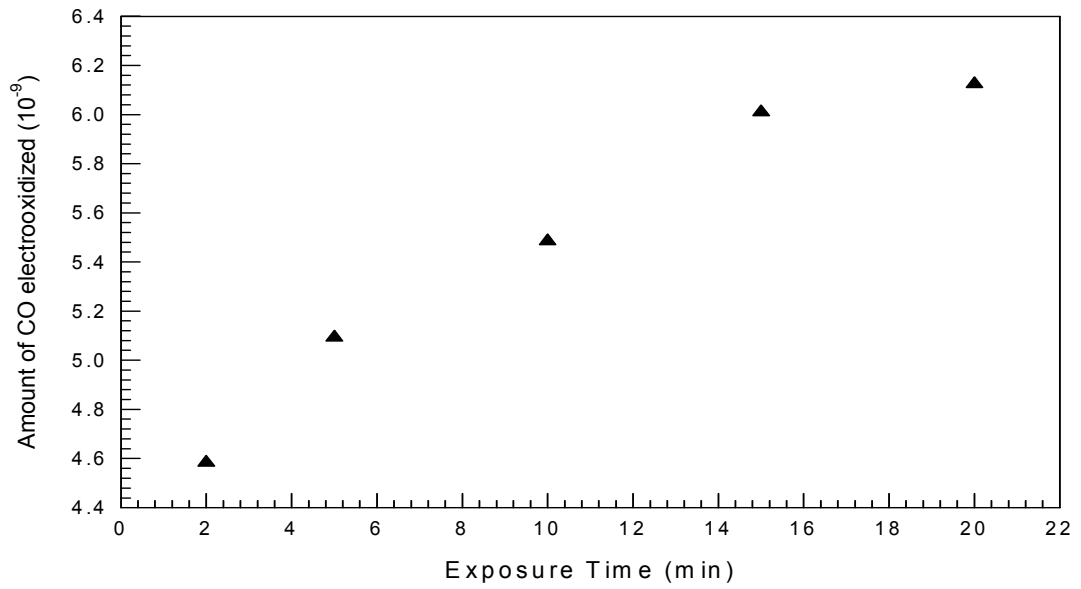


Figure 4-11: Amount of CO Electrooxidized vs Exposure Time at 10 ppm CO

From these plots it is clear that number of moles of carbon monoxide electrooxidized increases with exposure time. At lower exposure time, less carbon monoxide gets adsorbed on the electrode resulting in the smaller peak area. Similarly at higher exposure time, amount of carbon monoxide getting adsorbed on the electrode surface are much higher resulting in significantly higher carbon monoxide oxidation. But it is to be noted that charge variations (amount of CO oxidized) are not monotonous, representing absence of any linear relationship between the exposure time and carbon monoxide removal rate.

This phenomenon may be apparently due to either of the two reasons or a combination of these. Firstly, it may be due to the electrooxidation of any dissolved carbon monoxide that might not be purged. Secondly it might be due to the multilayer adsorption of carbon monoxide on the catalyst surface. Multilayer adsorption of carbon monoxide on Cu catalyst has also reported by Wonga et al. [76].

Also from the above figure, It is clear that moles of carbon monoxide electrooxidized at 20 and 25 minutes exposure time does differ only marginally, representing a saturation phenomenon. Hence, it can be inferred from the above graph that the saturation time of the Ni electrode is in the 25 minutes range with 1 % CO and 50 ml/min flow rate.

4.2.2. Effect of CO Concentration

As in the case of the exposure time study, it is anticipated that performance of the amount of carbon monoxide oxidation will also increases with concentration. Concentration of CO considerably affects the amount of CO getting adsorbed on the catalyst surface, hence

Exp #	Flow Rate (ml/min)	CO Concentration (ppm)
1	25	10
2		100
3		1000
4		1 %
5		Pure
6	125	10
7		100
8		1000
9		1 %
10		Pure
11	200	10
12		100
13		1000
14		1 %
15		Pure
16	275	10
17		100
18		1000
19		1 %
20		pure

Table 4-8: Details of Parametric Study on Planer Ni Electrode

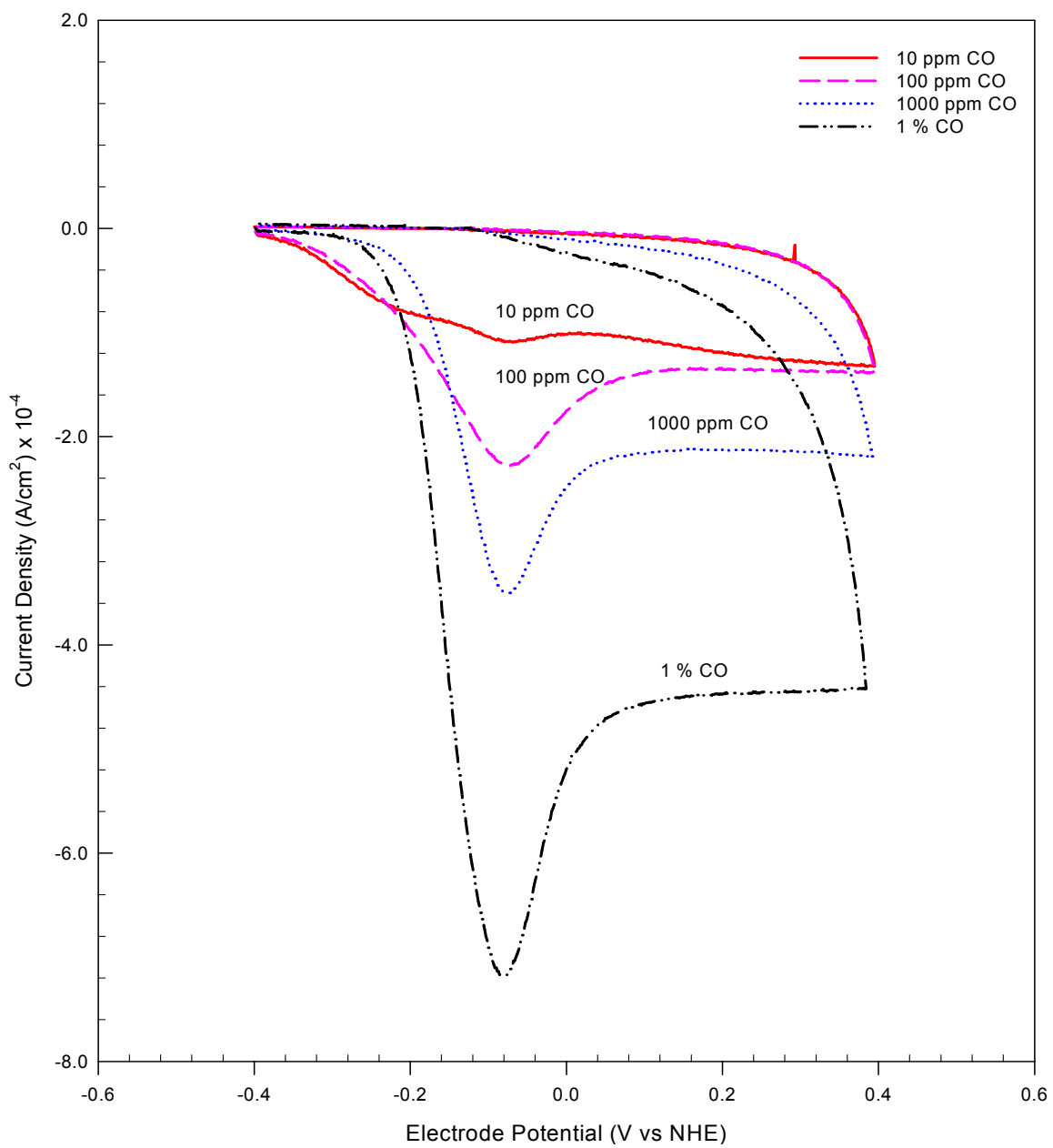


Figure 4-12: Effect of CO Concentration at 25 ml/min

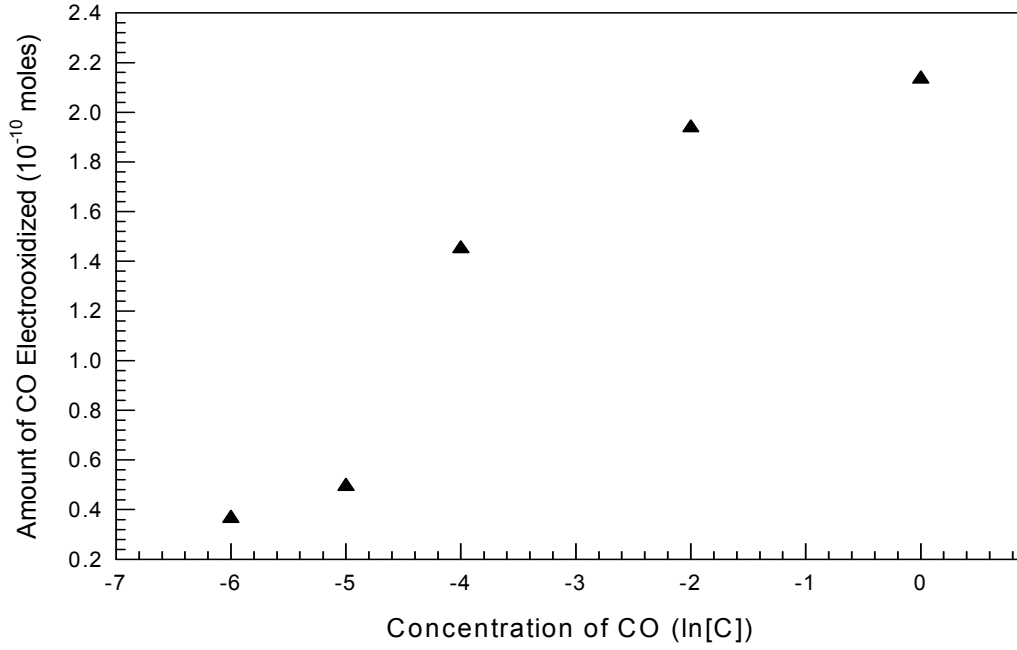


Figure 4-13: Amount of CO Electrooxidized vs Concentration at 25 ml/min

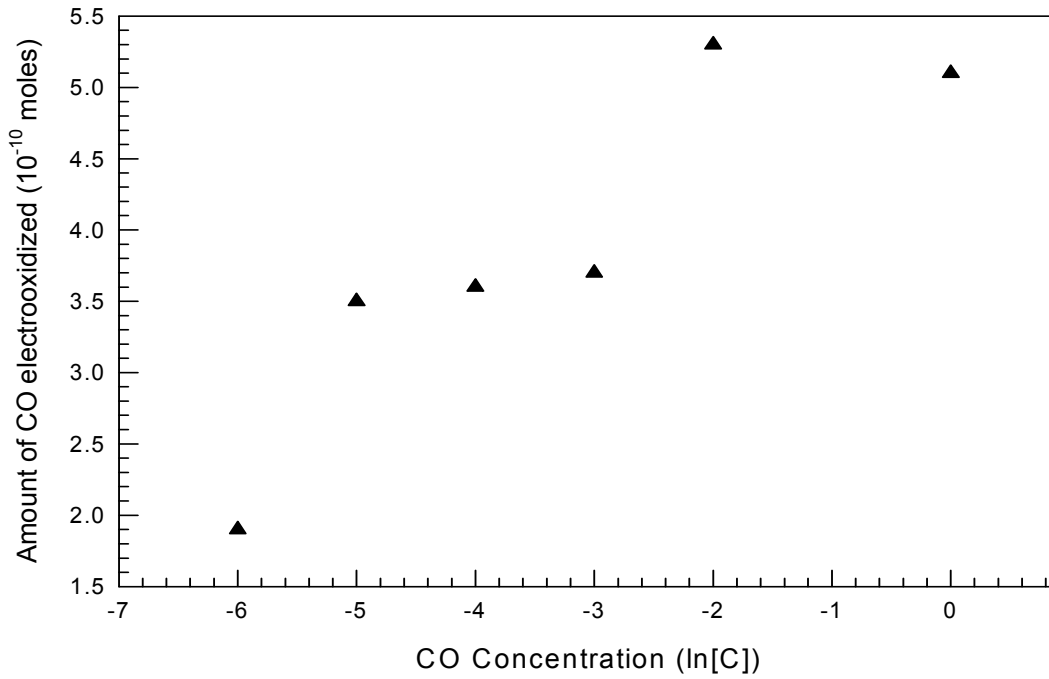


Figure 4-14: Amount of CO Electrooxidized vs CO Concentration at 125 ml/min

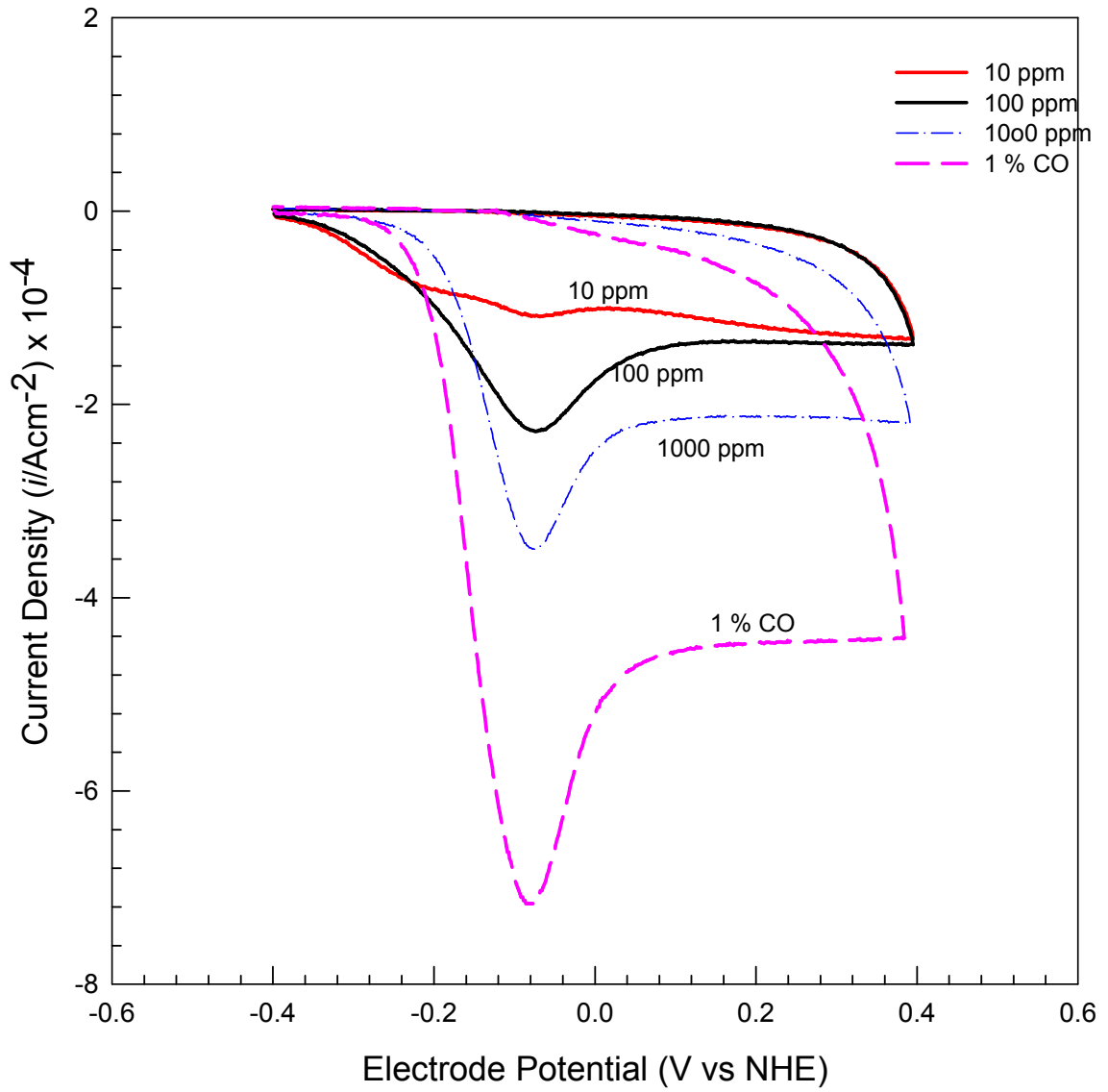


Figure 4-15: Effect of CO Concentration at 125 ml/min

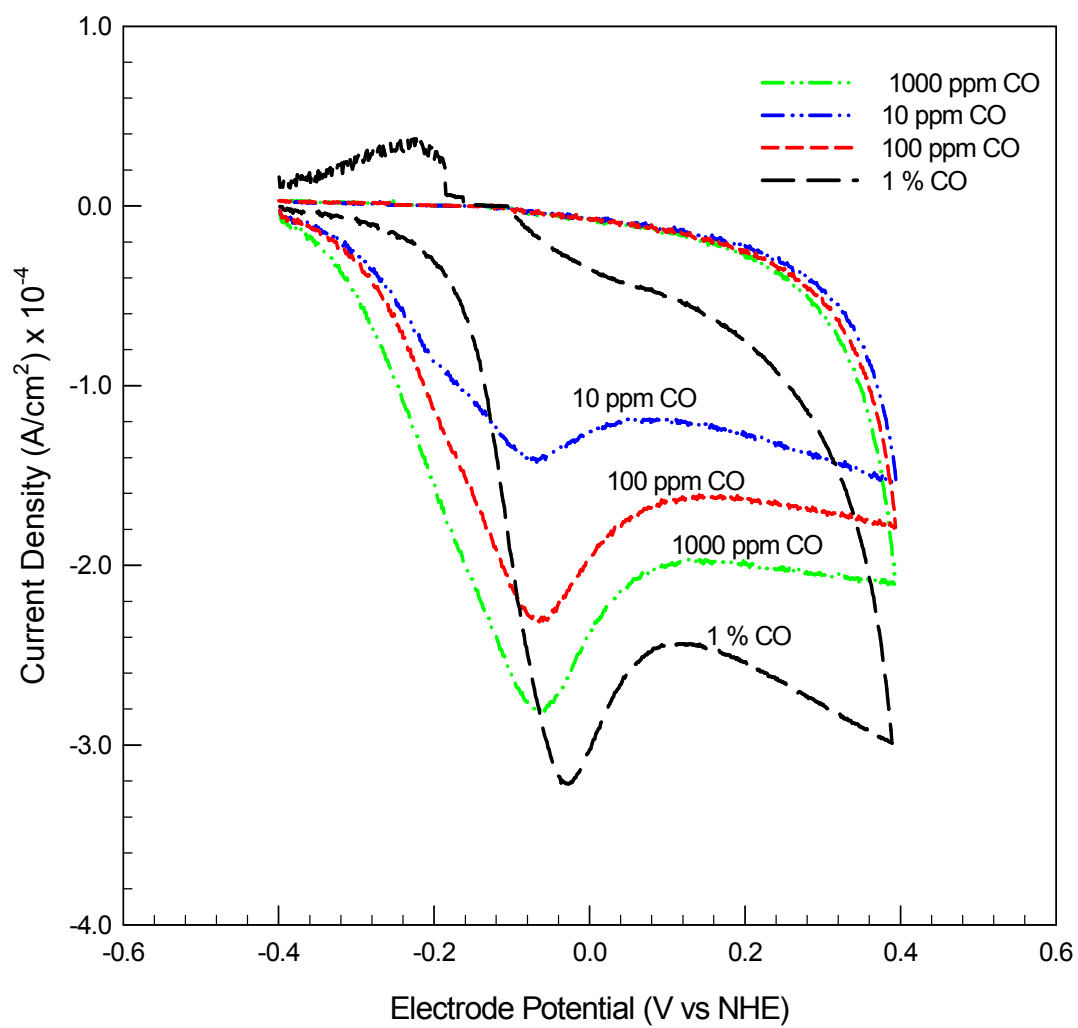


Figure 4-16: Effect of CO Concentration at 200 ml/min

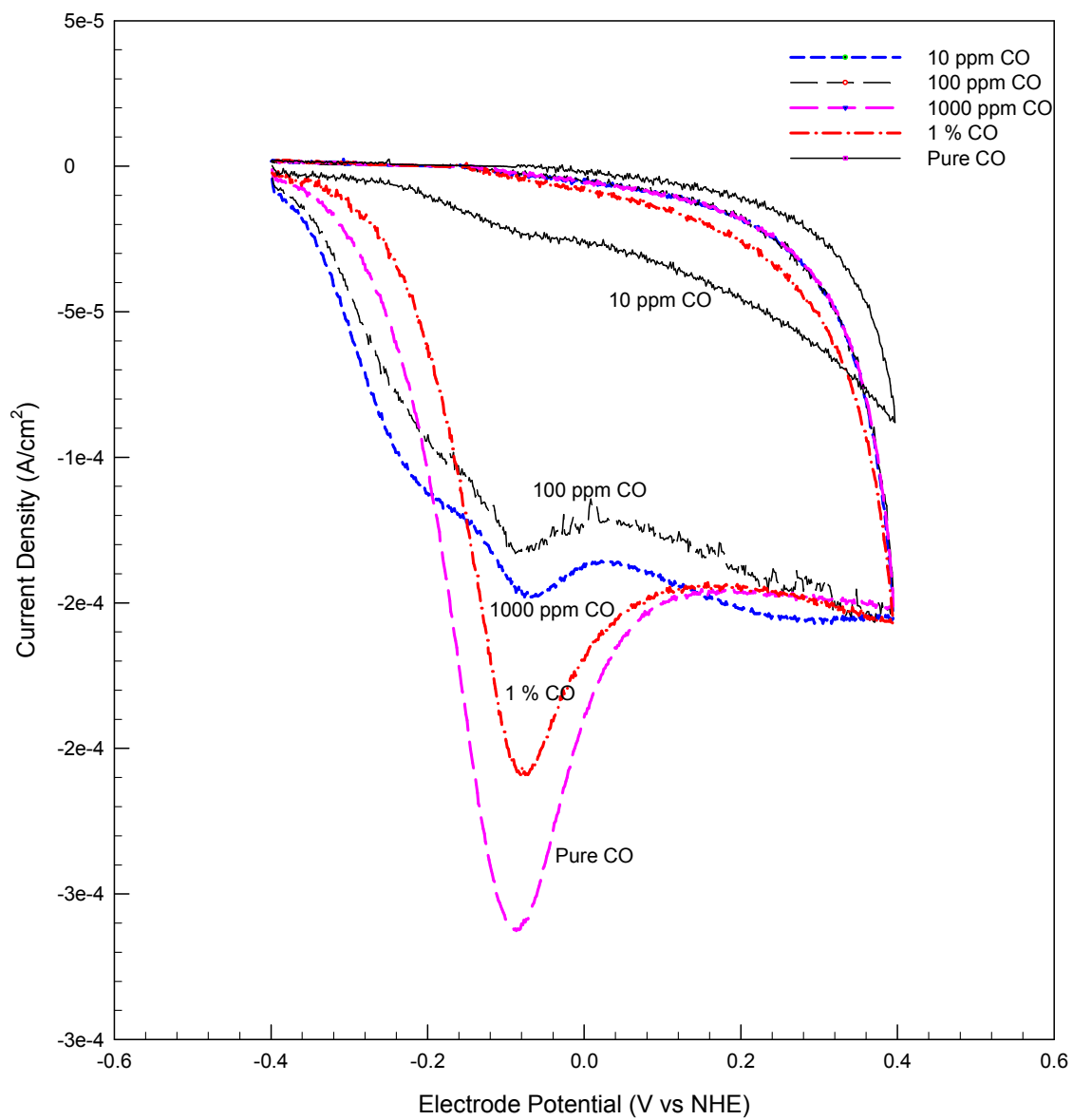


Figure 4-17: Effect of CO Concentration at 275 ml/min

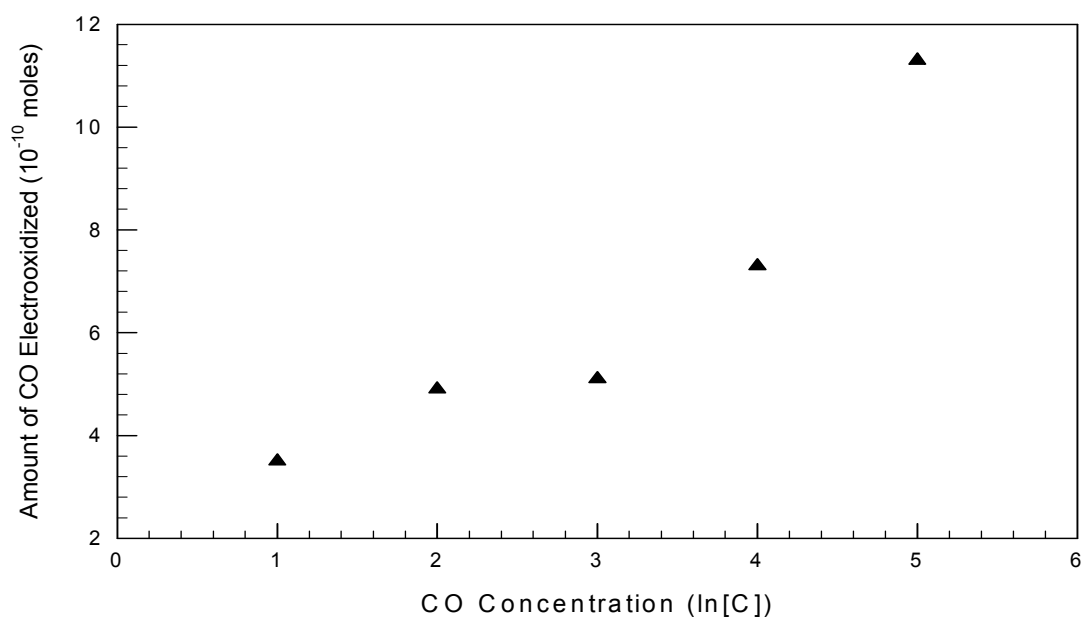


Figure 4-18: Amount of CO Electrooxidized vs CO Concentration at 200 ml/min

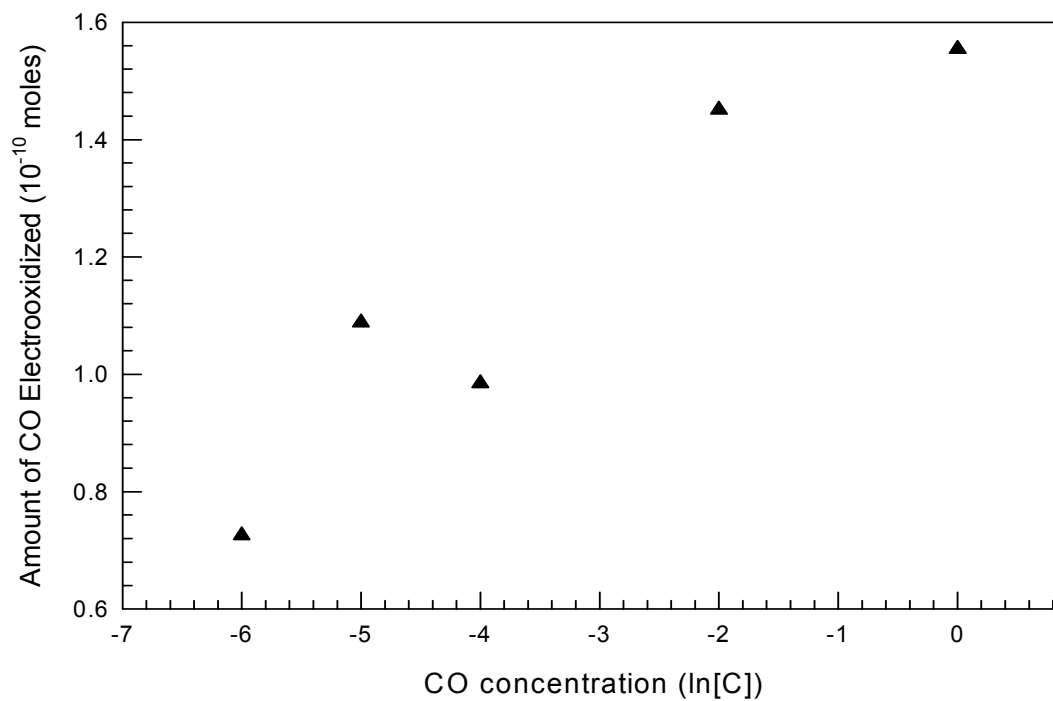


Figure 4-19: Amount of CO Electrooxidized vs CO Concentration at 275 ml/min

affects the carbon monoxide oxidation also. Since the flow rate of carbon monoxide is also important factor that affects the CO adsorption on Ni electrode. Therefore, in order to have complete assessment of the CO concentration effects, four different flow rates have been studied. The parameters of the experiments have been listed in Table 4-8.

Carbon monoxide electrooxidation voltammogram was observed after each exposure. Figure 4-12, Figure 4-15, Figure 4-16 and Figure 4-17 shows the effect of carbon monoxide concentration at 25, 125, 200 and 275 ml/min flow rate, respectively. From these plots it clears that, as in the case of the exposure time study, area of the carbon monoxide electrooxidation peaks seems to be increasing with the carbon monoxide concentration. However in this case variations of the carbon monoxide removal peak are relatively more monotonous and linear. Hence it can be inferred that the amount of CO removed by electrooxidation increasing with carbon monoxide concentration. Figure 4-13, Figure 4-14, Figure 4-18 and Figure 4-19 represents the above results in term of number of moles of CO electrooxidized at each at each concentration, respectively.

The behavior of these graphs indicates that oxidation of carbon monoxide increases with increasing carbon monoxide concentration. This phenomenon can be attributed to the availability of more carbon monoxide. However from the careful review of the above graph it can be inferred that amount of carbon monoxide electrooxidized does not increase monotonously or linearly with carbon monoxide concentrations. This strange behavior can be attributed to either of the two phenomena happening in the electrochemical cells. There is possibility that some carbon monoxide might be present in

the dissolved form in the electrolyte, which also gets oxidized during the process adding to the CO removal charges. The other possible reason of this inconsistency may be due to multilayer adsorption of CO at the catalyst surface, hence giving higher CO oxidation.

4.2.3. Effect of CO Flow Rate

Flow rate at which CO gas was passed through the electrolyte solution for CO exposing of the Ni electrode also affects the electrooxidation of CO. In order to access the affect of the flow rate, CO gas at four difference flow rate were used. The parametric details are given in Table 4-9. Carbon monoxide electrooxidation voltammogram were carried out after each exposure of the gas.

Figure 4-20, Figure 4-22, Figure 4-24 and Figure 4-26 represents the effect of flow rate at 1 % CO and 1000, 100, 10 ppm carbon monoxide at 25 minutes exposure time. Figure 4-21, Figure 4-23, Figure 4-25 and Figure 4-27 shows the number of the moles of CO electrooxidized at different flow rates respectively. It is clear from these plots that as the flow rate of the carbon monoxide is increased the area of area of the carbon monoxide peak is also increasing, indicating increase in carbon monoxide electrooxidation. The increase in the peak area (amount of CO electrooxidized) was essentially due to more availability of more CO at higher flow rate. But the important features of these plots are that the area change is only marginal. From these plots we can conclude that, in the investigated range of the flow rate, it does not significantly affect the CO electrooxidation. A possible explanation of this behavior can be attributed to the smaller active area of the catalyst that gets saturated easily with even very small flow rate.

Exp #	CO Concentration (ppm)	Flow Rate (ml/min)
1	10	25
2		125
3		200
4		275
5	100	25
6		125
7		200
8		275
9	1000	25
10		125
11		200
12		275
13	1 %	25
14		125
15		200
16		275
17	Pure	25
18		125
19		200
20		275

Table 4-9: Details of Parametric Study on Planer Ni Electrode

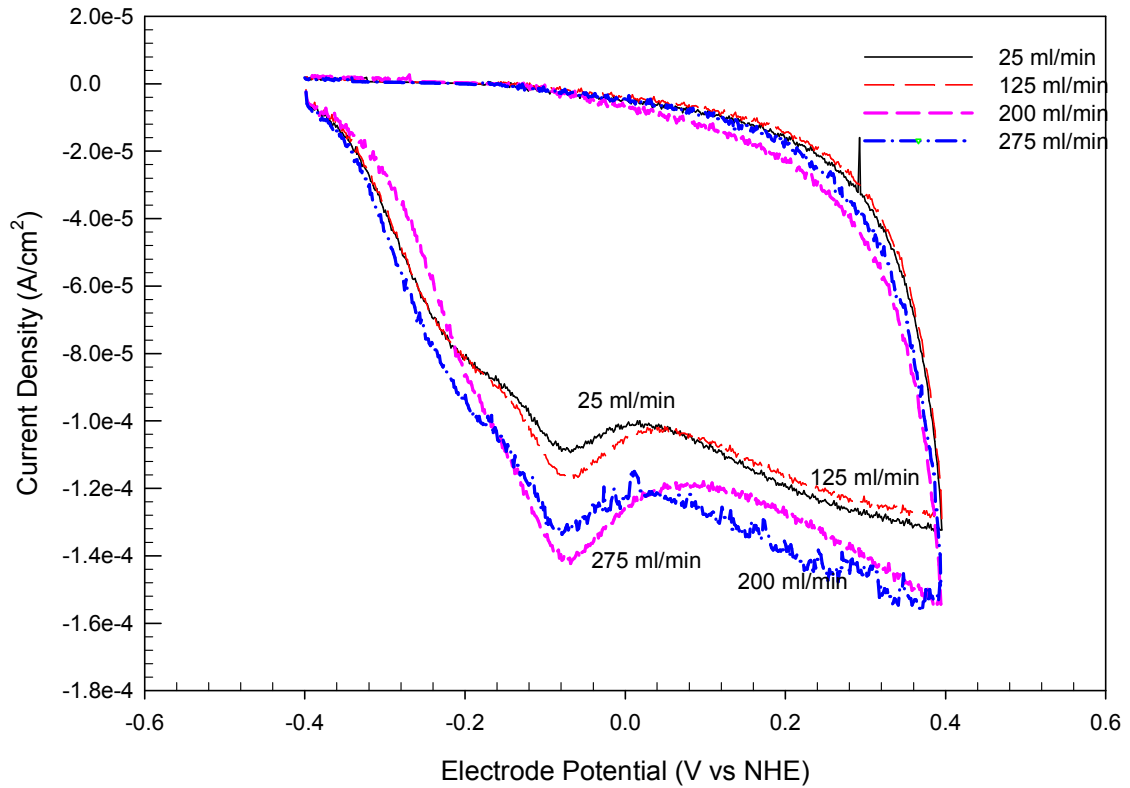


Figure 4-20: Effect of Flow Rate at 1 % CO

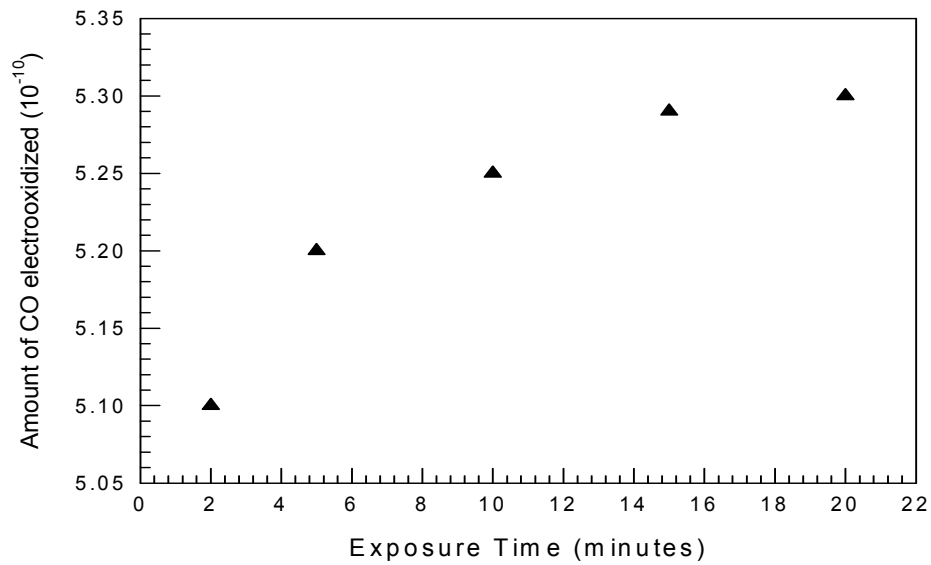


Figure 4-21: Amount of CO Electrooxidized vs Flow Rate at 10 ppm CO

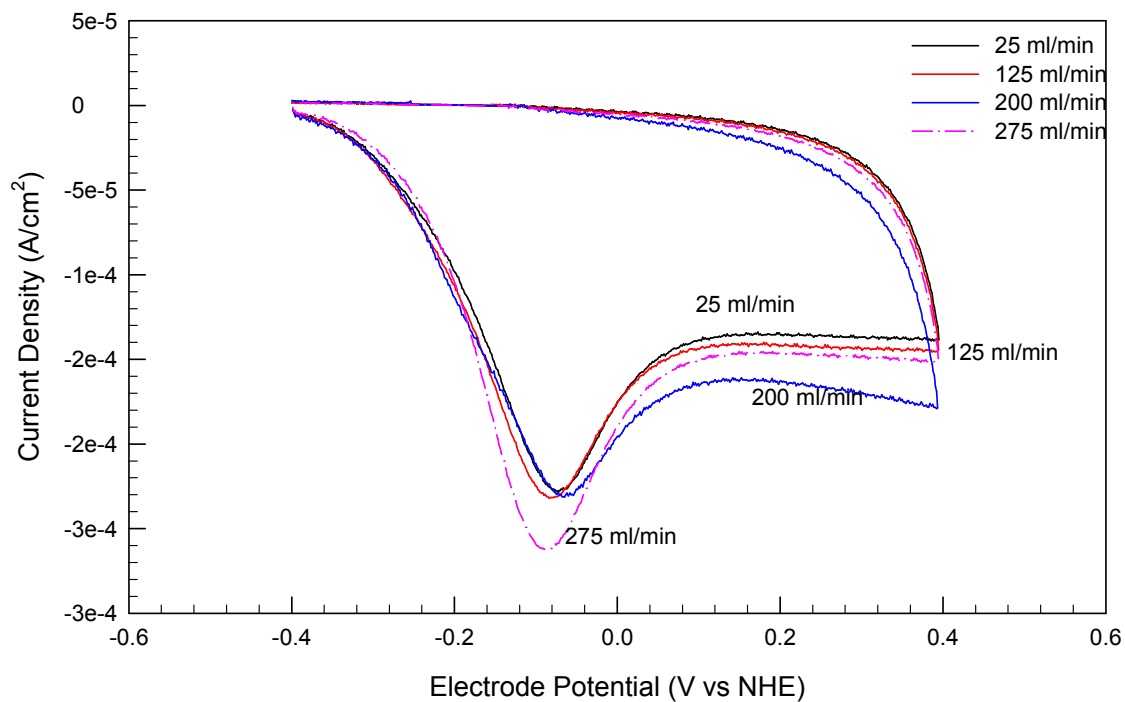


Figure 4-22: Effect of Flow Rate at 1 % CO

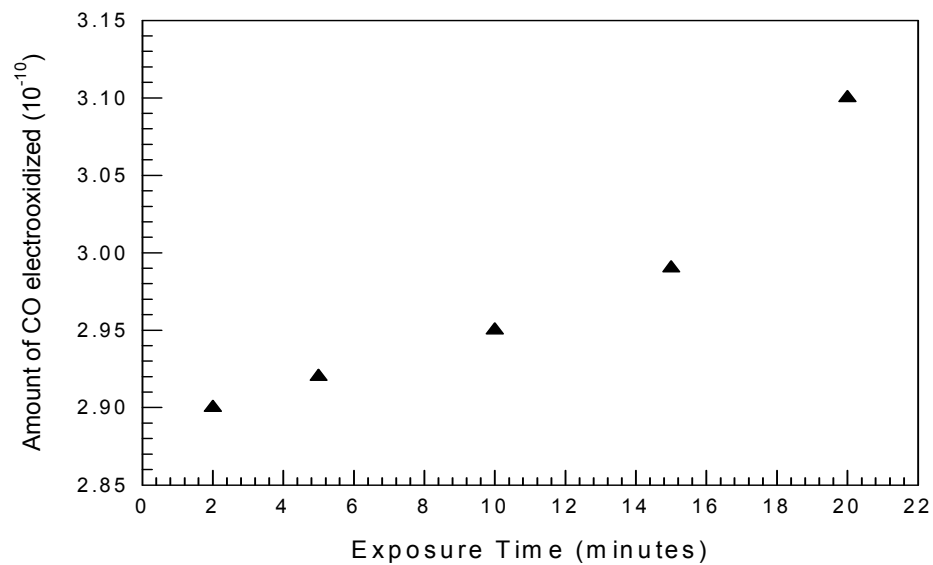


Figure 4-23: Amount of CO Electrooxidized vs Flow Rate at 10 ppm CO

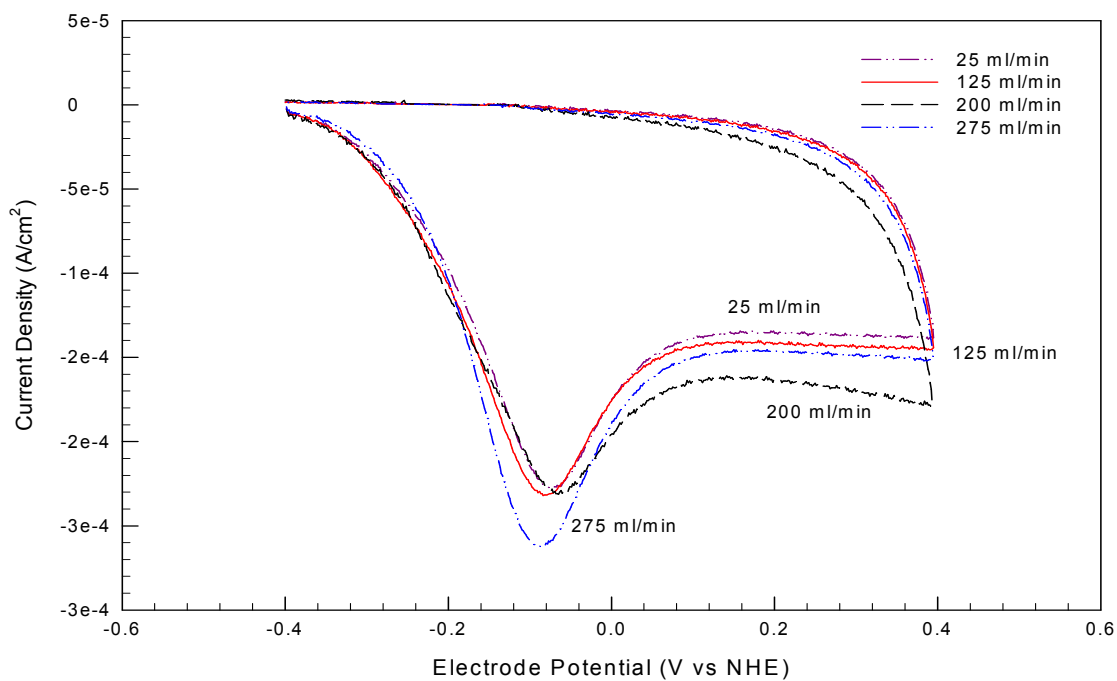


Figure 4-24: Effect of Flow Rate at 100 ppm CO

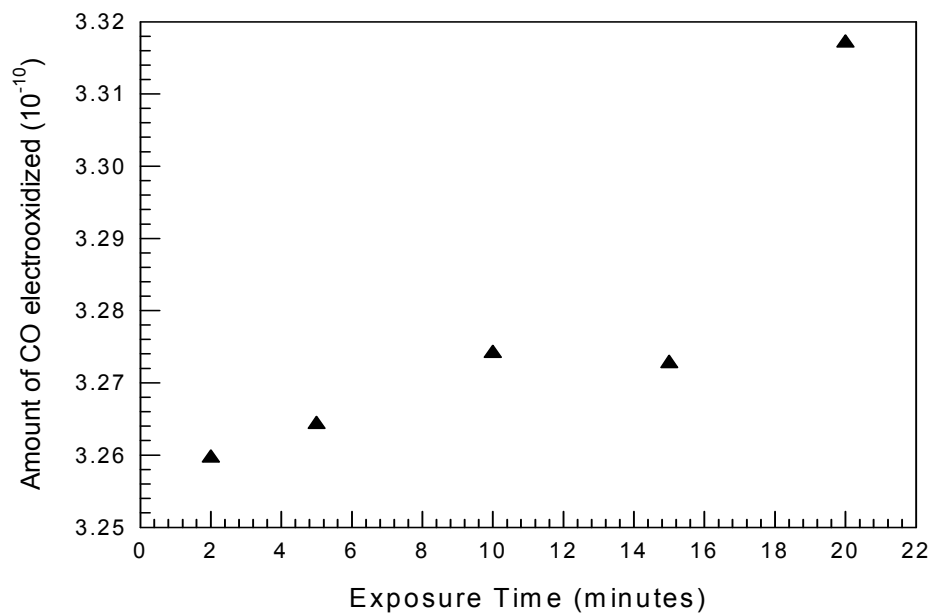


Figure 4-25: Amount of CO Electrooxidized vs Flow Rate at 10 ppm CO

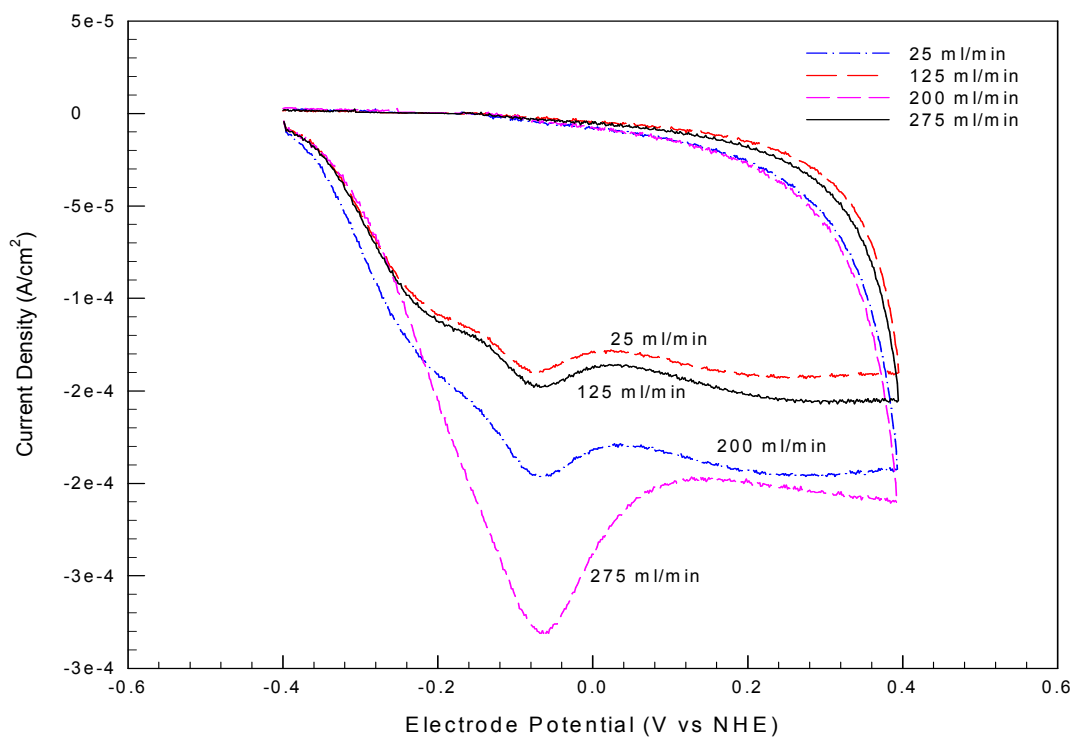


Figure 4-26: Effect of Flow Rate at 10 ppm CO

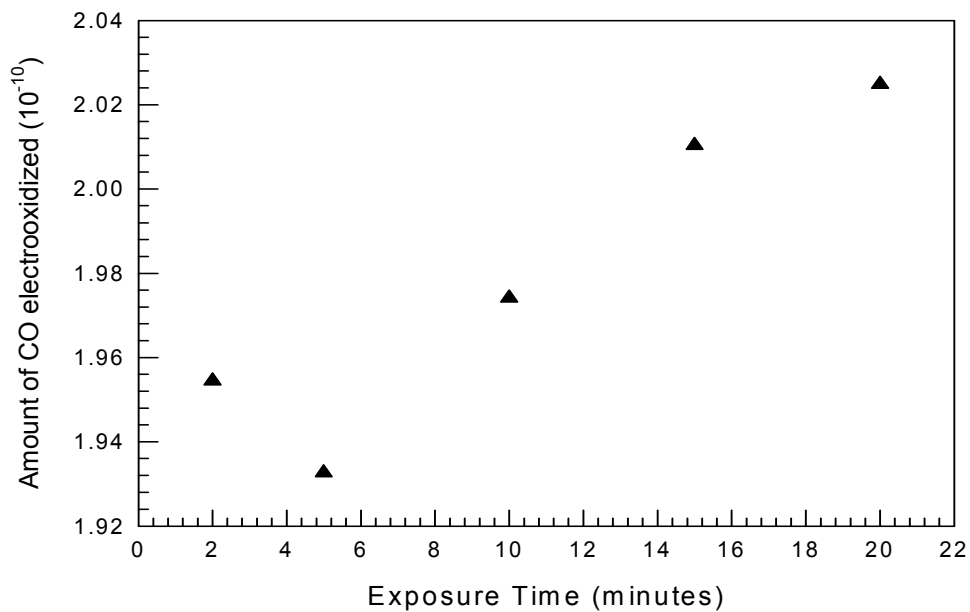


Figure 4-27: Amount of CO Electrooxidized vs Flow Rate at 10 ppm CO

4.3. Characterization of Raney-Ni Catalyst

In this section, details about the Raney-Ni catalyst characterization have been presented. Raney-Nickel catalyst is usually produced by leaching aluminum from Ni-Al alloy in a hot alkali. In this process H_2 gas evolves and gets adsorbed in the micropores of the Raney-Ni, which makes it highly pyrophoric as reaction of the adsorbed H_2 with air releases considerable amount of heat that can sinter catalyst. The pyrophoricity of the Raney-Ni catalyst prevents its characterization in active state. Hence the catalyst needs to be passivated for the characterization [81].

The pyrophoricity of the Raney-Ni catalyst can be eliminated by forming an oxide layer of a certain thickness on the surface of the active component and removing the adsorbed H_2 [81]. In the available literature numerous methods have been reported for the passivation of the pyrophoric Raney-Ni catalyst. Conventional method of catalyst passivation was described by Ewe et al [81]. H_2O_2 stabilization method was reported in a number of studies by Al-Saleh et al. [82], Rahman [83] and Kareemuddin [84]. It was found by these researchers that H_2 peroxide oxidation method using 15 % weight reported is one of the simplest and efficient methods of Raney-Ni catalyst passivation.

In this study the Raney-Ni catalyst was passivated by H_2O_2 oxidation for the characterization of the catalyst. The details about the experimental set up and procedure have been reported in literature [81-84]. The stabilized catalyst was characterized by scanning electron microscope (SEM), SEM-EDS, x-ray diffraction (XRD), inductive coupled plasma-absorption emission spectroscopy (ICP-AES) and BET surface area to

study the structure and active area of the catalyst. The details about the results of these characterizations have been presented in the following sections.

4.3.1. Inductive Coupled Plasma (ICP-AES)

The elemental analysis of the passivated catalyst was carried out by using inductive coupled plasma-absorption spectroscopy (ICP-AES) technique. The passivated catalyst sample was first digested in a 25 % of HCl solution under low heat until only a white film particle was formed. Resulting solution was finally diluted in 5 % HCl and screened with ICP for elemental analysis. By using four levels of mixed standard containing the elements found in the screening test, the final analysis of the catalyst sample were carried out. Table 4-10 gives the details of the elemental analysis of the passivated catalyst.

4.3.2. X-Ray Diffraction (XRD)

X-ray diffraction pattern of the passivated Raney-Ni catalyst was obtained to gain the insight about the structure and composition. High activity catalyst usually possesses high crystalline content. The technique is used to identify and compare the crystalline Ni, NiO and Ni (OH)₂ contents of the passivated Raney nickel catalyst. The absence of the Ni (OH)₂ peak indicates the absence in the sample. The x-ray diffraction patterns were obtained by using a Theta-2-theta scanning diffractometer. The scanning of sample was done from 4 degree to 80 degree two theta. The obtained XRD patterns were compared with standard Ni and NiO patterns of the Joint Committee of Powder Diffraction Services (JCPDS).

Elements	% By Weight
Al	2.7 %
Cu	<0.05%
Ni	88 %
Cr	<0.05%
Ti	<0.01%
Fe	<0.05%
Mn	<0.05%
Others(O)	9.34

Table 4-10: ICP-AES Analysis of H₂O₂ Passivated Raney Ni Catalyst

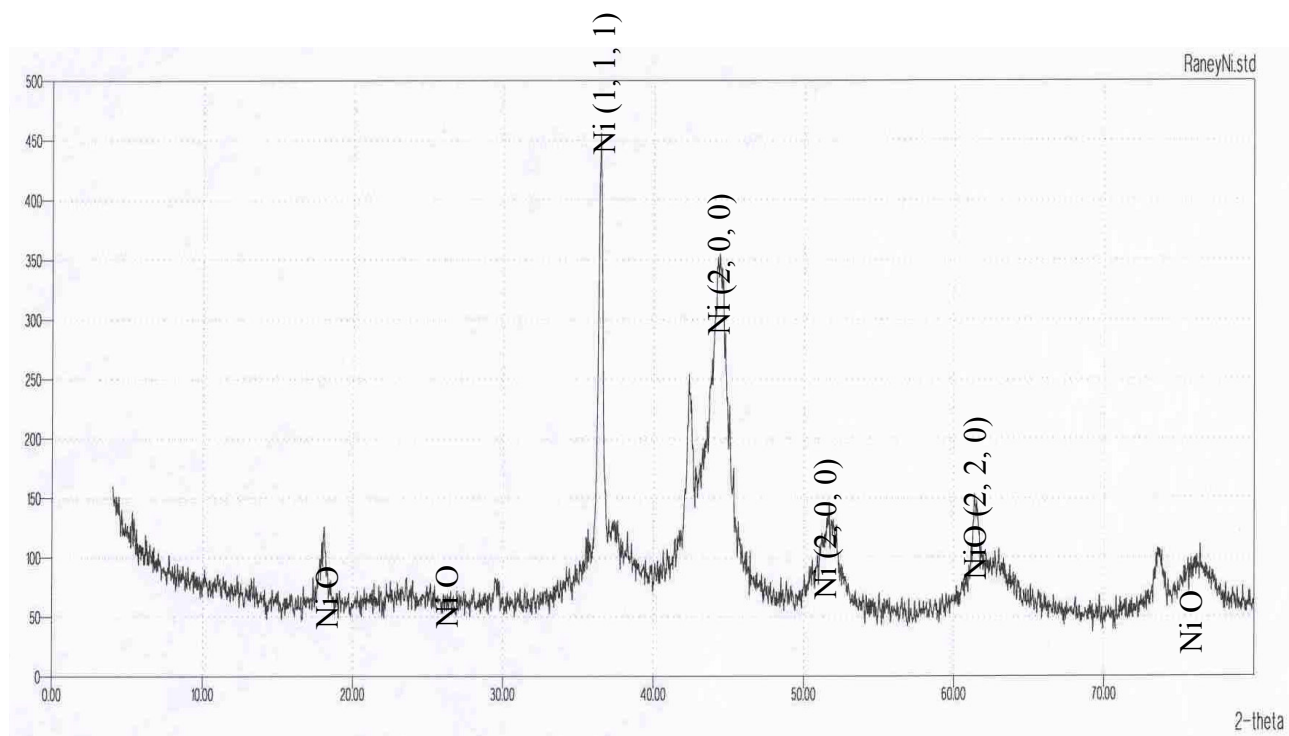


Figure 4-28: XRD Patterns of H₂O₂ Passivated Raney-Ni Catalyst

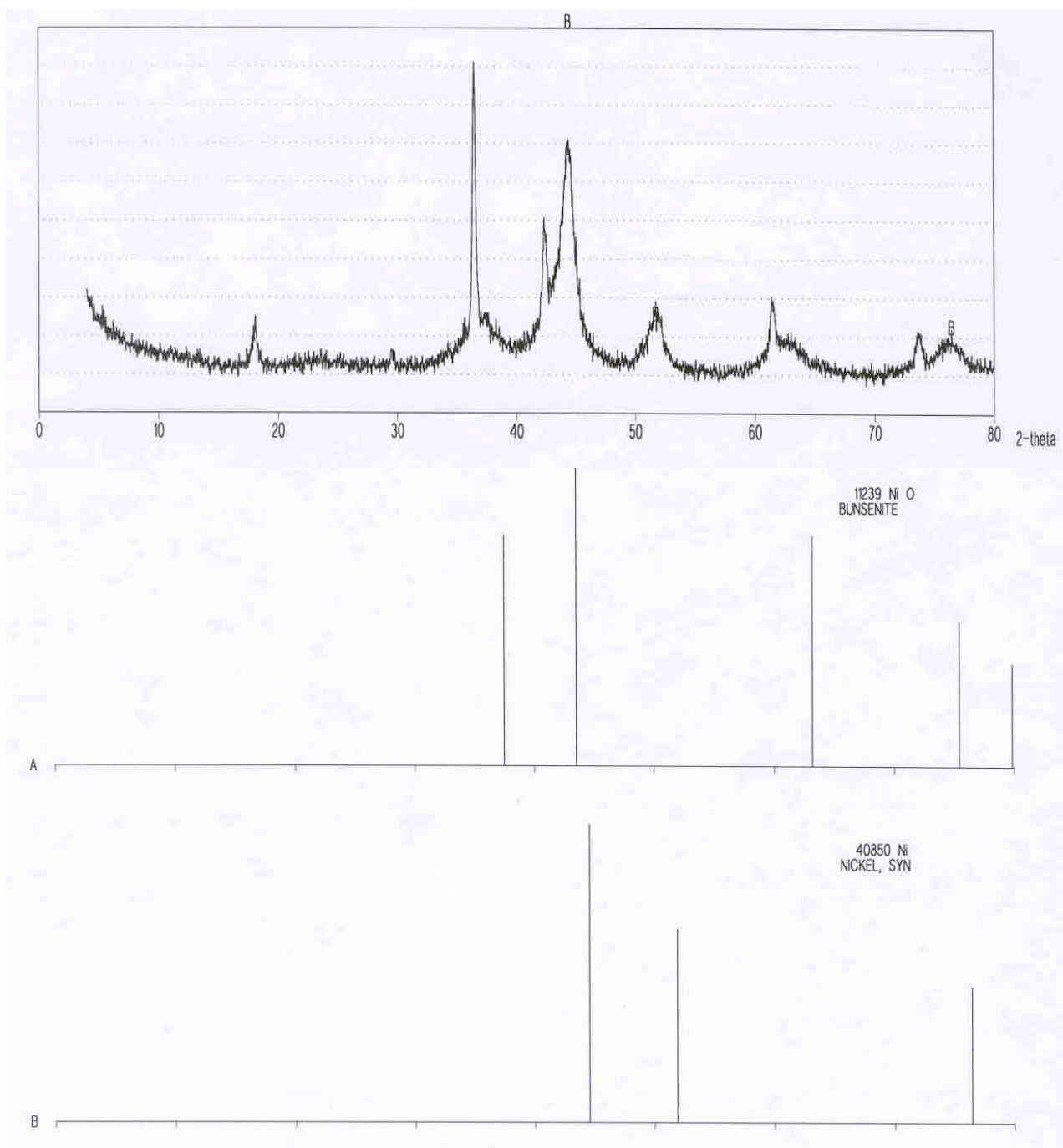
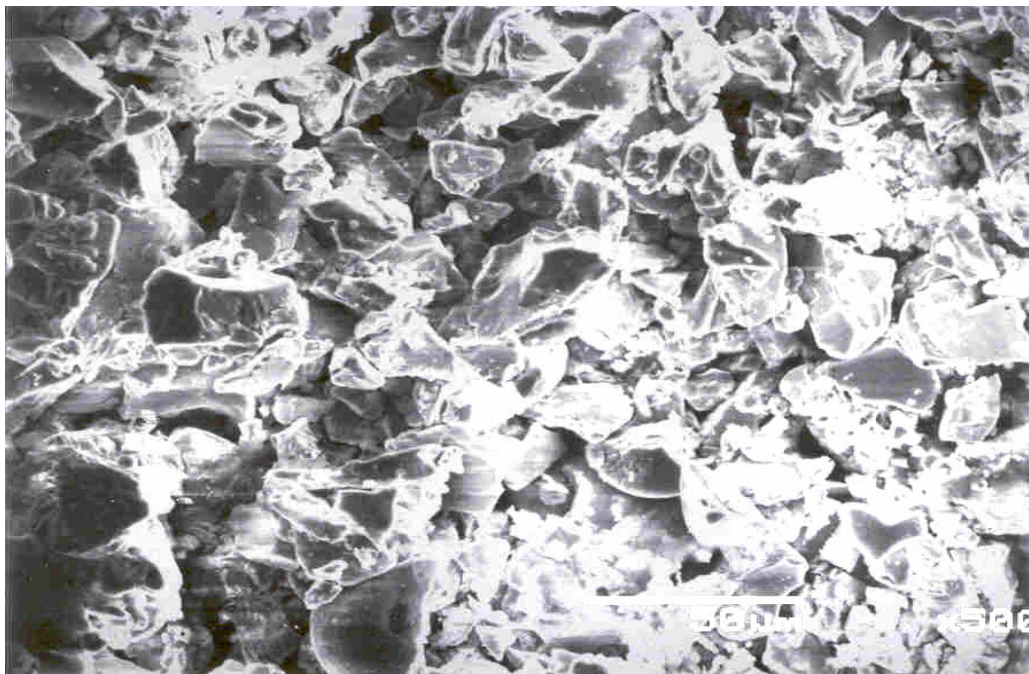
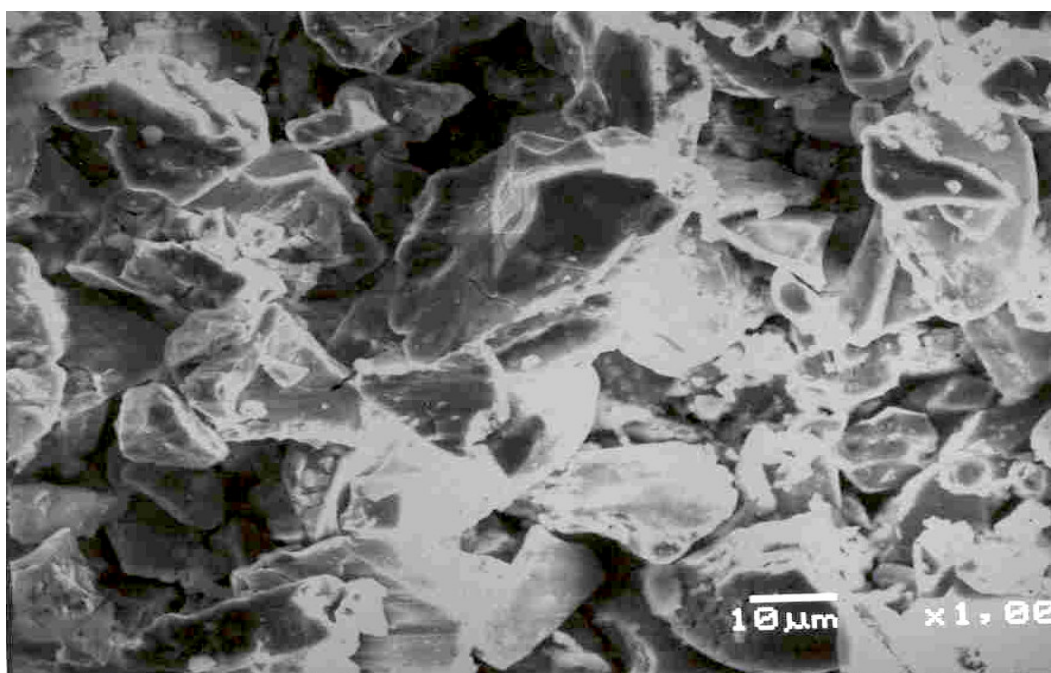


Figure 4-29: XRD Patterns of H_2O_2 Passivated Raney-Ni Catalyst



**Figure 4-30: SEM Micrograph of H₂O₂ Passivated Raney-Ni Catalyst
(500X magnification)**



**Figure 4-31: SEM Micrograph of H₂O₂ Passivated Raney-Ni Catalyst
(1000X magnification)**

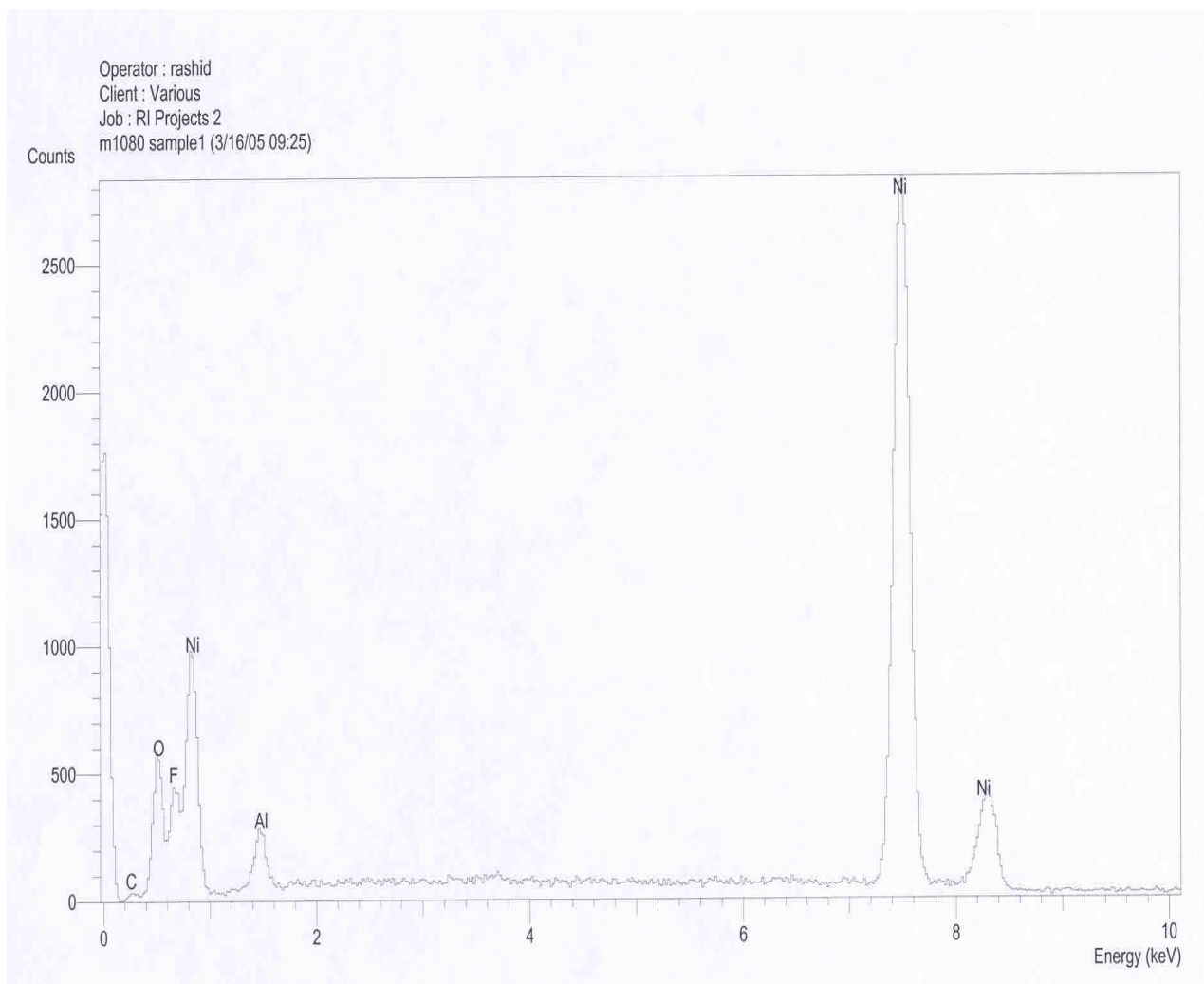


Figure 4-32: EDS Spectra of H_2O_2 Passivated Raney-Ni Catalyst

Parameters	Values (%)
Ni	87.8
O	9.34
Al	2.67
Si	0.14

Table 4-11: Elemental Analysis of H_2O_2 Passivated Raney Ni Catalyst

The XRD patterns in shown in figures have four prominent peaks which correspond to (1,1,1), (2,0,0), (2,2,0) and (2,2,2) of the standard nickel XRD patterns Higher crystallinity of the catalyst can be inferred from the sharp and pointed peaks. The peaks corresponding to NiO very small and swallow indicating that little NiO is present in the sample. The NiO content is less than 10 %. This may be hypothesized to be present on the surface as a result of the slow oxidation of Ni along with adsorbed H₂. Hence from the XRD patterns, it can be concluded that Raney-Ni catalyst contains crystalline Ni and little NiO representing higher active surface area and catalyst activity.

4.3.3. Scanning Electron Microscopy (SEM)

Scanning electron microscopy was carried out to determine the elemental composition and microstructure of the passivated catalyst sample. In this method an electron spot of 5 nm minimum is focused on the sample. This spot is then moved over a small area by means of a set of deflecting coils. This area is displayed highly magnified on a cathode ray tube (CRT) by focusing the current passing through the scanning coils to pass through the corresponding deflecting coils. The CTR image can be transferred to the photographic paper. The passivated catalyst sample was held with conducting black ink and adhesive conductive copper tape attached to sample holder. The imaging was performed in Secondary Electron (SEI) mode. The Energy dispersive spectral (EDS) and semiquantitative analysis data of the passivated Raney-Ni sample were obtained.

Figure 4-30 and Figure 4-31 represents the SEM micrograph the passivated catalyst samples. The micrographs have a magnified resolution of 500 and 1000 times

respectively. The micrograph clearly suggests that the particles are of irregular shape and have different sizes varying from submicron to 25 microns. The micrograph with 1000 resolution shows clearly that the particles have sharp edges and not fused into one another. This suggests that virtually no sintering of the catalyst took place. However, the sintering in the microporous structure having pores of less than 100 Å in each particle can not be identified in these micrographs.

Figure 4-32 represents the SEM-EDS micrograph of the passivated catalyst samples. The semiquantitative analysis of the EDS reveals that the passivated Raney-Ni have less than 3 % Al, while the content of NiO in the sample is approximately 10 %.

4.3.4. BET Surface Area and Pore Size Distribution

BET surface area and pore size distribution of the catalyst was obtained by Rahman [83]. Since the catalyst system and the experimental condition were identical to that being used in this study, the results obtained by him still hold for our H₂O₂ passivated catalyst system. The BET surface area of the passivated Raney-Ni catalyst can be measured by using the adsorption of a liquid N₂ on the catalyst surface. The value of the BET surface area of the H₂O₂ passivated catalyst was found to be 72 m²/g. Details about the experimental procedure and the other conditions have been reported by him [83]. The equipment used was SORPTOMATIC in which the volume of the gas adsorbed was obtained by measuring the decrease in the pressure resulting from the adsorption of a portion of N₂ gas. Experimental procedure and other details of the method have been given reported [83].

Pore Size (° A)	% Pores
37-100	0
100-1000	17
1000-10000	70
>10000	13

Table 4-12: Pore Size Distribution of Passivated Raney-Ni Catalyst

Parameters	Values
Particle Diameter	25.06 micron
BET Surface Area	72 m ² /g
Density	5.122 g/cm ³
Ni content	88 %
NiO content	10 %
Average Particle Size	25 micron
Mol Weight	58.71

Table 4-13: Characteristic Values of Passivated Raney-Ni Catalyst

Pore size distribution analysis of the catalyst was obtained by employing Quantachrome Microscan Particle Size Analyzer. The method consist of making sediment of the passivated catalyst in an appropriate liquid. The absorption of the falling particle in the liquid is measured and converted into particle size using sample density, liquid viscosity and temperature. The average particle diameter is 25.06 micron. Density of catalyst is required for the particle size analysis. The density of the catalyst was found to be 5.2212 g/cm³ by using helium displacement method [83].

Based on the XRD, SEM, pore size distribution and ICP-AES analysis, the complete characterization the passivated Raney-Ni catalyst have been listed in Table 4-13

4.4. CO Removal Study on Raney-Ni Electrode

The amount of CO oxidation on planer Ni electrode is of the order of few nano moles. As described earlier, CO removed by planer Ni electrode by exposing with of 1 % CO for 20 minutes is 1.88×10^{-4} μ moles. Smaller value of CO oxidation was apparently due to smaller active area of the planer electrode (0.3 cm²). In order to obtain a significant CO oxidation, Raney-Ni catalyst is used, which has significantly higher surface area.

4.4.1. Cyclic Voltammetry of Raney-Ni Electrode under N₂

Cyclic voltammogram of the N₂ exposed Raney-Ni electrode functioning as working electrode in the electrochemical cell was obtained under N₂ blanket. The Raney-Ni electrode was constructed in a cylindrical glass tube of approximately 14 mm diameter

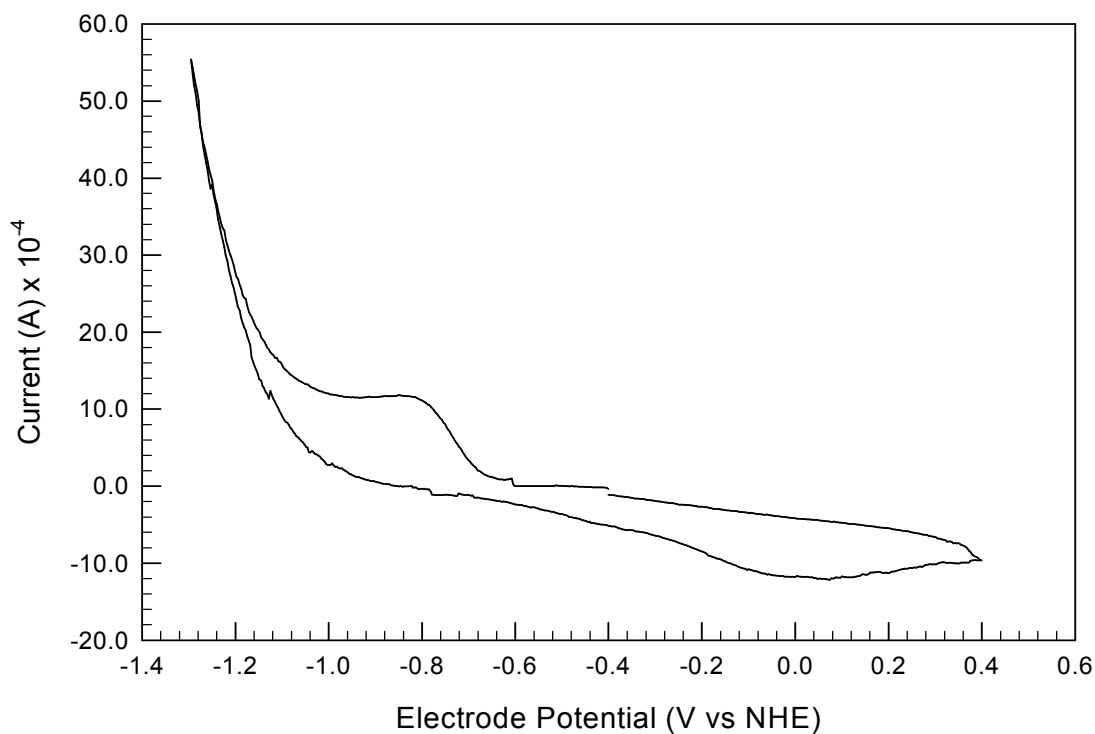


Figure 4-33: Complete CV of N₂ Exposed Raney-Ni Electrode

Parameters	Range/Values
Equilibration time (sec)	900
Initial potential (V vs NHE)	-0.4
First vertex potential (V vs NHE)	-1.4
Second vertex potential (V vs NHE)	+0.4
Final potential	-0.4
Scan rate (mV/sec)	10
Open circuit potential (V vs NHE)	-0.628

Table 4-14: CV Parameters of N₂ Exposed Raney-Ni Electrode

housing 0.9 gram of the Raney-Ni catalyst. The electrode was exposed to N₂ by continuously bubbling N₂ gas in the electrolyte solution over Raney-Ni catalyst bed at a flow rate of 50 ml/min for 30 minutes. The scan rate for the experimentation was 10 mV/sec. Exact parametric details of the experimentation have been listed in Table 4-14. Figure 4-33 and Figure 4-34 represents the cyclic voltammogram obtained for the N₂ exposed Raney-Ni electrode.

From the voltammogram, it is clear that at the beginning of the cathodic scan (-0.4 V) current response of the working electrode is zero representing absence of any electrochemical activity at the catalyst surface. As the electrode is further negatively scanned the current response of the cathodic current starts rising at -0.7 V and it keeps on rising with potential. This rise in the cathodic current is essentially due to the occurrence of the H₂ evolution reaction at the electrode surface. This observation is in agreement with the planer Ni electrode where H₂ evolution also takes place at the same potential.

However, contrary to the cathodic current response of the planer Ni electrode, it is to be noted that the current response seems to be following a plateau for a brief period before exponentially rising with the electrode potential. Observation of this plateau can be attributed to signifying higher surface area as compared to the planer Ni electrode. After this short plateau, H₂ evolution reaction further speeds up with the potential increasing to more cathodic values giving much higher current. In addition, it is to be noted that current response of the Raney-Ni electrode between -0.4 V upto -0.7 V potential scanning is not zero as was in the case of the planer electrode. This is essentially

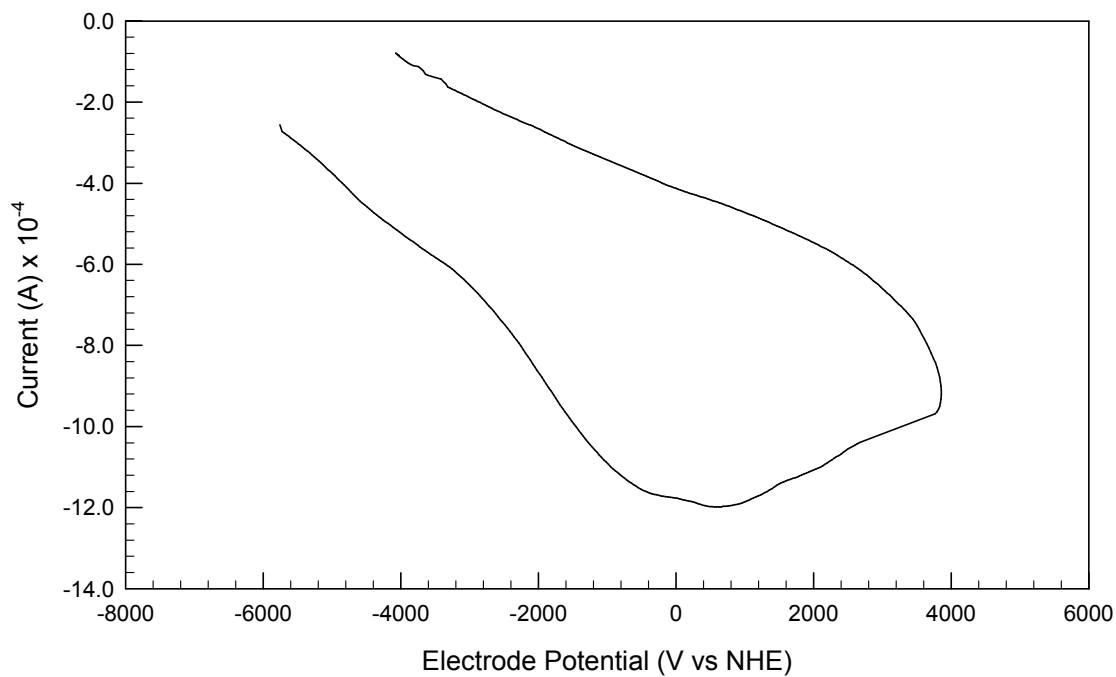


Figure 4-34: CV of N₂ Exposed Raney-Ni Electrode

Parameters	Range/Values
Equilibration time (sec)	600
Initial potential (V vs NHE)	-0.6
Vertex potential (V vs NHE)	+0.4
Final potential (V vs NHE)	-0.6
Scan rate (mV/sec)	10
Open Circuit Potential (V vs NHE) (measured)	-0.628
Area of the electrode (m ²)	63

Table 4-15: Parameters of N₂ Exposed Raney-Ni Electrode

due to the higher resistance of the electrolytic solution. Here, it is significantly higher because the catalyst is highly porous.

During the start of the anodic scan, the current response of the electrode is essentially zero due to the absence of any electrochemical activity at the electrode surface. As the electrode is further scanned a sharp peak is observed around 0.025 V, attributing to the electrochemical activity at that particular anodic potential. As in the case of the planer electrode, apparently this anodic peak is due to the dissolution of the Raney-Ni. However a major shift of 275 mV in the dissolution potential is observed. This huge shift in the dissolution potential is essentially due to significantly higher surface area of the Raney-Ni electrode. The active area of the Raney-Ni electrode is many times higher than that of the planner electrode suggesting significant double layer charging. Hence the occurrence of the peak at +0.025 V is essentially due to the passivation of the Raney-Ni electrode. The observation of the peak during the anodic scanning is in close agreement to that of the Ni oxidation results reported by Hori et al. [78].

From the preceding discussions about the cyclic voltammogram of the Raney-Ni electrode under N₂ environment, two important conclusions could be made. Firstly, Ni dissolution takes place at + 0.025 V. Secondly, H₂ evolution reaction starts at the -0.7 V.

4.4.2. Cyclic Voltammetry of CO Exposed Raney-Ni Electrode

In order to demonstrate the preferential adsorption of CO on Raney-Ni electrode surface, cyclic voltammetric experiments of Raney-Ni electrode were obtained

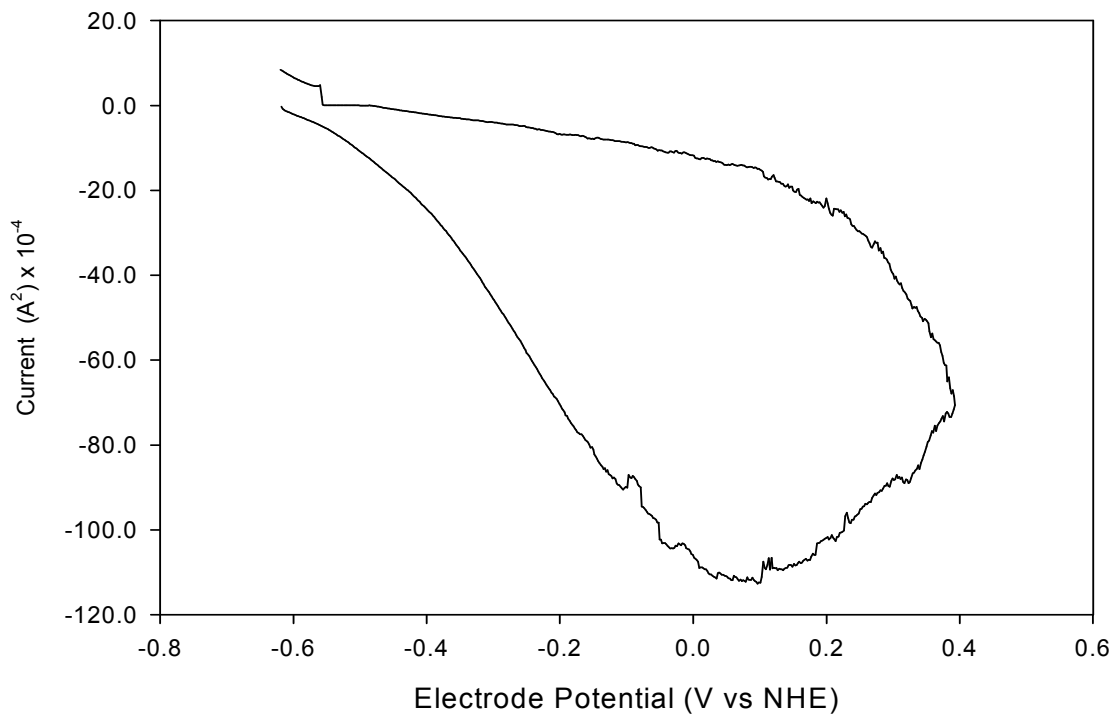


Figure 4-35: CV of CO Exposed Raney-Ni Electrode

Parameters	Range/Values
Equilibration time (Sec)	900
Initial potential (V vs NHE)	-0.6
Final potential	-0.4
Scan rate (mV/sec)	10
Open Circuit Potential (V vs NHE)	-0.630
Sample Area (m ²)	63
No of Cycles	3

Table 4-16: CV Parameters of CO Exposed Raney-Ni Electrode

Following the procedures experimental procedures discussed earlier. The details discussions about the feature of cyclic voltammogram of carbon monoxide exposed Raney-Ni electrode have been presented in this section.

The electrode surface was exposed to CO by continuously bubbling of 1 % CO gas through the electrolyte solution at a flow rate of 50 ml/min for 30 minutes. This flow rate of CO gas was maintained high enough to keep the catalyst bed in the fluidized state. This was done to achieve maximum adsorption of CO on the Raney-Ni catalyst surface. It was anticipated that during 30 minutes significant amount of CO gets adsorbed. During this process, CO might also get dissolved in the electrolytic solution, which was removed by continuous purging of N₂ through the electrolyte solution after flow of CO gas was stopped. Nitrogen was continuously passed through the electrolytic solution for 30 minutes, for the removal of CO. Subsequently flow of N₂ gas through the electrolyte solution was stopped and catalyst bed was allowed to settle. The flow of N₂ flow was still maintained atop of the electrolyte solution to prevent any unwanted dissolution of oxygen or oxygen containing species and to maintain the N₂ blanket over the electrolyte solution.

Figure 4-36 represents the voltammogram for the carbon monoxide exposed Raney-Ni electrode. The parametric details of the experimentation have been listed in Table 4-16 . Although CO exposed voltammogram of the Raney-Ni electrode has more or less similar trends and features but their characteristic are quite different than that obtained under N₂. Figure 4-36 also shows the comparison of the voltammogram under N₂ and CO. As in the case of the planer Ni electrode, during anodic scan Raney-Ni electrode also exhibits

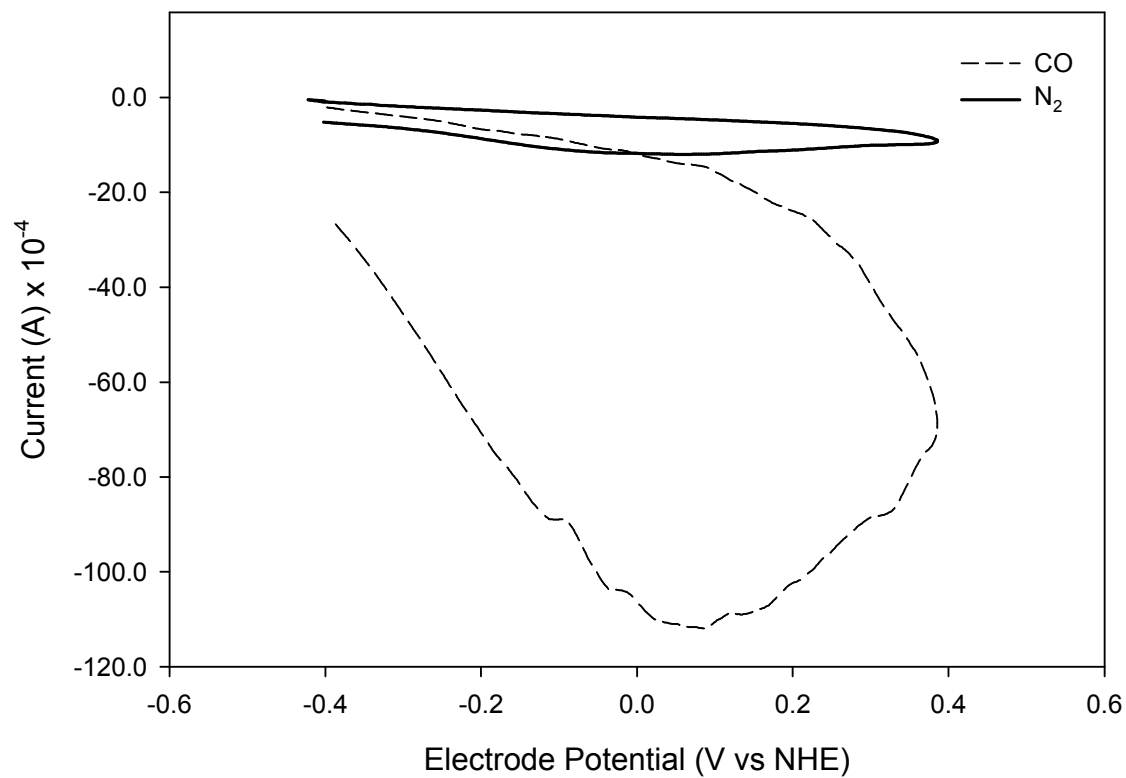


Figure 4-36: CV of CO and N₂ Exposed Raney-Ni Electrode

anodic peak at +0.225 V. The position of the anodic peak is significantly different than that observed in the case of the N₂ exposed Raney-Ni electrode, where dissolution occurs at +0.025 V. A potential shift of approximately 200 mV is observed in anodic peak position. As discussed earlier, in the case of carbon monoxide exposed planer Ni electrode, this anodic peak is essentially due to the oxidation of adsorbed carbon monoxide. This means that presence of carbon monoxide is preventing the oxidation of the Raney-Ni electrode. The magnitude of the peak shift in this case is considerably higher than that observed in the case of the planer Ni electrode where it was approximately 130 mV. This can be attributed to the higher surface area of the Raney-Ni electrode. From the above observations, it can be concluded that carbon monoxide gets adsorbed on Raney-Ni electrode.

4.4.3. Removal of Adsorbed CO from Raney-Ni Electrode

In agreement with the carbon monoxide removal from the planer Ni electrode, the adsorbed carbon monoxide from the Raney nickel electrode can be removed by using cyclic voltammetry. Figure 4-37 shows the cyclic voltammogram of the Raney-Ni electrode obtained during the electrooxidation of the adsorbed carbon monoxide. The details about the parameters of the experimentation have been listed in Table 4-17.

At the start of the anodic scanning (-0.6 V), the current response is zero representing absence of any electrochemical activity. However the current starts increasing at -0.4 V represents the onset of CO electrooxidation. As the electrode is scanned further anodically the current also increases, representing a peak at +0.15 V. Therefore from this

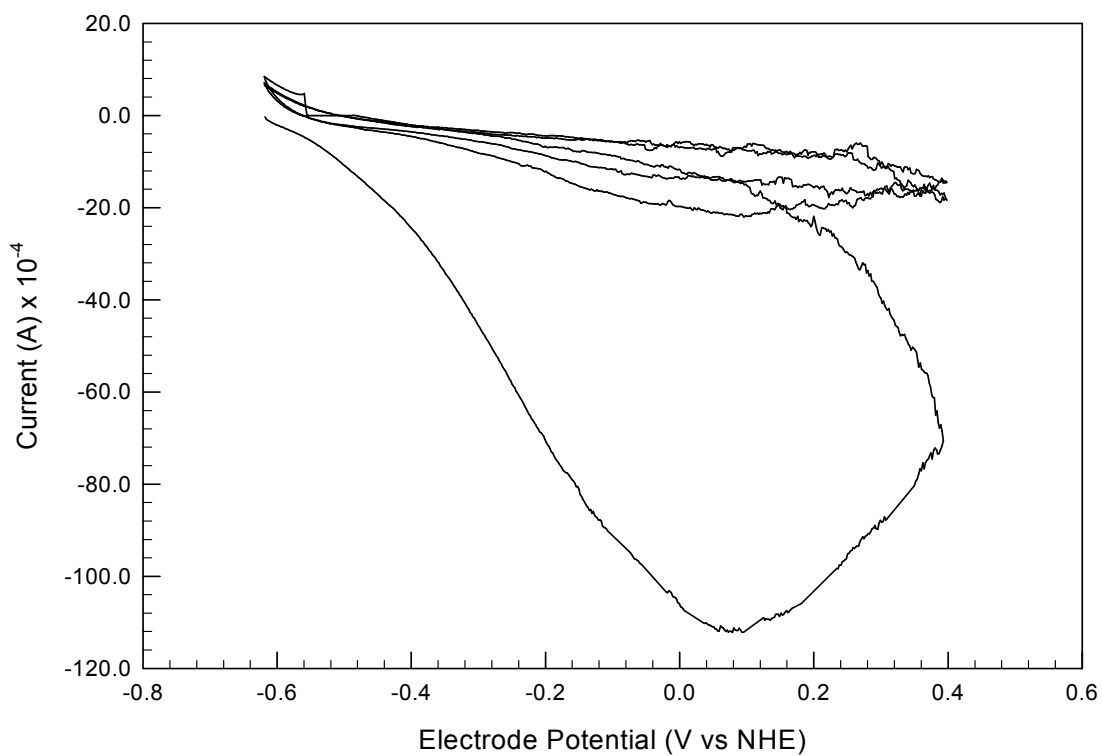


Figure 4-37: Cyclic Voltammogram of CO Electrooxidation on Raney Ni Electrode

Parameters	Range/Values
Equilibration time (Sec)	120
Initial potential (V vs NHE)	-0.4
Final potential (V vs NHE)	+0.4
Scan rate (mV/sec)	20
Open Circuit Potential (V vs NHE)	-0.638
No of cycles	3

Table 4-17: CV Parameters of CO Electrooxidation on Raney-Ni Electrode

voltammogram, it is clear that CO oxidation takes place at +0.15 V.

Multiple voltammogram of the CO exposed Raney-Ni electrode was observed in order to check the validity of the observation of the planer Ni electrode, where complete oxidation takes place in the first scan. Figure 4-37 represents the multiple cyclic voltammogram of the CO electrooxidation on Raney-Ni electrode. It is clear that during second and subsequent cycle, no CO removal peak is present. This observation essentially represents complete removal of CO took place.

As in the case of the planer Ni electrode, the area of the CO electrooxidation curve could be used to calculate the amount of the CO oxidized by the Raney-Ni electrode. The area of the peak in Figure 4-37 is approximately -500 m C. By using the Faraday's law given in equation 4.1, number of moles of CO electrooxidized is found to be 5.182 μ moles.

4.5. Parametric Study of CO Removal on Raney-Ni Electrode

As in the case of the planer Ni electrode, CO oxidation on Raney-Ni electrode also depends upon the CO concentration, exposure time and flow rate of the CO gas. It is anticipated that the affect of these parameter will be similar to that observed in the case of the planer Ni electrode. In addition to the above parameters, it was observed that the CO removal rate significantly depends upon the scan rate of the anodic scanning experiments. The effect of the scan rate on CO removal is presented in next section.

4.5.1.Effect of Scan Rate

In order to study the effect of the scan rate carbon monoxide electrooxidation voltammogram were obtained at 0.1, 1, 10 and 20 mV/sec, respectively.

Figure 4-38 shows variation of the carbon monoxide electrooxidation curves with scan rate. It is clear that, the peak area or moles of carbon monoxide electrooxidized varies significantly with the scan rate. It is also clear that the highest area of the carbon monoxide removal peak (moles of CO electrooxidized) is in the case of the highest scan rate (20 mV/sec) investigated, while the smallest area was observed in the case of the smallest scan rate of 0.1 mV/sec. This remarkable variation of the carbon monoxide removal can be attributed to the significantly higher surface area of the Raney-Ni catalyst.

From the above voltammogram, another interesting observation can be inferred regarding the variation of the carbon monoxide electrooxidation peak position with scan rate. The carbon monoxide peak is at 0.35 V potential for 20 scan rate, while it is observed approximately at +0.25 V at 10 mV/sec and in the case of 1mV/sec scan rate it is at +0.15 volt. Such shifting of the peak position was not observed earlier in the case of the planer Ni electrode due to smaller active area.

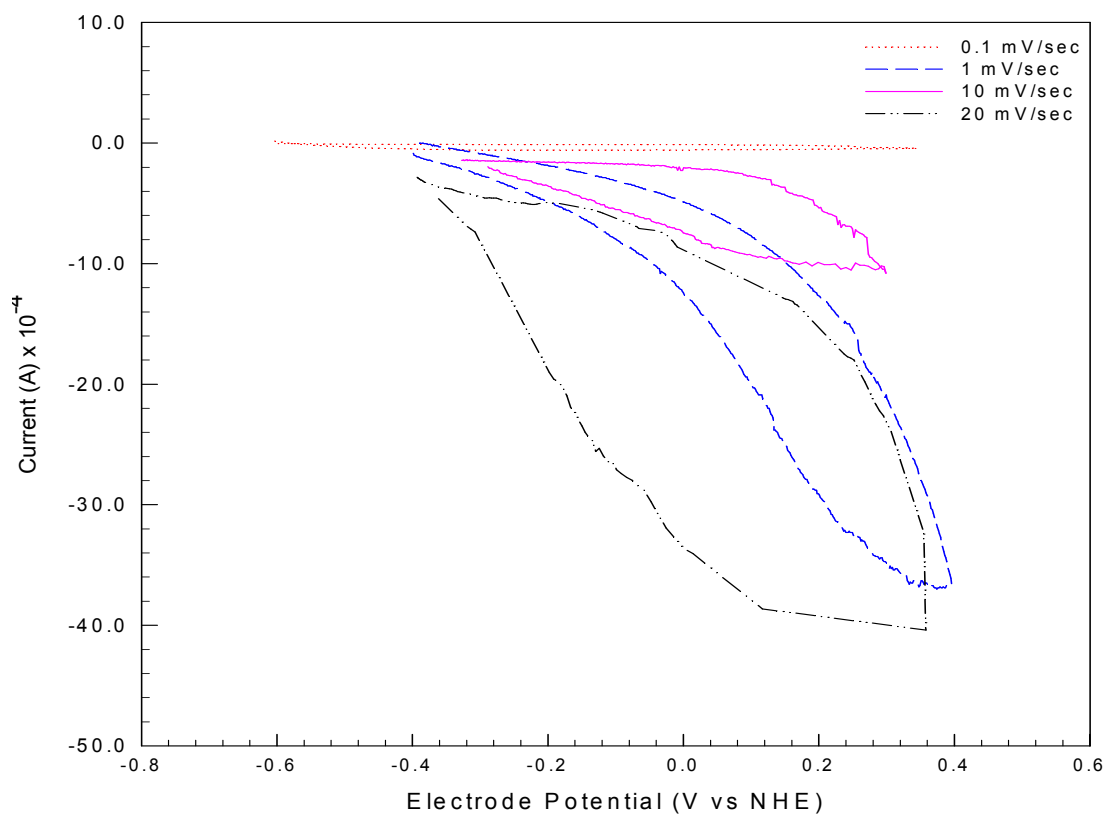


Figure 4-38: Effect of Scan Rate on CO Electrooxidation on Raney-Ni Electrode

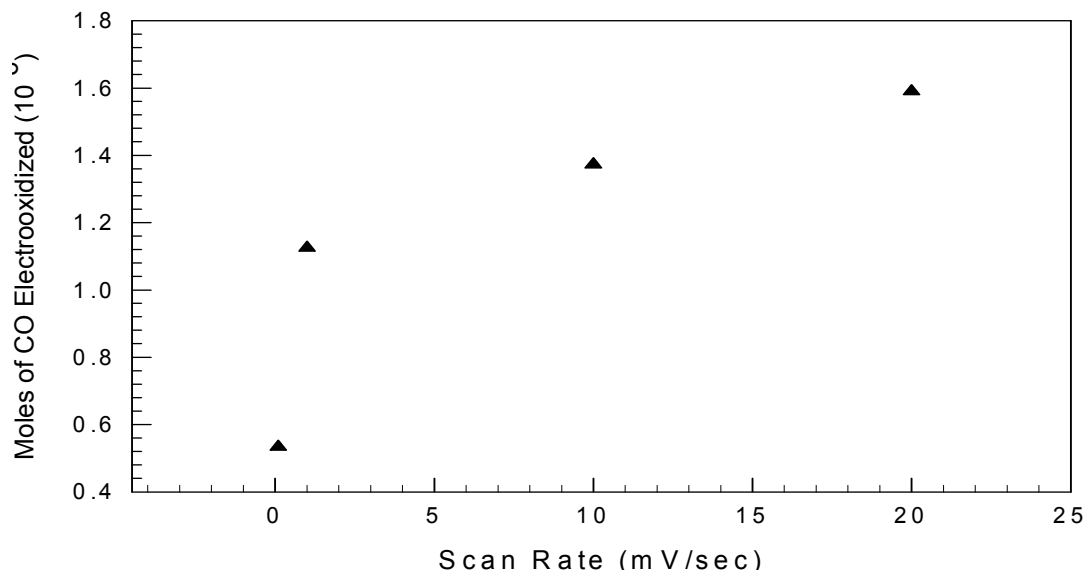


Figure 4-39: Amount of CO Electrooxidized vs Scan Rate

5. CONCLUSIONS & RECOMMENDATIONS

5.1. Conclusions

The search for an effective carbon monoxide removal method has led to the development of electrochemical filter proposes by Laxmanan et al [67-69]. It uses Pt-Ru as catalyst for the electrochemical filtering of carbon monoxide from reformat with excellent efficiency and effectiveness. Platinum is expensive and supply is limited.]. The present work was undertaken to explore the possibility of using Ni/Raney-Ni catalyst in the electrochemical filter for carbon monoxide removal from H₂ gas. The important conclusions from the present study can be stated as follows:

1. Electrochemical removal of carbon monoxide is possible on Ni/Raney-Ni catalyst, a much cheaper catalyst than platinum which is used in recently developed electrochemical filter.
2. In contrast to the earlier works, pertaining to carbon monoxide removal from Ni catalyst by using electroreduction, this work demonstrate that electrooxidation of carbon monoxide can be used for carbon monoxide removal from hydrogen.
3. From the cyclic voltammetric study Ni/ Raney-Ni electrode, it has been found that during cathodic scan hydrogen evolution reaction takes place and passivation of the Ni takes place during the anodic scan of the electrode under N_2 .
4. From the cyclic voltammetry of carbon monoxide exposed Ni/ Raney Ni electrode it has been found that preferential adsorption of CO takes place on Ni electrode.
5. The adsorption of carbon monoxide on Ni/Raney-Ni electrode prevents the Ni dissolution reaction and causes significant delay in the H_2 evolution reaction.
6. carbon monoxide removal depends upon a number of parameters such as active area of catalyst, CO concentration, CO exposure time, flow rate and scan rate etc.
7. Based on the study of the effect of exposure time, concentration and flow rate, it has been found that CO oxidation increases with increasing the exposure time.
8. Amount of carbon monoxide oxidized by Raney-Ni is significantly higher than planer Ni electrode verifying the dependence of active area.

5.2. Recommendations

This is the first work which establishes that Ni/Raney Ni catalyst could be used in the electrochemical filter to remove carbon monoxide from hydrogen streams (reformate

gas). Some of the recommendations for future study for pertaining to the performance improvement of the electrochemical method of carbon monoxide removal from hydrogen are as follows;

1. Use Raney-Ni gas diffusion electrode so that mass transfer resistance could be minimized.
2. Prepare a cell with higher surface area and demonstrate reduction in carbon monoxide concentration using gas chromatography.
3. Develop a mathematical model for the performance of the electrochemical filter so that parameters such as, effect of flow rate, exposure time and catalyst loading etc could be optimized.
4. Eventually its performance should be investigated under integrated reformer and fuel cell system.

NOMENCLATURE

NHE= Normal Hydrogen Electrode

SCE= Saturated Calomel Electrode

CV= Cyclic voltammetry

A= Surface area of the electrode

D = Average diameter of the carbon monoxide molecule

F= Faraday's constant

i = Exchange current density

N_A = Avogadro number

n = Number of the electron involves in the reaction

Q = Charge transferred during the reaction

N= Number of moles of carbon monoxide electrooxidized

REFERENCES

1. S. Kawatsu, "Advanced PEFC Development for Fuel Cell Powered Vehicles", *J. Power Sources*, **71**, 150-155 (1998).
2. B. Andreaus, L. Danon, L. Gulber and G. G. Schere, "Modeling Studies of the Carbon Monoxide Poisoning in Polymer Electrolyte Fuel Cells (PEFC)", *J. Electrochemistry*, **82-83** (1997).
3. S. U. Rahman, J. W. Weidner, S. M. J. Zaidi, N. A. Baghli and A. Nafees, "Approaches to Hydrocarbon Fuel Processing for Automotive and Fuel Cell Systems", *4th Middle East PetroTech-2003*, Manama, Bahrain, October (2003).
4. R. J. Bellows, "Technical Challenges for Hydrocarbon Fuel Processing", *DOE/ONR Workshop on Fuel Processing*, Baltimore, MD, October (1999).
5. C. Song, "Catalytic Fuel Processing for Low and High Temperature Fuel Cell Application: Challenges and Opportunities", *AIChE Spring Meeting, LA* March (2002).
6. Y. Y. Tong, H.S. Kim, P. K. Babu, P. Waszczuk, A. Wieckowski and E. Oldfield, "An NMR Investigation of CO Tolerance in Pt/Ru Catalyst", *J. American Chemical Society*, **124/3**, 468-473 (2002).
7. R. J. Bellows, "Less Conventional Approaches to Hydrocarbon Fuel Processing", *AIChE Spring National Meeting*, New Orleans, LA, March (2002).
8. S. H. Oh and R. M. Sinkeevitch, "CO Removal from Hydrogen Rich Fuel Feed Streams by Selective Catalytic Oxidation", *J. Catalysis*, **142**, 254-262 (1993).
9. P. Liu, "Two New approaches for CO Removal from Reformate Fuel for the PEMFC Application", *Fuel Cell Seminar Abstracts*, OR, November (2000).
10. T. Haung, R. E. White, J. W. Weidner and W Huang, "Development of a Novel Proton Exchange Membrane Fuel Cell Anode", *J. Electrochemical Society*, **149** (7), A862-A867 (2002)
11. S. Ball, A. Hodgkinson, G. Hoogers, S. Maniguet, D. Thompsett and B. Wong, "The Proton Exchange Membrane Fuel Cell Performance of a Carbon Supported Pt-Mo Catalyst Operating on Reformate", *Electrochemical and Solid State letters*, **5** (2) , A31 – A34 (2002).

12. Y. F. Han, M. J. Kahlich, M. Kinne, and R. J. Behm, “Kinetic study of the Selective CO Oxidation in H₂-Rich Gas on a Ru/-Al₂O₃ Catalyst”, *Physical Chemistry*, (2001).
13. M. M. Schubert, Wojtech Plzak, Jürgen Garcke and R. Jürgen Behm, “Activity, Selectivity and Long-Term Stability of Different Metal Oxide Supported Gold Catalysts for the Preferential Carbon Monoxide Oxidation in H₂-rich Gas”, *Catalysis Letters*, (2001).
14. M. M. Schubert, S. Hackenberg, A. C. van Veen, M. Muhler, V. Plzak and R. J. Behm, “CO Oxidation over Supported Gold Catalysts: I. Inert and Active Support Materials and their role in the Reaction Process”, *J. Catalysis*, **197**, 113-122 (2001).
15. T. J. Huang, K. L. Cheung, H., W., Yang and Wei-Ping Dow, “Effect of Cr Addition on Supported Cu Catalyst for CO Oxidation”, *Applied Catalysis A: General*, **174**, 199-206 (1998).
16. Watanabe, H. Igarashi and T. Fujino, “Design of Carbon Monoxide Tolerant Anode Catalysts for Polymer Electrolyte Fuel Cells”, *J. Electroanal. Chem.*, **67**(12), 1194-1196 (1999).
17. Hawk, A. Smirnova, J. M. Fenton and H. R. Kunz, “PEMFC Electrode Layer Modification for Improved High Temperature Performance”, *The 204th Meeting, The Electrochemical Society, Inc.*, Extended Abstract # **123**, October, (2003).
18. Y. Y. Tong, H.S. Kim, P. K. Babu, P. Waszczuk, A. Wieckowski and E. Oldfield, “An NMR Investigation of CO Tolerance in Pt/Ru Catalyst”, *J. American Chemical Society*, **124**/3 (2002).
19. A. Gasteiger, N. Markovic and P. N. Ross Jr., “H₂ and CO Electro-oxidation on well Characterized Pt, Ru and Pt-Ru. 1. Rotating Disk electrode Studies of CO/H₂ Mixtures at 62 °C”, *J. Physical Chemistry: B*, **99**, 16757–16767 (1995).
20. A. Gasteiger, N. Markovic and P. N. Ross Jr., “Hydrogen and Carbon Monoxide Electro-oxidation on well Characterized Pt, Ru and Pt-Ru. 2. Rotating Disk Electrode Studies of Pure Gases Including Temperature Effects”, *J. Physical Chemistry: B*, **99**, 829–8301 (1995).

21. D. C. Papageorgopoulos and F. A. de Bruijin, "Examining a Potential Fuel Cell Poison", *J. Electrochemical Society*, **149/2**, A140–A145 (2002).
22. W. Ruettinger, O. Ilinich and R. J. Farrauto, "A New Generation of Water Gas Shift Catalyst for Fuel Cell Applications", *J. Power Sources*, **118/1-2**, 61-65 May (2003).
23. G. Jacobs, P. M. Patterson, L. Williams, E. Chenu, D. Sparks, G. Thomas and B. H. Davis, "Water Gas Shift: In Situ Spectroscopic Studies of Noble Metal Promoted Ceria Catalysts for CO Removal in Fuel Cell Reformers and Mechanistic Implications", *Applied Catalysis: A, :General*, (2004).
24. T. Bunluesin, R. J. Gorte and G. W. Graham, "Studies of the Water-Gas-Shift Reaction on Ceria-supported Pt, Pd, and Rh: Implications for Oxygen-Storage Properties", *Applied Catalysis B: Environmental*, **15**, 107 (1998)
25. Y. Li, Q. Fu and M. F. Stephanopoulos, "Low-Temperature Water-Gas Shift Reaction over Cu and Ni-loaded Cerium Oxide Catalysts," *Applied Catalysis: B* **27**, 179 (2000).
26. G. Sedmak, S. Hocevar and J. Levec, "Kinetics of Selective Carbon Monoxide Oxidation in excess of H₂ over Nanostructured Cu_{0.1}Ce_{0.9}O_{2-y} Catalyst", *J. Catalysis*, **231**, 135 (2003).
27. A. Luengnaruemitchai, S. Osuwan and E. Gulari, "Selective Catalytic Oxidation of Carbon Monoxide in the Presence of Hydrogen over Gold Catalyst", *Int. J. Hydrogen Energy*, **29** (2004) 429.
28. G. Avgouropoulos, T. Ioannidis, "Selective Carbon Monoxide Oxidation over CuO-CeO₂ Catalyst Prepared via the Urea-Nitrate Combustion Method", *Applied Catalysis A: General*, **244**, 155 (2003).
29. P. V. Menacherry and W. C. Pfefferle; "Method for Operation of a Catalytic Reactor", *US Patent # 6514472*, February (2003).
30. M. A. Meltser and M. M. Hoch, "Controlled CO Preferential Oxidation", *US Patent # 5637415*, June (1997).
31. N. E. Vanderburgh, V. T. Nguyen and J. Guante, Jr., "Device for Staged CO Oxidation", *US Patent # 5271916*, June (1993).

32. T. Soma, T. Takahashi and M. Isomura, "Method for Removing CO from Reformed Gas", *US Patent # 5612012*, April (2002).
33. R. F. Buswell, R. Cohen, L. McNeilly and S. D. Watkins, "Apparatus for the two-stage Selective Oxidation of CO in a H₂ containing Gas Mixture", *US Patent # 750076*, May (1998).
34. C. D. Dudfield, R. Chen and P. L. Adcock, "Evaluation and Modeling of a CO Selective Oxidation Reactor for Solid Polymer Fuel Cell Automotive Applications", *J. Power Sources*, **85**, 237-244 (2000).
35. M. Nagamiya, M. Yamashita, I. Maeda, M. Yamaoka, M. Taki, S. Aoyama and Y. Araki, "CO Reducing Device for Reducing CO in Reformate Gas", *US Patent # 6332901*, December (2001).
36. J. W. Park, J. H. Jeong, W. L. Yoon, C. S. Kim and Y. W. Rhee, "Selective Oxidation of CO in Hydrogen Rich Stream over Cu-Ce Catalyst Promoted with Transition metals", *2nd European PEMFC Forum*, 733-745, Lucerne, Switzerland; 30th June–4th July (2003).
37. M. Myers, "Reformate Post Processing for CO Clean Up", *Annual National Laboratory R&D Meeting*, Los Alamos, NM, 28-29 July (2000).
38. M. Inbody, R. Borup, J. Tafuya, J. Hedstorm and B. Morton, "Carbon Monoxide Clean Up Developments", *DOE Review, OTT Fuel Cell Program*, June (2000).
39. P. Chin, G.W. Roberts, J. J. Spivey and X. Sun, "CO Preferential Oxidation Support Study for Fuel Cell Applications", *DOE NETL Meeting*, June 2003.
40. R. M. Privette, T. J. Flynn, M. A. Pema, K. E. Kneidel, D. L. King and M. Cooper, "Compact Fuel Processor for Fuel Cell Powered Vehicles", *DOE/EPR/GRI Fuel Cell Technology Conference*, Chicago, Illinois, US, 3-5 August (1999).
41. L. Bromberg, D. R. Cohn and A. Robinovitch, "Plasma Reformer Fuel Cell Systems for Decentralized Power Applications", *Int. J. Hydrogen Energy*, **22**, 83 - 94 (1997).
42. L. Bromberg, D. R. Cohn, A. Robinovitch and N. Alexei, "Hydrogen Manufacturing using Low Current Non Isothermal Plasma Boosted Fuel

- Converter”, *Energy for 21st Century: Hydrogen Energy*, ACS Proceedings, San Diego, LA, (2001).
43. M. Yardimci, O. Sarelie, A. V. Friedman and L. A. Kennedy, “Employing Plasma as Catalyst in H₂ Production”, *Int. J. Hydrogen Energy*, **23**, 1109-1111 (1998).
 44. C. D. Dudfield, R. Chen and P.L. Adcock, “Evaluation and Modeling a CO Selective Oxidation Reactor for Solid Polymer Fuel Cell Automotive Application”, *J. Power Sources*, **85**, 237–244 (2000).
 45. K. H. Ledjeff, J. Rose and R. Wolters, “CO₂ Scrubbing and Methanation as Purification System for PEFC”, *J. Power Sources*, **86/1**, 556-551 (2000).
 46. M. Murthy, M. Esayian, A. Hobson, S. McKenzie, W. Lee and J. M. V. Zee, “The Performance of PEM Fuel Cell Exposed to Transient CO Concentrations”, *Electrochemical and Solid state letters*, October (2001).
 47. S. Takaneka, T. Shimuzu and K. Otsuku, “Complete Removal of CO in Hydrogen Rich Gas Stream through Methanation over Supported Metal Catalysts”, *Int. J. Hydrogen Energy*, (2004).
 48. R. Bellows, “Fuel Processing for PEM Fuel Cell: Engineering Hurdles and Science Opportunity”, *National Science Foundation Workshop.*, VA, USA, November (2001).
 49. S. Sircar and T.C. Golden, “Purification of Hydrogen by Pressure Swing adsorption”, *Separation Science and Technology*, **35/5**, 667-687 (2000).
 50. H. Tamon, K. Kitamura and M. Okazaki, “Adsorption of CO on Activated Carbon Impregnated with Metal Halide”, *AIChE Journal*, **42/2**, 422 (1996)
 51. S. E. Iyuke, W. R. W. Daud, A. B. Mohammed, A. A. H. Kadhum, Z. Faisal and A. M. Shariff, “Application of Sn-Activated Carbon in Pressure Swing Adsorption for Purification of Hydrogen”, *Chemical Engineering Science*, **55**, 4745–4755 (2000).
 52. T. Rehg, D. J. Liu and J. C. Williams and M. Kaiser, “Electro-catalytic Oxidation (ECO) Device to Remove CO from Reformate for Fuel Cell Application”, *US Patent # 6245214*, Jun (2001).

53. E. Yasumoto, K. Hatoh and T. Gamou, "Fuel Cell Device Equipped with Catalyst Material for Removing CO and Method for Removing CO", *US Patent # 5702838*, June (2001).
54. Y. Yasuda, H. Moritsuka and Y. Izaki, "Preparation and Evaluation of CO₂ Permselective Membrane for High Temperature Gas Separation", *JSME International Journal*, **41/4**, 1012 (1998).
55. Saracco and V. Specchia, "Catalytic Inorganic Membrane Reactors: Present Experience and Future Opportunities", *Catalysis Review Science and Engineering*, **36**, 305–384 (1994).
56. S. Uemiya, "State of the Art of Supported Metal Membranes for Gas Separations", *Separation and Purification Methods*, **28**, 51–85 (1999).
57. S. N. Paglieri and J. D. Way, "Innovations in Palladium Membrane Research", *Separation and Purification Methods*, **31/1**, 1-169 (2002).
58. W. S. Winston Ho, "Development of Novel Water Gas Shift Membrane Reactor for Hydrogen Enrichment", *University of Kentucky*, (2002).
59. T. Utaka, K. Sekizawa and K. Eguchi, "CO Removal by Oxygen Assisted Water Gas Shift Reactions over Supported Cu Catalyst", *Applied Catalysis A: General*, **194-195**, 21-26 (2000).
60. D. P. Wilkinson, H. H. Voss, J. Dudley, G. J. Lamont; and V. Basura, "Method and Apparatus for Oxidizing CO in the Reactant Stream of an Electrochemical Fuel Cell", *US Patent # 5432021*, July (1995).
61. M. Hashimoto, M. Mizubuchi, M. Sei, K. Kinugawa and A. Igarshi, "Development of Compact and Efficient Reformer Using a new Catalyst for Shift Converter", *Scientific Advances in Fuel Cell Systems*, Amsterdam, 24-26 September 2(002).
62. V. Keulen, A. J. Nicolaas and J. G. Reinkingh, "Hydrogen Purification", *US Patent# 640049*, June (2002).
63. D. J. Edlund; J. Pledger; W. A. Studebaker and R. Todd, "Hydrogen Purification Membrane", *US Patent # 6632270*, October (2003).

64. D. A. G. Aranda, V. M. Souza, A. C. C. Rodriguez, I. S. Lopes and F. B. Passos, "Selective CO Oxidation on Pt/Nb₂O₅ Catalyst for Fuel Cell Applications", *UFRJ*, Brazil (2002).
65. S. D. Lee, R. Kumar and M. Krumplet, "Removal of CO from Reformate for Polymer Electrolyte Fuel Cell Application", Fuel Cell Seminar, Palm Spring, California, November (1998).
66. L. Cordaro, A. Pino, M. Vita, V. Lagena and V. Rucupero, "Development of a CO-Clean up System Based on Sorption Desorption Process", Scientific Advances in Fuel Cell Systems, Amsterdam, September (2002).
67. B. Lakshmanan, J. W. Weidner and W. Huang, "Electrochemical Filtering of Carbon Monoxide from Fuel-Cell Reformate", *Electrochemical and Solid State letters*, **5**, A267-A270 (2002).
68. B. Lakshmanan and J. W. Weidner, "Electrochemical Filtering of CO from Fuel-Cell Reformate", Extended *Abstract*, 204th Meeting, The Electrochemical Society, Inc., October (2003).
69. B. Lakshmanan and K. Chokkalingam, "CO Filter", *US Patent # 6517963*, February (2003).
70. C. Terreblanche, "South Africa May Become Power House of the World", *Sunday Argus*, IOL, South Africa, June 27, 2004.
71. S. Bridge, "South Africa Could Become a Global Energy Leader", *Business Report & Independent Online (Pty) Ltd.*, June 27, 2004.
72. Y. Hori, K. Kikuchi and S. Suzuki, "Production of CO and CH₄ in Electrochemical Reduction of CO₂ at Metal Electrodes in Aqueous Hydrogen Carbonate Solution", *Chemistry Letters*, 1695-1698, (1985).
73. Y. Hori, A. Murata, R. Takahashi and S. Suzuki, "Electrochemical Reduction of CO to Hydrocarbons at various Metal Electrodes in Aqueous Solution", *Chemistry Letters*, 1665-1668, (1987).
74. M. Azuma, K. Hashimoto, M. Watanabe and T. Sakata, "Carbon Dioxide Reduction on Various Metal Electrodes", *J. Electroanalytical Chemistry*, **260**, 441-445 (1989).

75. Y. Hori and A. Murata, "Electrochemical Evidence of Intermediate Formation of Adsorbed CO in Cathodic Reduction of Carbon Dioxide at a Nickel Electrode", *Electrochimica Acta*, **35** (11-12), 1777 - 1780 (1990).
76. K. Wang, G. Chottinger and D. A. Scherson, "Electrochemical Oxidation of Ni (111) c (4x2) -CO in Alkaline Electrolytes", *J. Physical Chemistry*, **96**, 6742-6744 (1992).
77. Y. Hori, A. Murata and Y. Yoshinami, "Adsorption of CO, Intermediately Formed in the Electrochemical Reduction of CO₂, at Copper Electrode", *J. Chemical Society, Faraday Transaction*, **87/1**, 125-128 (1991).
78. O. Koga and Y. Hori, "Reduction of Adsorbed CO on a Ni Electrode in Connection with the Electrochemical Reduction of CO₂", *Electrochimica Acta*, **38/10**, 1391 - 1394 (1993).
79. A. Cuesta and C. Gutierrez, "Study by Potential-Modulated Reflectance Spectroscopy of CO on Ni in alkaline Medium", *J. Electroanalytical Chemistry*, **382/1-2**, 153-159 (1995).
80. S. Gultekin, M. A. Al-Saleh and A. S. Al-Zakri, "Effect of CO Impurity in Hydrogen on the Performance of Ni/PTFE Diffusion Electrodes in Alkaline Fuel Cells", *Int. J. Hydrogen Energy*, **19/2**, 181-185 (1994).
81. H. H. Ewe, E. W. Justi and H. Selbach, "Storage of Hydrogen", *Energy Conversation and Management*, **24/1**, 89-96 (1984).
82. M. A. Al-Saleh, S. U. Rahman, S. M. M. J. Kareemuddin and A. S. Al-Zakri, "Novel Methods of Stabilization of Raney-Ni Catalyst for Fuel-Cell Electrodes", *J. Power Sources*, **72**, 159-164 (1998).
83. S. U. Rahman, "Development of Raney-Nickel Gas Diffusion Electrodes for Fuel Cells", PhD Dissertation, *King Fahd University of Petroleum and Minerals*, Saudi Arabia (1995).
84. S. M. M. J. Kareemuddin, "Stabilization of Raney-Nickel Catalyst for Fuel Cell Electrodes", MS Thesis Dissertation, *King Fahd University of Petroleum and Minerals*, Saudi Arabia (1996).

APPENDIX

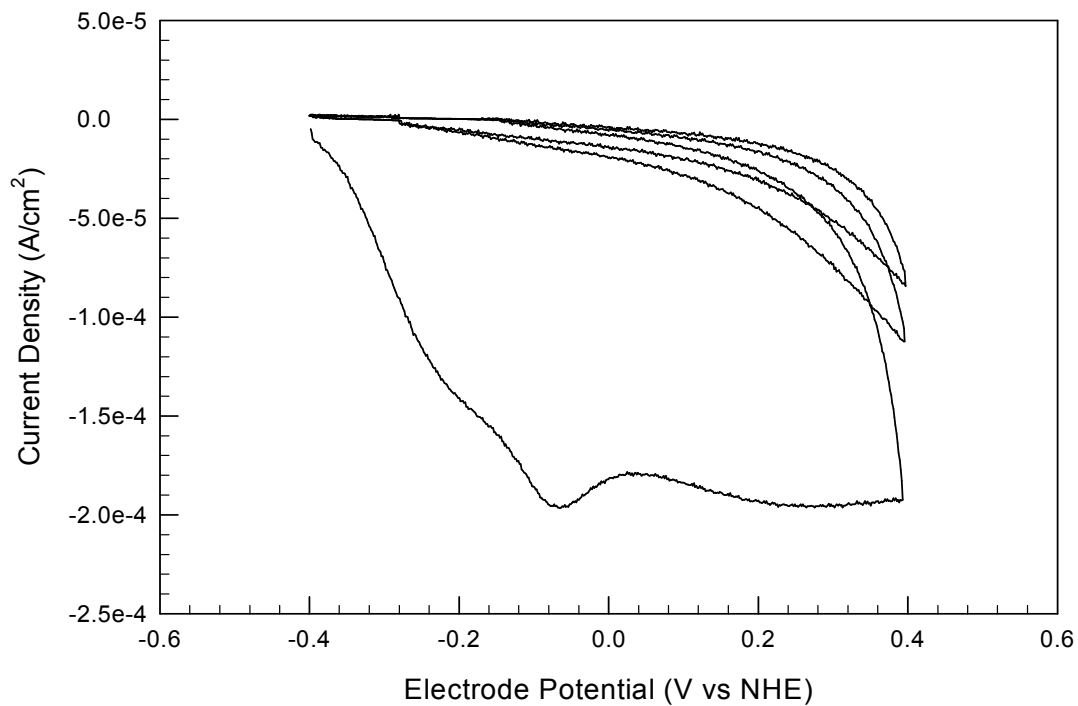


Figure A 1: Multiple Voltammogram of 10 ppm CO @ 25 ml/min

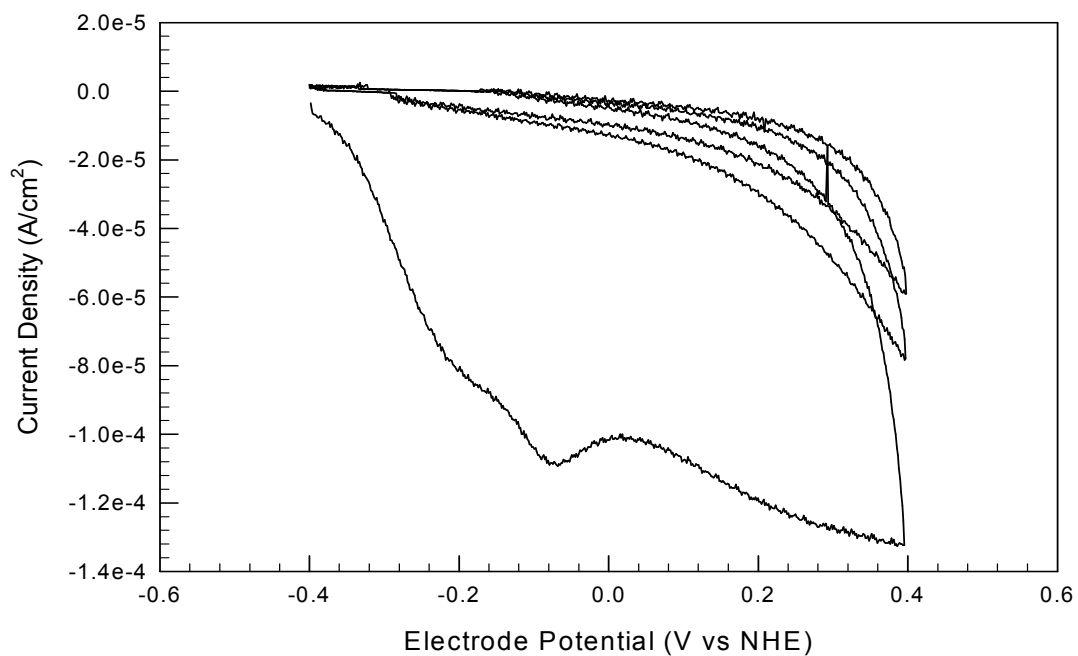


Figure A 2: Multiple Voltammogram of 100 ppm CO @ 25 ml/min

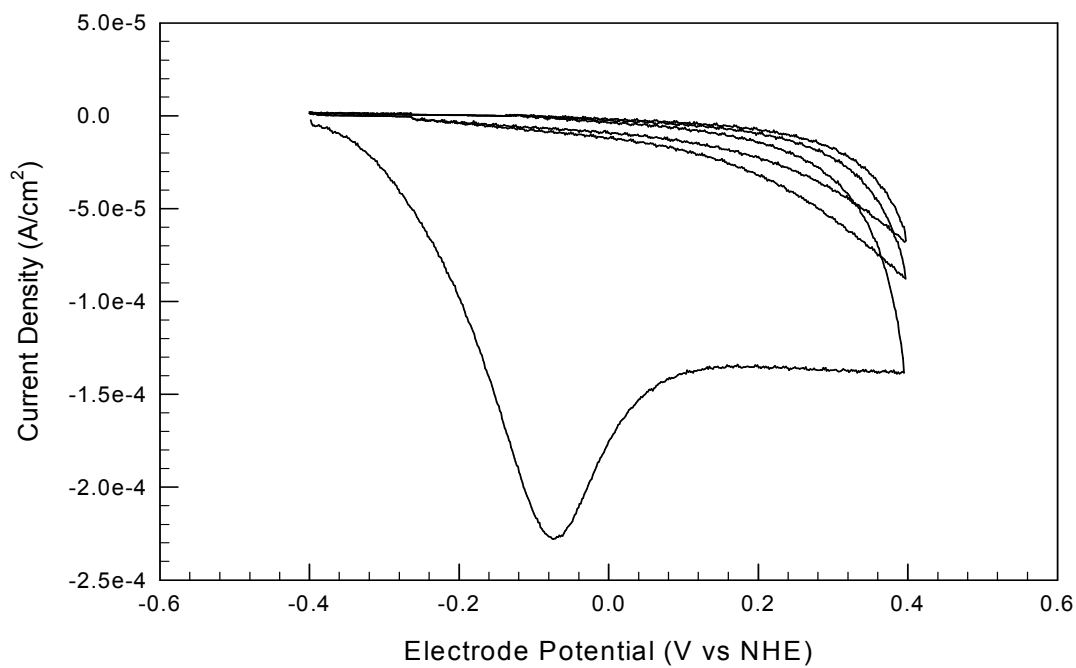


Figure A 3: Multiple Voltammogram of 1000 ppm CO @ 25 ml/min

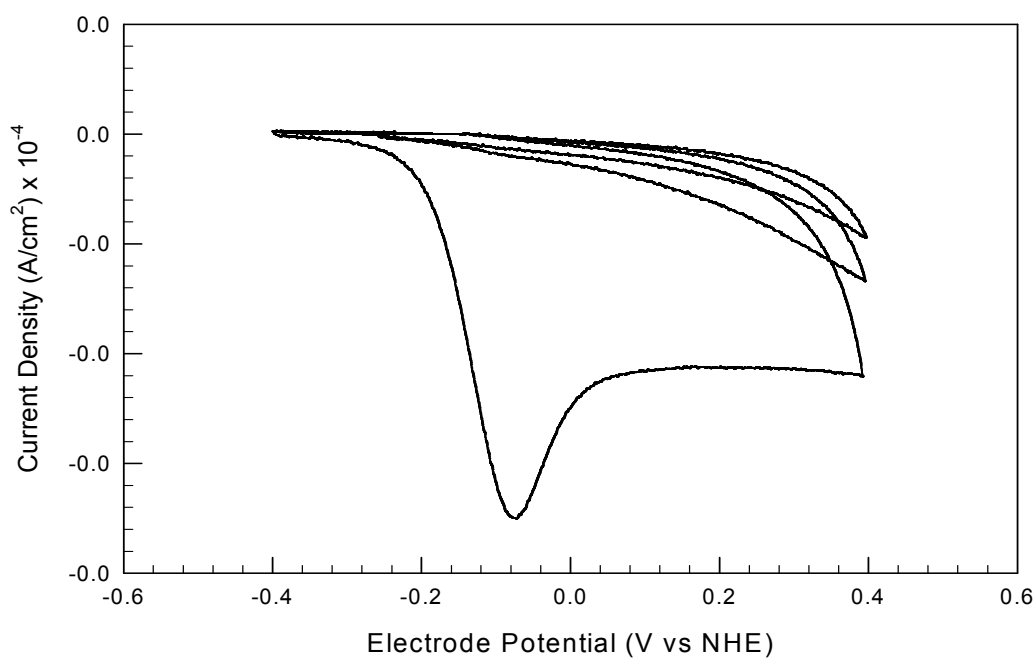


Figure A 4: Multiple Voltammogram of 1 % CO @ 25 ml/min

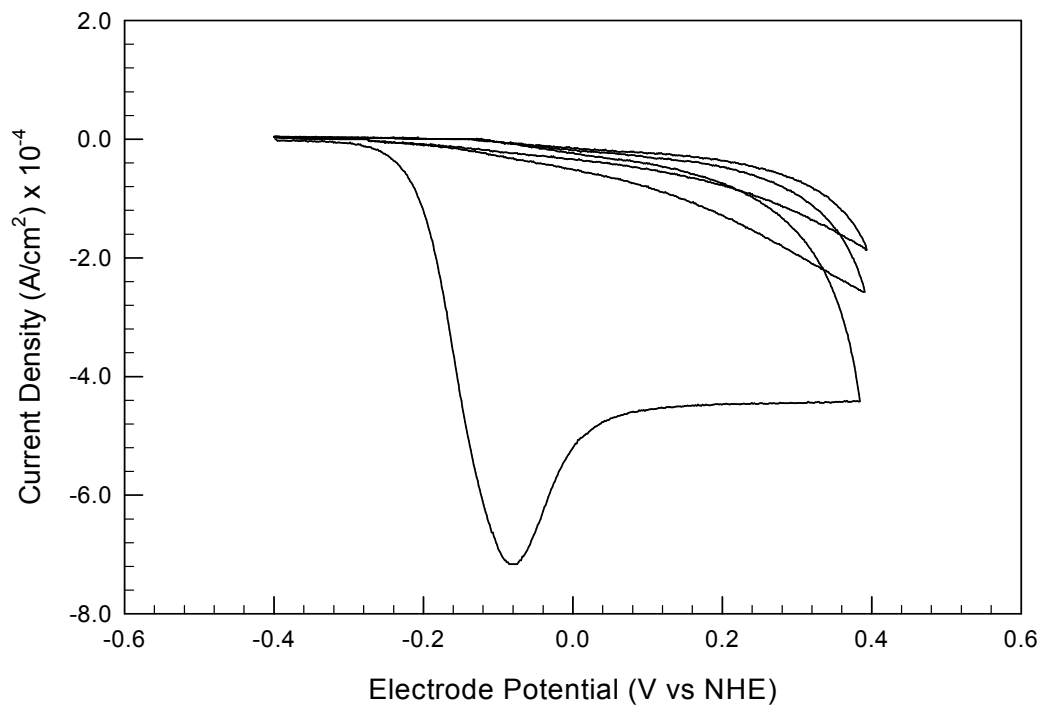


Figure A 5: Multiple Voltammogram of Pure CO @ 25 ml/min

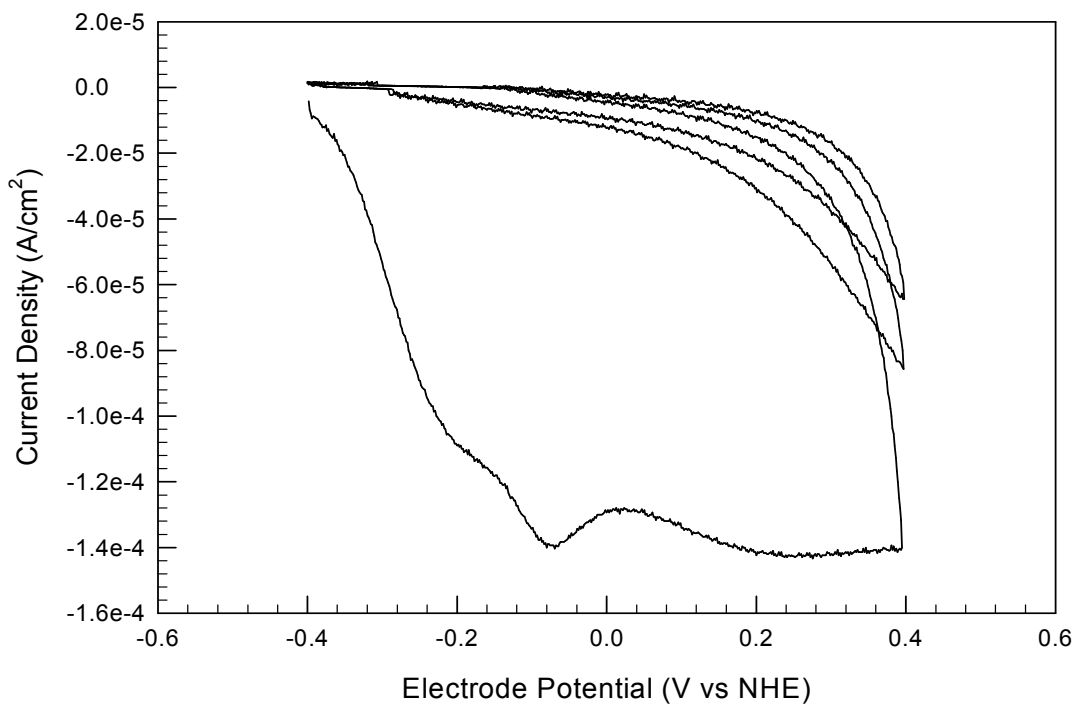


Figure A 6: Multiple Voltammogram of 10 ppm CO @ 125 ml/min

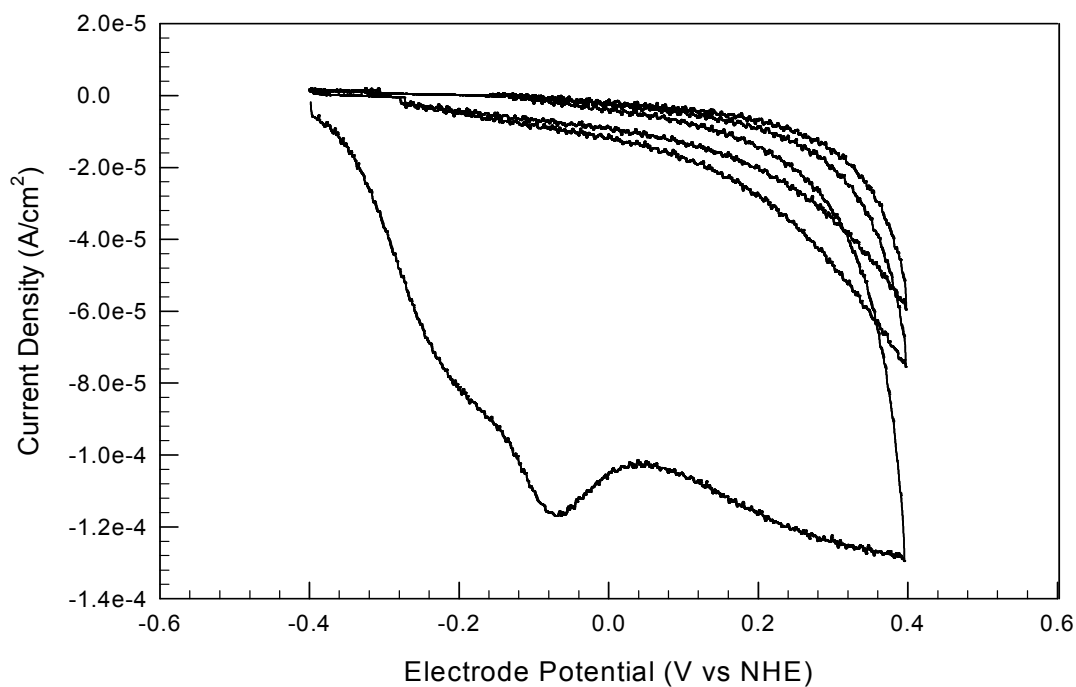


Figure A 7: Multiple Voltammogram of 100 ppm CO @ 125 ml/min

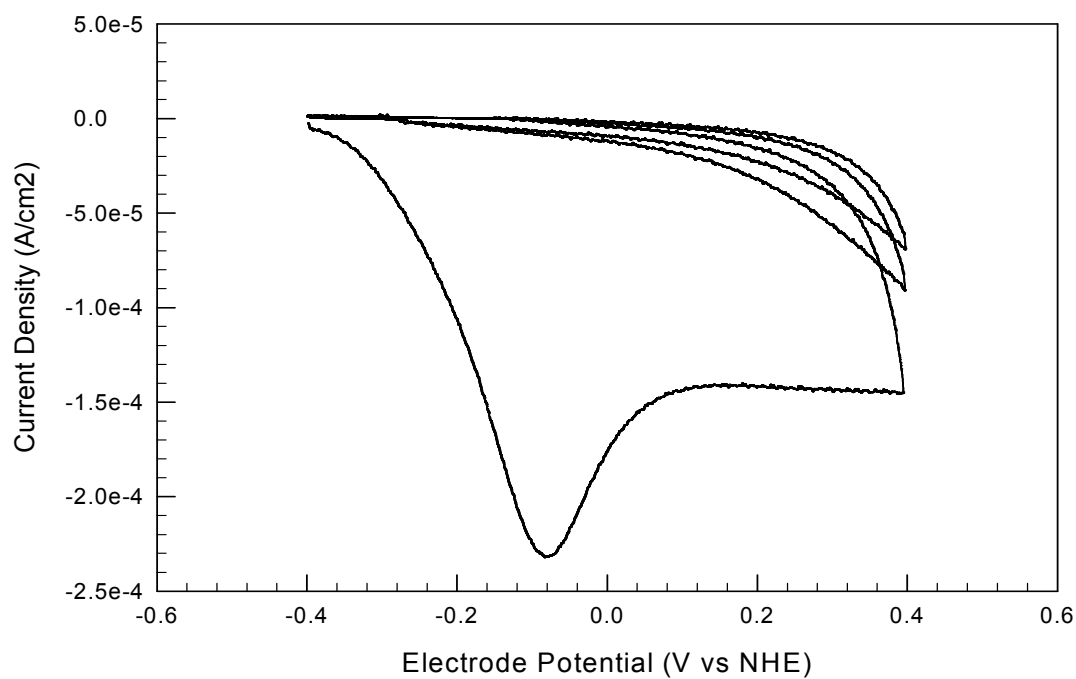


Figure A 8: Multiple Voltammogram of 1000 ppm CO @ 125 ml/min

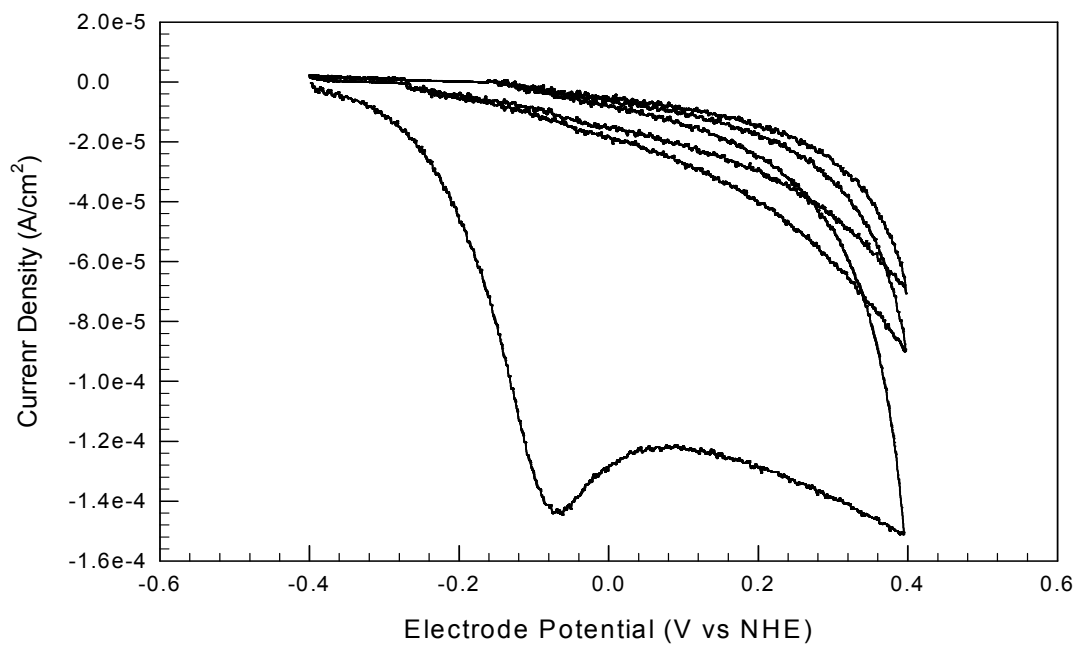


Figure A 9: Multiple Voltammogram of 1% CO @ 125 ml/min

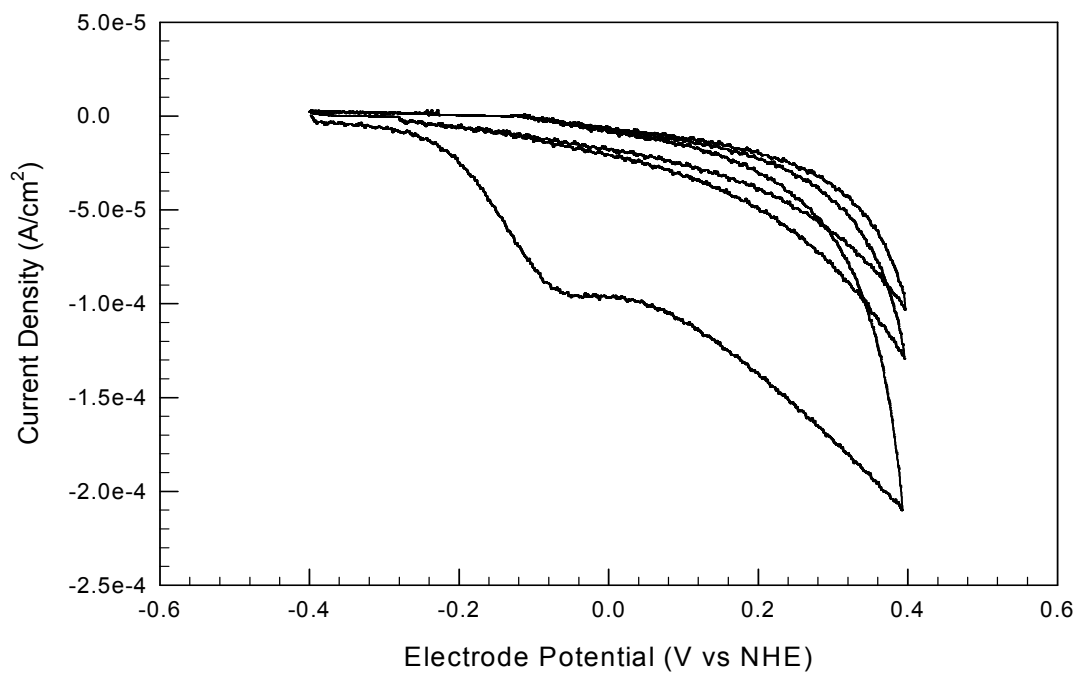


Figure A 10: Multiple Voltammogram of Pure CO @ 125 ml/min

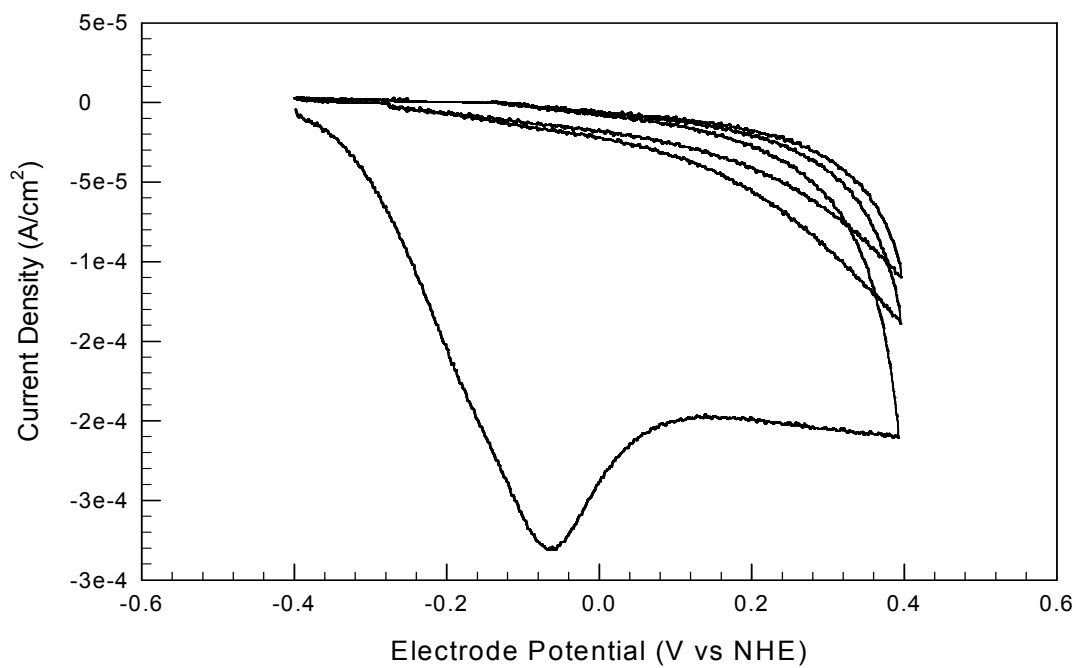


Figure A 11: Multiple Voltammogram of 10 ppm CO @ 200 ml/min

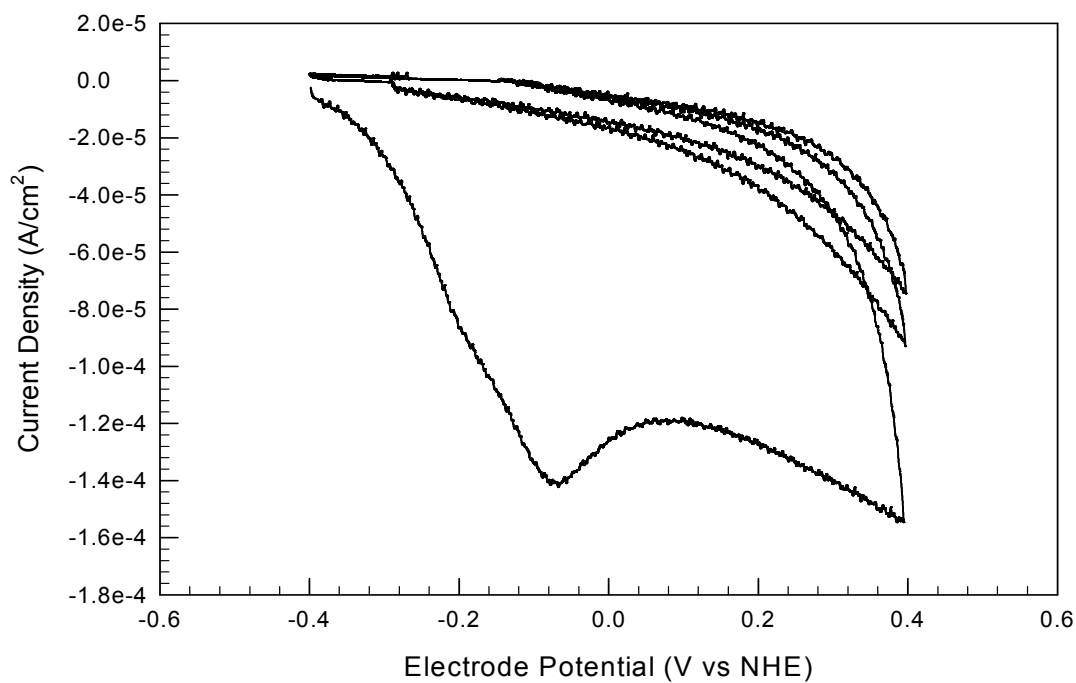


Figure A 12: Multiple Voltammogram of 100 ppm CO @ 200 ml/min

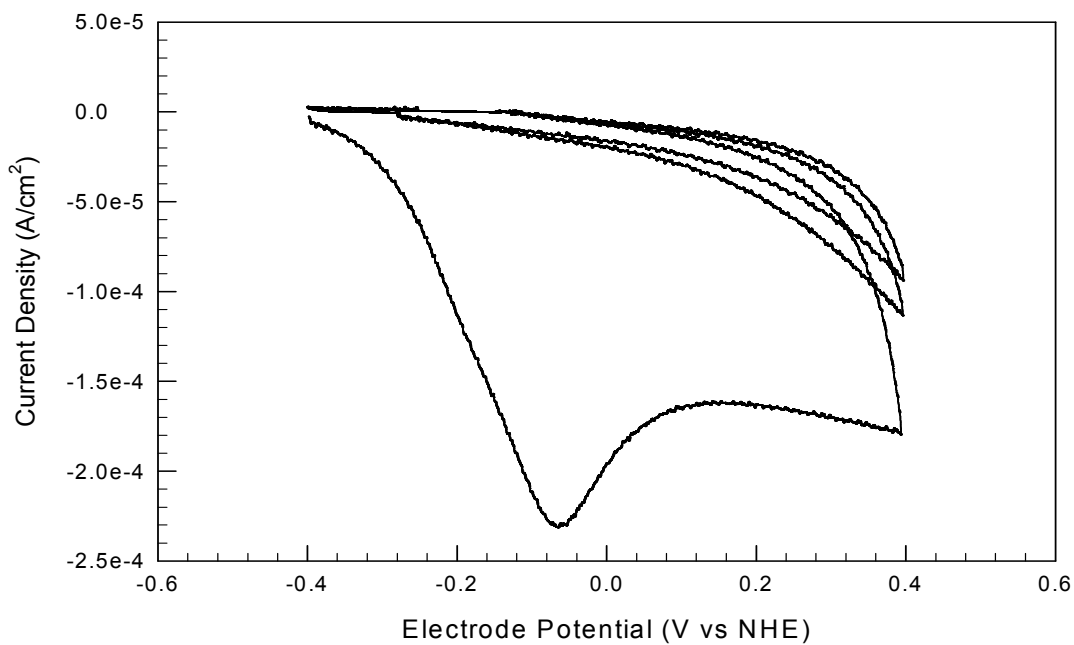


Figure A 13: Multiple Voltammogram of 1000 ppm CO @ 200 ml/min

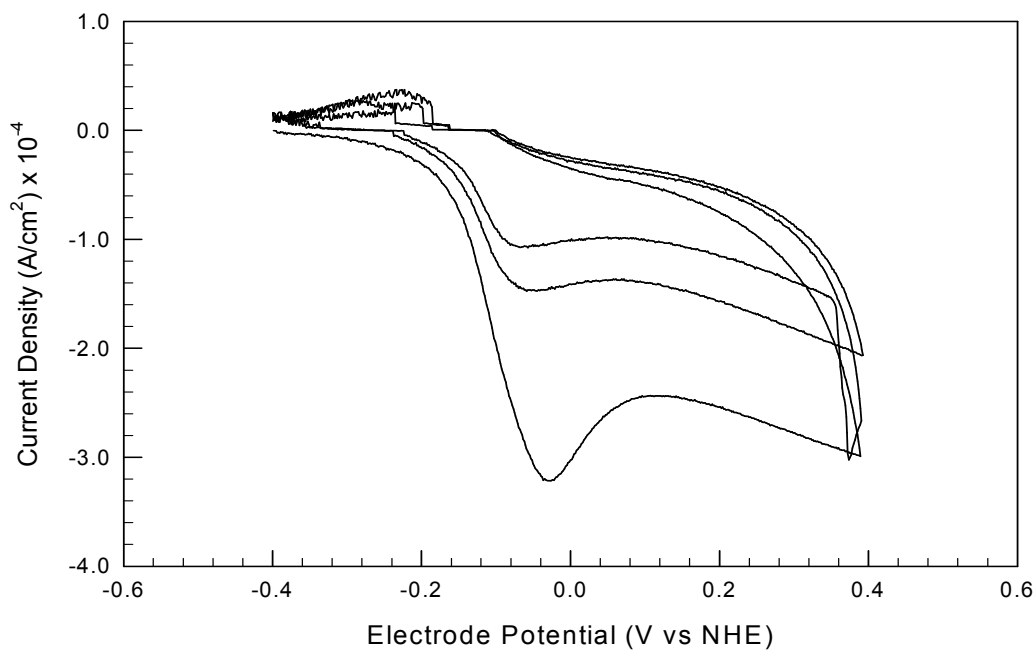


Figure A 14: Multiple Voltammogram of 1 % CO @ 200 ml/min

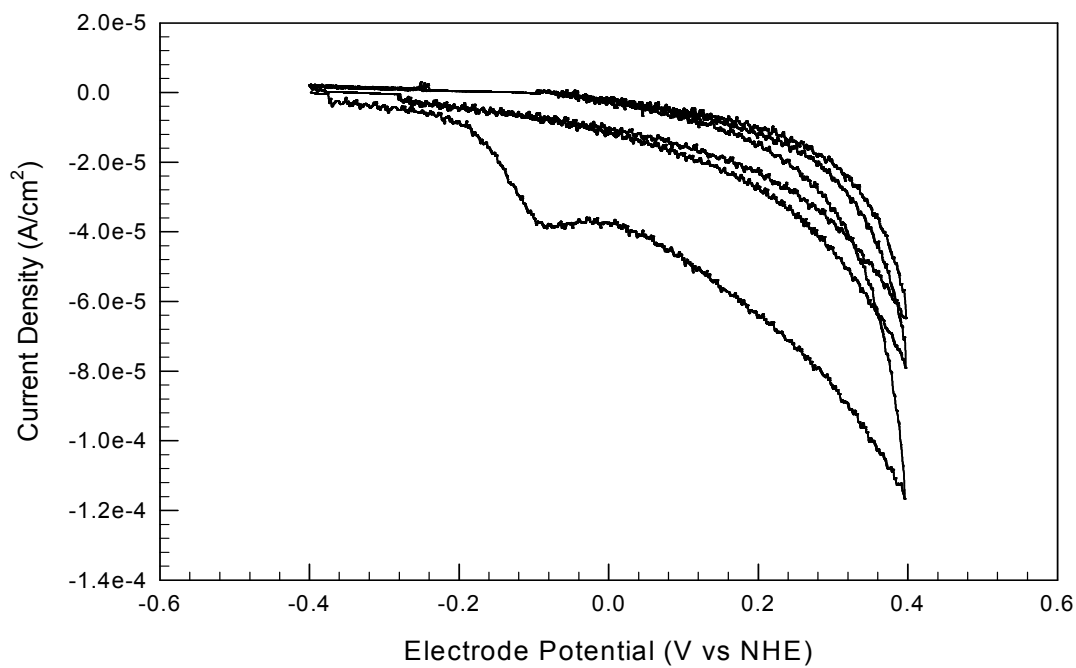


Figure A 15: Multiple Voltammogram of Pure CO @ 200 ml/min

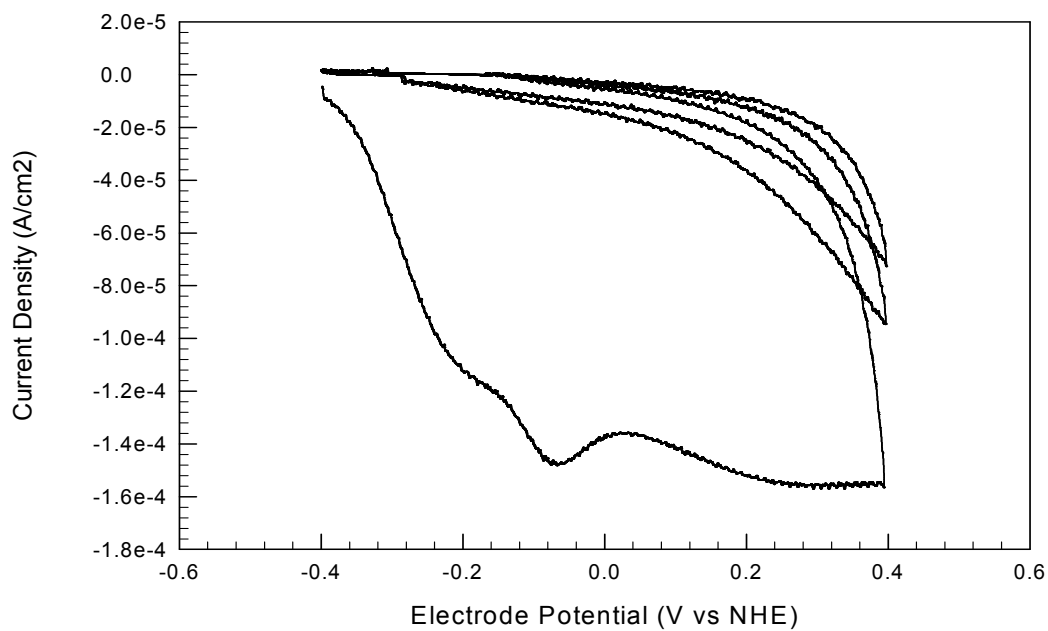


Figure A 16: Multiple Voltammogram of 10 ppm CO @ 275 ml/min

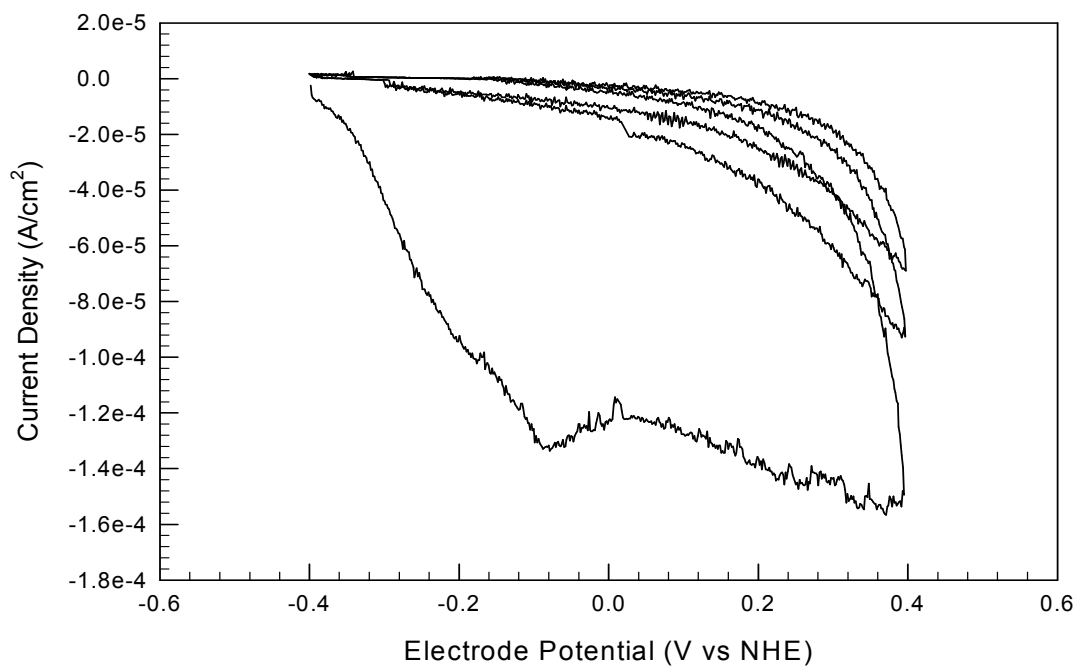


Figure A 17: Multiple Voltammogram of 100 ppm CO @ 275 ml/min

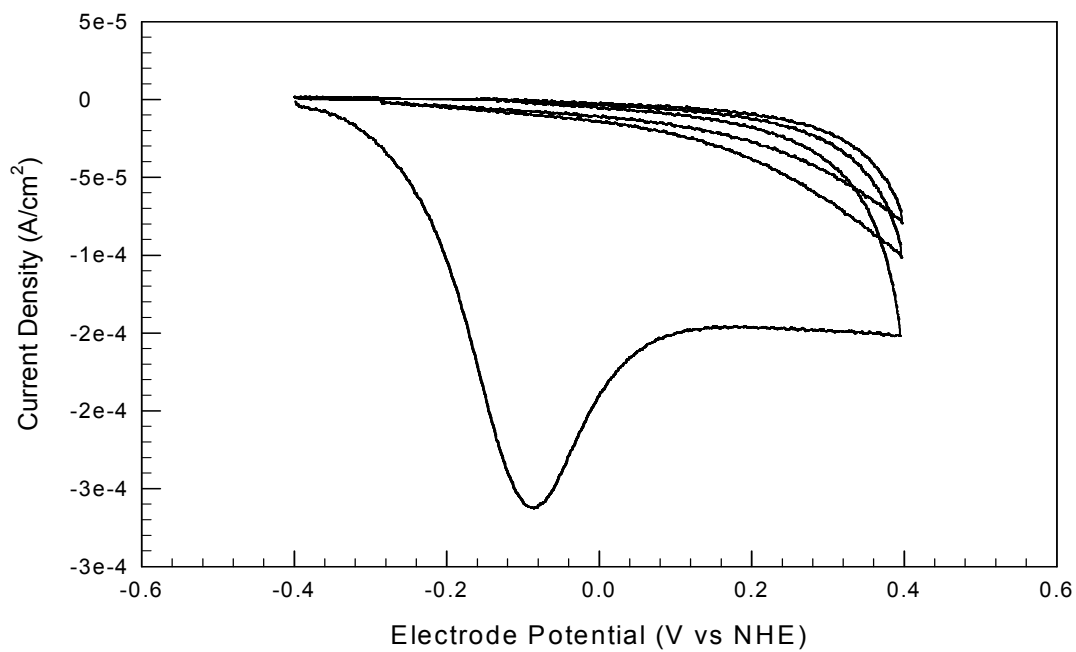


Figure A 18: Multiple Voltammogram of 1000 ppm CO @ 275 ml/min

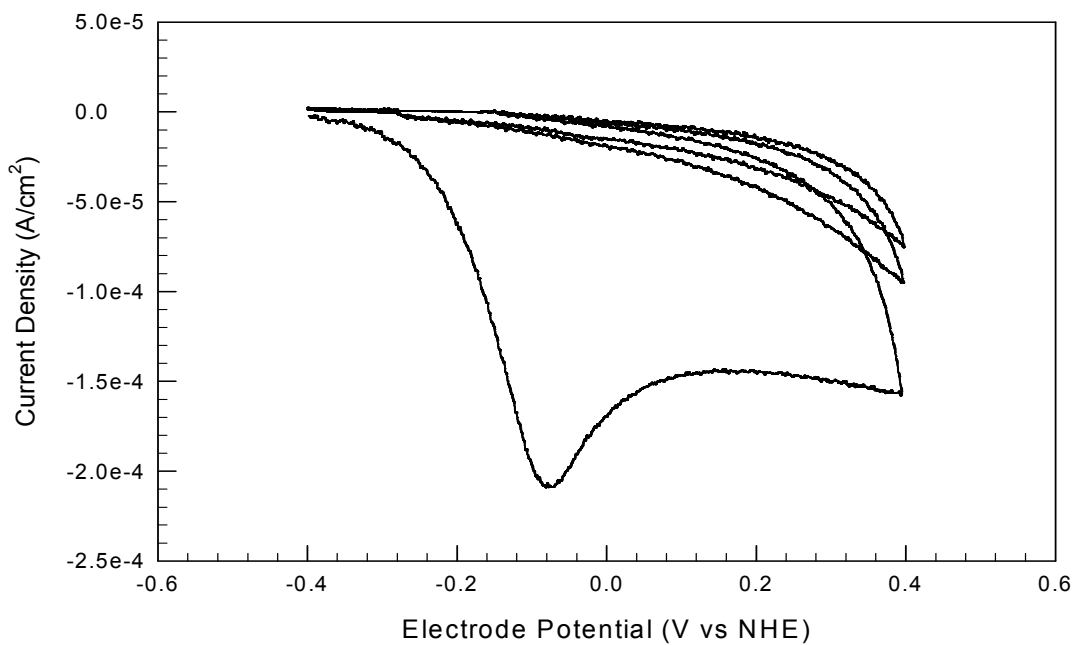


Figure A 19: Multiple Voltammogram of 1 % CO @ 275 ml/min

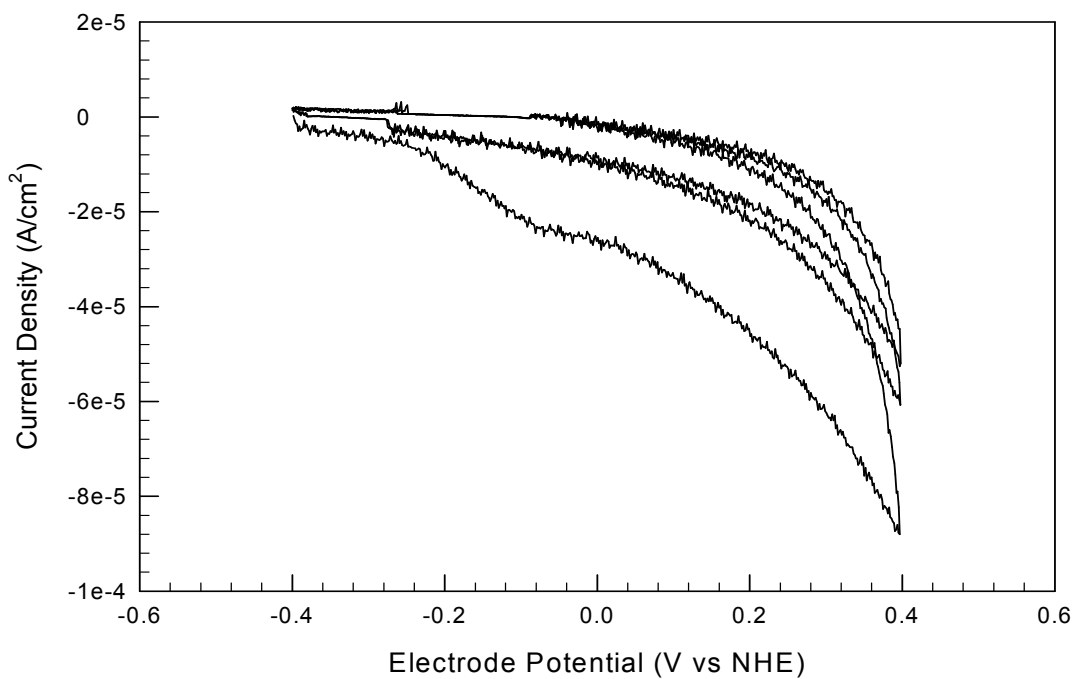


Figure A 20: Multiple Voltammogram of Pure CO @ 275 ml/min

VITAE

EDUCATION

1. Master of Science in Chemical Engineering (May 2005)

King Fahd University of Petroleum and Minerals, Dhahran-31261, KSA

2. Bachelor of Technology in Petrochemical Engineering (May 2002)

Zakir Hussain College of Engineering and Technology,
Aligarh Muslim University, Aligarh -202002, INDIA

PROFESSIONAL EXPERIENCE

Research Assistant (September 2002 – November 2005)

King Fahd University of Petroleum and Minerals, Dhahran-31261, KSA

CONFERENCE & PUBLICATION

1. Ahmad Nafees, S.U. Rahman and S.M.J. Zaidi, “*Electrochemical Removal of Carbon Monoxide from Hydrogen Using Nickel Catalyst*”, Submitted (Electrochimica Acta).
2. Ahmad Nafees, S.U. Rahman, S.M.J. Zaidi, “*Approaches to Solve the Problem of CO Poisoning in Hydrocarbon based PEM Fuel Cell Systems*”, Chemistry in Industry Conference and Exhibition CHEMINDIX-2004, September 2004, Bahrain.
3. Ahmad Nafees, S.U. Rahman, S.M.J. Zaidi, “*Carbon Monoxide Removal from Reformate on Ni Catalyst for Proton Exchange Membrane Fuel Cell*”, 208th Meeting of the Electrochemical Society, 16-21st October 2005, Los Angeles, California, USA
4. S.U. Rahman, S.M.J. Zaidi, N.A. Al-Baghli, Ahmad Nafees, J.W. Weidner, “*Approaches to Hydrocarbon Fuel Processing for Automotive and Stationary Fuel Cell Systems*”, 4th Middle East Refining and Petrochemicals Exhibition and Conferences, PETROTECH, October 2003, Bahrain.

PERSONAL INFORMATION

Email : ahmadnafeessajid@yahoo.com & nafeesansari@gmail.com

Homepage: <http://staff.kfupm.edu.sa/che/mnafees>

Home Address: Mohalla-Sakrawal (West), Tanda, Faizabad, U. P. 224190, INDIA